

Development of new insecticide
technologies against urban pests based on
biomolecules

Núria Farrús Bartolo

DOCTORAL THESIS UPF/ 2024

THESIS DIRECTORS

Dr. José Luis Maestro

Dr. Maria Dolors Piulachs

INSTITUT DE BIOLOGIA EVOLUTIVA (CSIC-UNIVERSITAT

POMPEU FABRA)



This industrial thesis is a collaboration between the Institute of Evolutionary Biology (CSIC-Universitat Pompeu Fabra) and the company Mylva S.A., and it was supported by Pla de Doctorats Industrials de la Secretaria d'Universitats i Recerca del Departament d'Empresa i Coneixement de la Generalitat de Catalunya (grant number 2021 DI 059)



Als meus pares

Acknowledgments

Vull començar donant les gràcies a tots els qui han fet possible aquest doctorat industrial. D'una banda als meus directors de tesi, José Luis Maestro i Maria Dolors Piulachs, agrair-los les ensenyances, haver-me transmès la seva passió per la ciència i el recolzament que m'han donat al llarg d'aquest camí. D'altra banda a la direcció de l'empresa Mylva, Albert Picas i Sílvia Sorribes, agrair-los l'entusiasme pel projecte, el suport i fer-me sentir part de l'equip. Moltes gràcies a ambdues parts per brindar-me aquesta oportunitat i per confiar-me aquest projecte tan ambiciós. Agrair també al Pla de Doctorats Industrials de la Secretaria d'Universitats i Recerca del Departament d'Empresa i Coneixement de la Generalitat de Catalunya (2021 DI 059) pel suport econòmic rebut.

També vull mostrar el meu agraïment al Roger Brunet, per assumir aquest repte amb tantes ganes, pels valuosos consells i per la confiança dipositada en mi. Així mateix, vull agrair-li al Xavier Bellés les enriquidores discussions científiques, els seus consells i la seva contagiosa passió pel saber.

A tots els membres del p129 que m'han fet costat al llarg d'aquests tres anys – Alfonso, Celeste, David, Denis, Jorge, Judit, Mireia, Thiago, Vivi, Yu, i Zeynab – gràcies per fer-ho tot més fàcil, per tot el que m'heu ensenyat i per les bones estones compartides. Tots i cadascun de vosaltres heu estat una part essencial d'aquesta tesi; us considero família. Agrair-li també a la Cristina la feina feta amb tanta cura i haver compartit amb mi l'amor pels insectes i la fotografia.

Donar les gràcies també a l'equip humà que conforma l'administració del IBE, així com a tota la gent del Institut. Sou una llista extensa de persones que heu format part del meu dia a dia, des de les xarrades al passadís i els *coffee breaks*, fins les reunions d'estudiants i les birres al Bar Magatzem. Gràcies a tots vosaltres per fer més lleuger aquest camí; us tinc a tots molt presents.

Vull agrair a l'equip de I+D de Mylva que m'ha acompanyat durant aquest temps – Andrea, Carlota, Marta, Raúl i Tristan – per haver-me acollit amb els braços oberts i estar sempre disposats a ajudar-me. No he tingut la sort de conèixer-vos en profunditat, però sou persones extraordinàries.

Un especial agraïment als meus amics, que m'han escoltat, m'han aconsellat i m'han recolzat quan ho he necessitat. Particularment a l'Anna, que ha viscut aquesta tesi en primera persona i ha estat el meu gran suport en els moments més complicats, gràcies per ser-hi sempre. Gràcies també a la Júlia J., perquè sense ella avui no estaria aquí.

I per últim però no menys important, als meus pares, als quals va dedicada aquesta tesi, gràcies per creure en mi, per animar-me a seguir amb els estudis i per ser el meu refugi segur. Al meu germà, gràcies per donar-me sempre suport i confiar en el que faig. A les meves padrines, que tot i no ser-hi de ben segur n'estarien molt orgulloses. A la Rosita, pels ànims i la confiança. I als meus tiets i cosins, pel seu suport, que sempre he sentit molt a prop.

A tots vosaltres, gràcies per haver fet aquesta tesi una realitat.

Abstract

This industrial thesis provides insights into the development of new insecticide technologies against the cockroach *Blattella germanica*. We have focused this work on the design of an oral insecticide using RNA interference (RNAi) methodology, as an alternative to synthetic chemical insecticides. We first evaluated essential genes in *B. germanica* by injection, and then selected one of them as the best candidate for RNAi oral delivery experiments. We also studied the function of this candidate gene in *B. germanica* oogenesis. For oral delivery experiments, we used nanomaterials to preserve the stability of the double-stranded RNA (dsRNA) as it passes through the insect gut. Results in RNAi oral delivery showed no insect mortality but oviposition was compromised in certain cases. We identified the potential barriers that limit RNAi efficiency in oral experiments, reinforcing the importance of their understanding for the successful development of oral RNAi-based insecticides. Additionally, we propose antisense oligonucleotides (ASOs) as alternative nucleic acid-based molecules to manage *B. germanica* pest.

Resum

Aquesta tesi industrial aporta coneixement sobre el desenvolupament de noves tecnologies insecticides contra la panerola *Blattella germanica*. Hem centrat aquest treball en el disseny d'un insecticida oral mitjançant la metodologia d'interferència d'ARN (ARNi) com a alternativa als insecticides químics sintètics. Primer de tot, hem estudiat per injecció els gens essencials en *B. germanica* i després hem seleccionat un d'ells com el millor candidat per als experiments d'administració oral d'ARNi. També hem estudiat la funció d'aquest gen candidat en l'oogènesi de *B. germanica*. Per als experiments d'administració oral, hem utilitzat nanomaterials per preservar l'estabilitat de la doble cadena de RNA (dsRNA) mentre passa pel digestiu de l'insecte. En els resultats d'administració oral d'ARNi no es va observar mortalitat en els insectes, però l'oviposició es va veure compromesa en alguns casos. Hem identificat les barreres potencials que limiten l'eficiència de l'ARNi en experiments orals, fet que reforça la importància de la seva comprensió per a l'exitós desenvolupament d'insecticides orals basats en ARNi. A més, proposem els oligonucleòtids antisentit (ASOs), molècules basades en àcids nucleics, com alternativa per controlar la plaga de *B. germanica*.

Preface

In the latter half of the 20th century and the early 21st century, the climate change and the urban expansion have exacerbated the problem of urban pests. Among them, the cockroach *Blattella germanica* is one of the most alarming and disturbing. This nuisance pest, found in urban environments worldwide, can transmit important diseases and cause significant economic losses. At present, the main approach to manage this pest is the use of synthetic chemical insecticides. However, these compounds can harm non-target organisms, contaminate the environment, and ultimately affect human health.

The demonstrated side effects of certain widely used synthetic chemical compounds, the appearance of resistances to them, and their growing prohibition by the European Union have created the necessity of the development of alternatives more target-specific and environmentally friendly. This has motivated the company Mylva to explore potential alternatives for managing urban pests, starting several lines of research. Among these efforts, the company launched the initiative to establish this industrial doctorate, focused on the use of acid nucleic molecules against *B. germanica*. This thesis is the result of the collaboration between the company Mylva with more than 35 years of experience in pest management together with José Luis Maestro and Maria Dolors Piulachs, principal investigators of the Institute of Evolutionary Biology (CSIC-Universitat Pompeu Fabra) with more than 35 years of experience in *B. germanica* and molecular biology techniques.

In this industrial thesis, the main objective was the design of a species-specific and environmentally-friendly oral insecticide based on acid nucleic molecules, mainly taking advantage of the RNA interference (RNAi) mechanism to target an essential gene. This thesis aimed to address the challenges of achieving mortality in *B. germanica* by RNAi oral delivery, since we know that injection of double-stranded RNA (dsRNA) is highly effective in this insect species. We described how nanoparticles could preserve the stability of dsRNA, together with the potential barriers that limit RNAi efficiency in *B. germanica*. We provided valuable insights for the future development of insecticides based on nucleic acid molecules, both mRNAs and non-coding RNAs.

Table of contents

Acknowledgments	vii
Abstract.....	ix
Resum.....	xi
Preface.....	xiii
1. INTRODUCTION AND OBJECTIVES.....	1
1.1. INTRODUCTION	3
1.1.1. <i>Blattella germanica</i> as a pest.....	3
1.1.1.1. Anatomical characteristics	3
1.1.1.2. Habitat and geographic spread	4
1.1.1.3. Health problem.....	5
1.1.1.4. Economic impact.....	5
1.1.2. <i>Blattella germanica</i> as a model insect.....	6
1.1.3. Insecticides for pest control.....	6
1.1.3.1. Disadvantages of common insecticides.....	8
1.1.3.2. Current pest management strategies.....	9
1.1.3.3. New pest management strategies based on nucleic acid molecules.....	9
1.1.3.3.1. RNA interference (RNAi)	10
1.2. OBJECTIVES	13
1.3. BIBLIOGRAPHY	13
2. DEPLETION OF ESSENTIAL GENES IN <i>Blattella germanica</i> USING RNA INTERFERENCE.....	19
2.1. INTRODUCTION	21
2.1.1. Selection of essential genes	21
2.2. MATERIALS AND METHODS	22
2.2.1. Cockroach colony and tissues sampling.....	22
2.2.2. RNA extraction, cDNA synthesis and quantitative real-time PCR analysis	23
2.2.3. dsRNA synthesis and RNAi experiments by injection.....	24
2.2.4. Statistical analysis	24
2.3. RESULTS	25
2.3.1. Mortality determined by the depletion of candidate genes in adult <i>Blattella germanica</i> females.....	25
2.3.2. Depletion of [REDACTED] mRNA levels in different tissues of adult <i>Blattella germanica</i> females.....	26

2.3.3. Mortality determined by [REDACTED]-treatment in adult <i>Blattella germanica</i> males and sixth nymphal instar <i>Blattella germanica</i> females	28
2.3.4. Depletion of [REDACTED] mRNA levels in different tissues of adult <i>Blattella germanica</i> females.....	29
2.4. DISCUSSION	31
2.5. BIBLIOGRAPHY	33

3. CHMP4B CONTRIBUTES TO MAINTAINING THE FOLLICULAR CELLS INTEGRITY IN THE PANOISTIC OVARY OF THE COCKROACH *Blattella germanica*..... 39

ABSTRACT	43
3.1. INTRODUCTION	44
3.2. MATERIALS AND METHODS	46
3.2.1. Insects sampling	46
3.2.2. RNAi experiments.....	46
3.2.3. RNA extraction, cDNA synthesis, and quantitative real-time PCR analysis	47
3.2.4. Quantification of total ovarian proteins.....	48
3.2.5. Tissue staining and immunohistochemistry	48
3.2.6. Statistical analysis	48
3.3. RESULTS	49
3.3.1. <i>Chmp4b</i> expression in the ovaries of <i>Blattella germanica</i>	49
3.3.2. Effects of <i>Chmp4b</i> depletion on the ovary of 5-day-old <i>Blattella germanica</i> adults	49
3.3.3. Expression of genes related to cell planar polarity in ds <i>Chmp4b</i> -treated <i>Blattella germanica</i> adult ovaries.....	56
3.3.4. Effects of <i>Chmp4b</i> depletion on the basal ovarian follicle of <i>Blattella germanica</i> last instar nymphs	58
3.4. DISCUSSION	62
3.5. BIBLIOGRAPHY	64
3.6. SUPPLEMENTARY MATERIAL	69

4. CHARACTERIZATION OF [REDACTED]-NANOPARTICLES..... 73

4.1. INTRODUCTION	75
4.1.1. Nanoparticles for dsRNA oral delivery.....	75
4.1.2. Selection criteria of nanomaterials for dsRNA oral delivery .	77
4.2. MATERIALS AND METHODS	78
4.2.1. Cockroach colony.....	78
4.2.2. [REDACTED] dsRNA	78
4.2.3. Preparation of [REDACTED]-nanoparticles	79
4.2.3.1. Chitosan nanoparticles	79

4.2.3.2. Liposome nanoparticles.....	80
4.2.3.3. PAMAM nanoparticles	81
4.2.3.4. PEI nanoparticles.....	82
4.2.4. Efficiency of complexation or encapsulation of dsRNA using nanomaterials	83
4.2.5. Characterization of dsRNA-nanoparticles in the Scanning Electron Microscope	83
4.2.6. Determination of particle size by Dynamic Light Scattering .	84
4.2.7. RNAi experiments by injection.....	85
4.2.8. Statistical analysis	85
4.3. RESULTS	85
4.3.1. Chitosan-based nanoparticles.....	85
4.3.1.1. Capacity of chitosan for complexing [REDACTED]	85
4.3.1.2. Morphology and size of chitoplex (CX).....	86
4.3.2. Liposome-based nanoparticles	87
4.3.2.1. Capacity of liposomes for encapsulating [REDACTED]	87
4.3.1.2. Morphology and size of lipoplex (LX).....	88
4.3.3. Polyamidoamine-based nanoparticles	89
4.3.3.1. Capacity of PAMAM for complexing [REDACTED]	89
4.3.3.2. Morphology and size of PAMAM-complex (PAX).....	90
4.3.4. Polyethylenimine-based nanoparticles	91
4.3.4.1. Capacity of PEI for complexing [REDACTED]	91
4.3.4.2. Morphology and size of PEI-complex (PEIX).....	92
4.3.5. Mortality induced by [REDACTED]-NPs injection in adult <i>Blattella germanica</i> females	93
4.4. DISCUSSION	94
4.5. BIBLIOGRAPHY	96

5. dsRNA ORALLY DELIVERED TO ADULT FEMALES..... 101

5.1. INTRODUCTION	103
5.1.1. The insect gut	103
5.1.2. dsRNA feeding and the barriers that limit its efficiency.....	104
5.1.2.1. Degradation of dsRNA by RNases and effect of pH.....	105
5.1.2.2. Cellular uptake of dsRNA and systemic spreading of the dsRNA effect.....	106
5.1.2.3. Endosomal escape of dsRNA.....	107
5.1.2.4. Other factors influencing dsRNA efficiency.....	108
5.1.3. Enhancing dsRNA efficiency using nanoparticles	109
5.1.3.1. The transient pore model.....	109
5.1.3.2. The proton-sponge effect model.....	110
5.2. MATERIALS AND METHODS	112
5.2.1. Cockroach colony and tissues sampling.....	112

5.2.2. RNA extraction, cDNA synthesis and quantitative real-time PCR analysis	112
5.2.3. [REDACTED] dsRNA	113
5.2.4. [REDACTED] and dsPolyH synthesis.....	114
5.2.5. Preparation of [REDACTED]-nanoparticles	114
5.2.6. dsRNA oral delivery.....	114
5.2.6.1. [REDACTED]	114
5.2.6.1.1. Persistence of dsRNA [REDACTED]	115
5.2.6.2. Forced feeding.....	116
5.2.6.3. Water-feeder bottles	116
5.2.7. Statistical analysis	116
5.3. RESULTS	117
5.3.1. Feeding of naked dsRNA to adult females.....	117
5.3.1.1. Persistence of naked dsRNA in [REDACTED]	117
5.3.1.2. Effect of naked [REDACTED] and [REDACTED] delivered using [REDACTED] on reproduction and survival.....	118
5.3.1.3. Effect of naked [REDACTED] delivered in water solutions on reproduction and survival.....	119
5.3.2. Feeding of [REDACTED]-nanoparticles to adult females.....	120
5.3.2.1. Effect of [REDACTED]-nanoparticles delivered in [REDACTED] on reproduction and survival.....	120
5.3.2.2. Effect of [REDACTED]-nanoparticles delivered by forced feeding on reproduction and survival.....	123
5.3.2.3. Effect of [REDACTED]-nanoparticles delivered in water solutions on reproduction and survival	125
5.4. DISCUSSION	128
5.5. BIBLIOGRAPHY	130

6. UNRAVELING THE ABSENCE OF MORTALITY IN THE dsRNA-NPs FEEDING EXPERIMENTS..... 137

6.1. INTRODUCTION	139
6.2. MATERIALS AND METHODS	140
6.2.1. Cockroach colony and tissues sampling.....	140
6.2.2. [REDACTED] dsRNA	140
6.2.3. Preparation of [REDACTED]-nanoparticles	140
6.2.4. Collection of midgut juice and hemolymph	141
6.2.5. <i>Ex vivo</i> dsRNA degradation assay.....	141
6.2.6. Characterization of Peritrophic Membrane in the Scanning Electron Microscope	143
6.2.7. Statistical analysis	144
6.3. RESULTS	145
6.3.1. <i>Ex vivo</i> degradation of dsRNA conjugated with nanomaterials in the midgut juice of <i>Blattella germanica</i>	145

6.3.2. Structure of the peritrophic membrane of <i>Blattella germanica</i>	147
6.4. DISCUSSION	149
6.5. BIBLIOGRAPHY	150
7. A piRNA REGULATING OOGENESIS AND EMBRYO DEVELOPMENT IN COCKROACHES	153
7.1. INTRODUCTION	157
7.2. MATERIALS AND METHODS	159
7.2.1. <i>Blattella germanica</i> colony and tissue sampling	159
7.2.2. Small RNA library processing	160
7.2.3. RNA extraction and expression studies	160
7.2.4. Treatments with antisense oligonucleotides	161
7.2.5. Microscopy methodologies	162
7.2.5.1. <i>In situ</i> hybridization	162
7.2.5.2. DAPI-TRITC-Phalloidin staining	162
7.2.5.3. Embryo observations	163
7.2.6. Statistical analysis	163
7.3. RESULTS	163
7.3.1. piRNA-83679 in the ovary	163
7.3.2. piRNA-83679 and basal ovarian follicle development	166
7.3.3. piRNA-83679 function on reproduction and embryo development	168
7.4. DISCUSSION	171
7.5. BIBLIOGRAPHY	173
7.6. SUPPLEMENTARY MATERIAL	179
8. DISCUSSION	181
8.1. GENERAL DISCUSSION	183
8.2. BIBLIOGRAPHY	186
9. CONCLUSIONS	189
ANNEXES	193

1. INTRODUCTION AND OBJECTIVES

1. INTRODUCTION AND OBJECTIVES

1.1. Introduction

1.1.1. *Blattella germanica* as a pest

Cockroaches are among the most primitive winged insects and their origin dates back to approximately 300 million years ago to the Carboniferous period. At the present time there are about 4,000 described species of cockroaches, most of them of tropical origin, and less than 1% are considered pest species (Grimaldi & Engel, 2005). Insect pests are defined as insects that cause harm to humans, their livestock, crops or possessions (Hill, 1997). Within cockroaches, the German cockroach *Blattella germanica* (L., 1758) (Blattodea: Blattellidae), the American cockroach *Periplaneta americana* (L., 1758) (Blattodea: Blattidae), and the Oriental cockroach *Blatta orientalis* L., 1758 (Blattodea: Blattidae), are the species with the highest global impact (Toukhsati & Scanes, 2018). Among these, *B. germanica* is the most widespread and abundant species in urban areas (Tang et al., 2024; Wang et al., 2021).

1.1.1.1. Anatomical characteristics

The German cockroach adults measure between 1.5 to 1.8 cm in length. They have a general light brown coloration with two dark parallel bands in the pronotum, which are generally broader in nymphs (Figure 1.1). Male and female adults are easily distinguishable: females are more robust than males; the tegmina completely cover the abdomen in females, while in males, the terminal abdominal segments remain visible; in females abdominal tergites are uniform, whereas in males the tergal glands are located in the 7th abdominal tergites; females possess cerci with twelve segments, whereas males have eleven (Figure 1.1) (Cornwell, 1968).

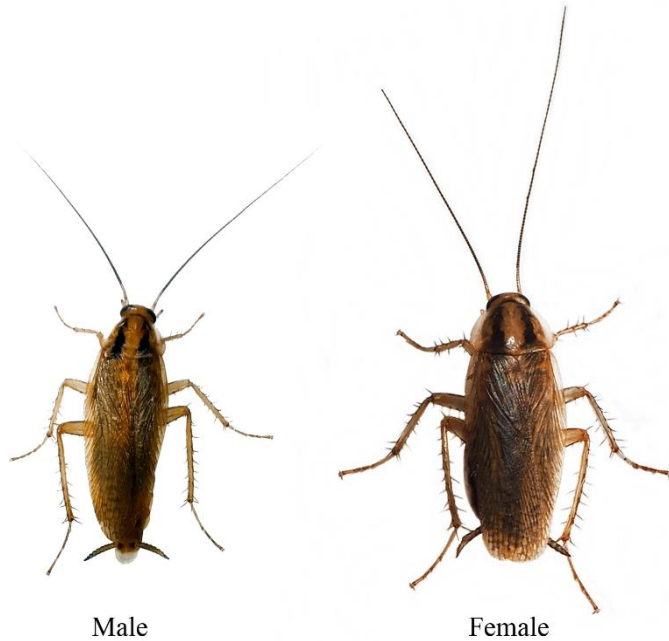


Figure 1.1. Male and female adult *Blattella germanica* cockroaches. Images courtesy of Cristina Olivella.

1.1.1.2. Habitat and geographic spread

The German cockroach, *B. germanica* have been originated from the Asian cockroach *Blattella asahinai* (Mizukubo, 1981) (Blattodea: Ectobiidae) approximately 2,100 years ago, probably by adapting to human settlements in India or Myanmar (Mukha et al., 2002; Roth, 1985; Tang et al., 2024). Recent genomic analyses indicate that the global spread of *B. germanica* followed two main routes: an older westward expansion to the Middle East, dating back about 1,200 years, coinciding with commercial and military activities of Islamic dynasties; and a recent eastward route, occurring approximately 390 years ago, aligned with European colonial commercial activities. This most recent global spread was accelerated with the European advances in long-distance transportation, and temperature-controlled housing (Tang et al., 2024).

The density of *B. germanica* population increased during the first half of the 20th century, especially in ports extensively trading with Europe, where it has been inadvertently carried by man (Tang et al., 2019). In the second

half of the 20th and the beginning of the 21st century, climate change and urban expansion have favored the presence of this pest (Bonney et al., 2008). Nowadays, *B. germanica* is the most widespread and cosmopolitan cockroach, found exclusively in areas with human presence and never endemic to natural habitats (Tang et al., 2019).

About its habitat in urban environments, *B. germanica* prefers a warm, moist, dark environment. It is commonly found in kitchens, larders, hotels, restaurants, and hospitals where food, warmth and moisture create the optimal conditions (Cornwell, 1968; Wang et al., 2021).

1.1.1.3. Health problem

Cockroaches are not only a nuisance pest but also have a significant impact on public health. Cockroaches can contaminate food through the mechanical spread of diverse human pathogens, predominantly bacteria such as *Escherichia coli*, *Pseudomonas aeruginosa*, *Klebsiella spp.*, but also fungi and different type of parasites, including hookworms and nematodes, which may cause serious human diseases (Fotedar et al., 1991). Moreover, cockroaches have greater health relevance in allergies, representing one of the most common sources of indoor allergens worldwide, and triggering serious allergic reactions, such as allergic asthma and rhinitis (Sohn & Kim, 2012).

1.1.1.4. Economic impact

Cockroach infestations cause economic losses in many ways, such as the materials and labor cost to treat infestations, wasted food due to its contamination, medical expenses from exposure to allergens, and costs associated with regulatory compliance. The medical problems associated with cockroaches are difficult to estimate because there are no data distinguishing between respiratory diseases caused by cockroach allergies and those caused by other factors (Wang et al., 2021).

In 2024, the market for cockroach control is estimated to be worth \$551.2 million, with a projected annual growth rate of 5% from 2024 to 2031. The economic impact varies by region, with North America being the largest market, having a market size of \$220.48 million in 2024. It is followed by

Europe with a market size of \$165.36 million in 2024. Asia-Pacific ranks third with a market size of \$126.78 million in 2024 (Dharmadhikari, 2024).

1.1.2. *Blattella germanica* as a model insect

The German cockroach is a well-studied insect species, in great measure due to the work of our laboratory since the 1980's (Bellés et al., 2024). This extensive research allows us to closely monitor most of the aspects of the life cycle of our model organism under laboratory conditions. Moreover, the availability of the *B. germanica* genome (Harrison et al., 2018), provide us with the tools to understand the insect not only at the physiological level, but also at the molecular one.

The cockroach *B. germanica* is an hemimetabolous insect, therefore with incomplete metamorphosis, being nymphs similar to adults except for size and the fact that their wings and genitalia are undeveloped. *B. germanica* life cycle consists of three differentiated stages: egg, nymph and adult. Adult females deposit the eggs in a protective structure called ootheca. The ootheca, which is formed by the female and can contain around 30-40 eggs, is externally carried during all embryogenesis until the nymphs emerge (Roth & Willis, 1954). This ootheca is produced at the end of the 7th day or at the beginning of the 8th day of every gonadotrophic cycle, regardless of whether the females were mated or not (Bellés et al., 2024). Under our laboratory conditions (29 °C), adult females produce around five oothecae during their lifetime, the embryogenesis lasts around 18 days, and the postembryonic development, comprising six nymphal stages, lasts between 22 to 24 days. In addition, adult females can live up to 250 days.

1.1.3. Insecticides for pest control

Insecticides are defined as any toxic substance used to eradicate and control insect populations at any life stage. Their usage dates back 4,500 years by Sumerian people, who used sulphur to kill insects and mites, and also 3,200 years ago mercury and arsenic were used by Chinese people to control body lice (Araújo et al., 2023). The use of chemical compounds was followed by botanical preparations, with *Chrysanthemum spp.* as the most relevant due to its active compound, pyrethrin. This compound was effective against various pests, including cockroaches, bedbugs, flies, and mosquitoes (Davies et al., 2007).

Pest control experienced significant advances during mid-19th and early 20th centuries, with the development of the first synthetic chemical insecticides made of organochloride compounds. One of these was the dichlorodiphenyltrichloroethane (DDT), highly effective in eliminating insects, but later banned due to its long-lasting residues that negatively affected the environment and human health (Thuy, 2015). Shortly thereafter, researchers chemically modified natural pyrethrin to create pyrethroids, photodegradable alternatives extensively used to control *B. germanica*. Unfortunately, the widespread use of these insecticides led to the development of resistances (Davies et al., 2007; World Health Organization, 2006).

Neonicotinoids emerged as an alternative, with imidacloprid becoming the most used insecticide worldwide from 1999 to 2018 (Ihara & Matsuda, 2018). Two neonicotinoids, imidacloprid and dinotefuran, were extensively employed to control *B. germanica* (World Health Organization, 2006). However, in 2018, the European Union banned the outdoor use of imidacloprid, together with other neonicotinoids, due to their negative impact on bees. However, its indoor application, such as for controlling *B. germanica*, remains permitted (Blacqui re et al., 2012; Regulation 2018/783). Currently, besides neonicotinoids, the other two most used insecticides are organophosphates and carbamates (Ara jo et al., 2023).

In recent years, there has been a significantly increase in the use of biorational insecticides, which have a minimal impact in the environment and non-target organisms. These insecticides can be divided into three main categories: juvenile hormone analogues, chitin synthesis inhibitors, and sexual pheromones. Juvenile hormone (JH) analogues and chitin synthesis inhibitors are insect growth regulators (IGRs); the first one induces a biological effect similar to natural JH, inhibiting metamorphosis, while the second one impairs exoskeleton formation, preventing molting. Unlike IGRs, sexual pheromones do not directly cause insect mortality; instead, sexual pheromones are used to attract insects to traps or confuse them to prevent mating (Bell s, 1988). IGRs are commonly used for *B. germanica* control, such as pyriproxyfen and hydroprene (JH analogs), or flufenoxuron (chitin synthesis inhibitor) but, because IGRs are relatively slow acting, they are generally used in combination with a fast-acting insecticide (Koehler & Patterson, 1991; Kramer et al., 1990; Reid et al., 1992).

Currently, biopesticides, a less explored type of insecticides, have gained attention to control *B. germanica*. Biopesticides are focused on the use of entomopathogenic bacteria, fungi, viruses, nematodes, and natural enemies (including parasitoids and predators), to cause infections to *B. germanica* leading to its death; and plant-derived substances, including alkaloids, flavonoids, and plant essential oils, that can control this pest by contact toxicity, stomach toxicity, repellent effects, and also interfering in insect development (Pan & Zhang, 2020).

1.1.3.1. Disadvantages of common insecticides

Chemical insecticides have been and continue to be essential for controlling *B. germanica*, thereby reducing its associated health problems and economic costs. However, their usage causes some relevant disadvantages (Tang et al., 2019).

One of these disadvantages is the appearance of resistances in the insects, which are transmitted to the descendants, causing those highly effective insecticides were converted in innocuous in a short time in certain insect populations. Nowadays, *B. germanica* has been reported worldwide to have developed resistance at least to 45 insecticide active ingredients (Mota-Sanchez & Wise, 2024). These resistances appeared due to the massive use of carbamates, organochlorines, organophosphates and pyrethroids to control this pest, exerting selective pressure. Moreover, *B. germanica* lives in relatively closed populations, which facilitates rapid selection of the high-level resistances (Tang et al., 2019). The insecticide resistance mechanisms documented in *B. germanica* are: enzymatic detoxification, target site insensitivity, reduced cuticular penetration and behavioral aversion (Fardisi et al., 2019).

Another negative consequence of certain synthetic chemical insecticides was their low selectivity, affecting non-target organisms, and introducing ecological disequilibrium and the appearance of new pests. Additionally, the use of insecticides can cause environmental contamination, affecting the health of humans and other species (Bellés, 1988).

1.1.3.2. Current pest management strategies

Initially, the insecticides targeting *B. germanica* were used in an indiscriminate manner, without considering the appropriate dosages or potential consequences for human health, the environment, and non-target organisms. Nowadays, pest management of *B. germanica* is commonly based on Integrated Pest Management (IPM) approaches aiming to control the pest while guarding human health and the environment (Brader, 1979). For *B. germanica* control, IPM incorporates strategies such as education, sanitation, trapping, vacuuming, and sealing of harborages, with pesticides applied when needed. Moreover, IPM strategies focus on the reduction of the use of insecticides, low toxicity products, and prioritizing baits than spray formulations (Dingha et al., 2016).

The use of sprays to control *B. germanica* populations started to be replaced in the mid-1980s by insecticide baits. This new application method minimizes the development of resistances compared to sprays, as cockroaches receive a lethal dose of the insecticide from their first consumption. This is not the case with spray insecticides, which often result in exposure to sublethal doses (Khoobdel et al., 2022). However, resistances using baits were also observed, being behavior aversion one of the most relevant ones. Baits often contain feeding stimulants such as D-glucose to attract cockroaches, but the aversion to these compounds can result in the failure of these baits (Wada-Katsumata et al., 2013). To prevent resistances, it is recommended to rotate between different products or use mixture products with multiple modes of action, rather than using a single active ingredient with a single mode of action (Fardisi et al., 2019).

1.1.3.3. New pest management strategies based on nucleic acid molecules

Recent advances in genomic and genetic technologies have facilitated the development of alternative urban pest management strategies, such as the ones based on the use of nucleic acid molecules (Pan & Zhang, 2020). The most common strategy is based on RNA interference, that contrary to conventional insecticides, have a specific sequence-dependent mode of action, providing a high species-selectivity, and its active ingredient, based on RNA, has a short environmental lifespan, minimizing ecological impact (Bachman et al., 2020; Christiaens et al., 2020). The successful

effectiveness of the RNA interference (RNAi) mechanism in controlling insect pests has led to the exploration of other nucleic acid-based molecules more cost-effective, such as antisense oligonucleotides (ASOs) (Oberemok et al., 2018).

1.1.3.3.1. RNA interference (RNAi)

RNAi is a highly evolutionary conserved cellular mechanism that regulates gene expression throughout all eukaryotes (Hannon, 2002). It is a post-transcriptional gene-silencing mechanism that operates in sequence-specific manner, using small RNA molecules together with different effector proteins to inhibit or degrade complementary RNAs. Three RNA interference pathways were described in eukaryotic organisms which are mediated by small interfering RNA (siRNA), microRNA (miRNA), and piwi-interacting RNA (piRNA), respectively (Cooper et al., 2019). Each pathway is thought to have evolved to play a distinct role; the miRNA pathway is involved in internal gene regulation, the piRNA pathway protects the genome against transposons and the siRNA pathway regulates gene expression and protects the cells against both exogenous and endogenous genetic elements (viruses and transposable elements) (Obbard et al., 2009).

The siRNA pathway was first discovered in the nematode *Caenorhabditis elegans* by the introduction of target gene-specific double-stranded RNA (dsRNA) (Fire et al., 1998). Since its discovery, RNAi has rapidly evolved into a powerful genetic tool for studying gene function, regulation, and interaction at both cellular and organismal levels (Bellés, 2010). The siRNA pathway is exploited by experimentally introducing exogenous dsRNA into the cells to silence specific genes (Figure 1.2). Once inside, this long dsRNA is subsequently cut into siRNA duplexes typically ranging from 19-22 bp by the RNase III endonuclease Dicer 2 (Dcr2) (Cooper et al., 2019; Montañés et al., 2021). Then, Dcr2 assisted by dsRNA-binding proteins such as R2D2, transfers the siRNA duplex onto the RNA-induced silencing complex (RISC), which comprises various protein components, among them the endonuclease Argonaute 2 (Ago2). The passenger strand of siRNA is then cut and eliminated, and the guide strand directs RISC to the mRNA region complementary to the guide siRNA. The guide siRNA complements by Watson-Crick base pairing to the target mRNA, leading to its

degradation by Ago2, resulting in post-transcriptional gene silencing (Figure 1.2) (Cooper et al., 2019).

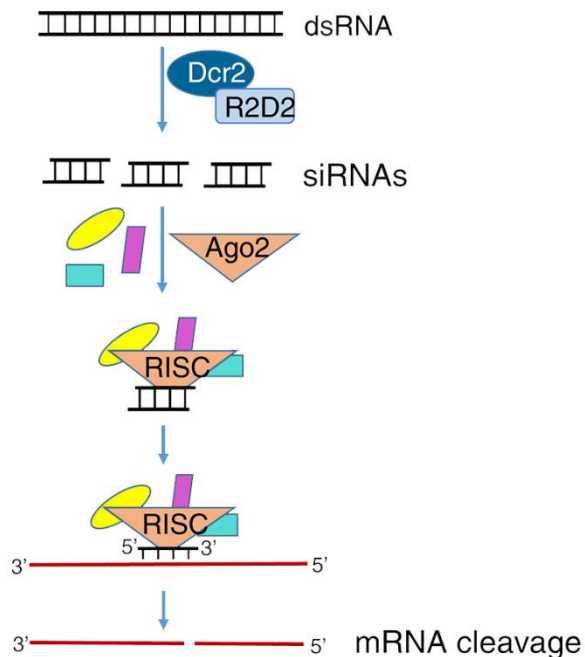


Figure 1.2. The exogenous small interfering RNA (siRNA) pathway in eukaryotes. Exogenous dsRNA targeting a specific gene is internalized inside the cytoplasm of the cells. dsRNA is cut by the RNase III endonuclease Dicer 2 (Dcr2) into siRNAs typically of 19-22 bp. Dcr2, assisted by R2D2, loads the siRNA onto the RNA-induced silencing complex (RISC), which includes various protein components and Argonaute 2 (Ago2). RISC keeps the guide strand of the siRNA to find the complementary mRNA. Ago2 then degrades this target mRNA, resulting in post-transcriptional gene silencing. Modified from Cooper et al. (2019).

Before the RNAi breakthrough, most molecular and genetic research in insects was conducted in just a few model species, such as the fruit fly *Drosophila melanogaster* (Meigen, 1830) (Diptera: Drosophilidae) and the red flour beetle *Tribolium castaneum* (Herbst, 1797) (Coleoptera: Tenebrionidae) because of their low cost, rapid generation time and well-established genetic tools. RNAi discovery has led to a revolution in insect molecular biology research, since it facilitated the expansion of reverse functional genomics studies in non-model species, where obtaining stable

mutants was more challenging (Bellés, 2010; Christiaens et al., 2020). Reverse functional genomics, whereby the gene is chosen first and its function studied later, had evolved thanks to genome and transcriptome sequencing that had broadly increased the number of genes and mRNAs available in insect species (Zhu & Palli, 2020). RNAi plays a decisive role in deciphering the function of the genes identified through sequencing.

During the last decade, RNAi not only has generated interest in the field of reverse functional genomics but has also garnered attention for pest protection, essentially to protect crops. RNAi strategy for pest management involves, in the case of siRNA pathway, the designing of dsRNA sequences targeting essential genes of the pest insect, silencing those genes and finally, leading the animal to death. For functional genomics, RNAi methodology consists in most of the cases, in the injection of dsRNA into the abdomen of the insect, a procedure not suitable for field applications. To achieve effective pest control, the organism should be able to autonomously uptake the dsRNA, either through feeding or direct contact (Bonina & Arpaia, 2023).

Nowadays, only two RNAi-based products are commercially available to control agricultural pests, with none yet developed for urban pest control. The first RNAi-based product, named SmartStax[®], was developed by Monsanto (now Bayer Crop Science) and launched into the market in 2009. SmartStax[®] consists of a transgenic corn crop that expresses a hairpin dsRNA targeting the *Snf7* gene of the Western corn rootworm *Diabrotica virgifera virgifera* (LeConte, 1868) (Coleoptera: Chrysomelidae), together with *Bacillus thuringiensis* Cry proteins to delay the evolution of resistance (Bayer Crop Science, 2022). Furthermore, in 2023, Calantha[™], a foliar RNAi-based insecticide, was launched by GreenLight Biosciences to act against the Colorado potato beetle *Leptinotarsa decemlineata* (Say, 1824) (Coleoptera: Chrysomelidae) (GreenLight Biosciences, 2024). Although only these two products are currently available, others are undergoing regulatory approval or are in development.

1.2. Objectives

The general objective of the present thesis was the design of an oral insecticide against the cockroach *B. germanica* using RNAi methodologies, allowing to reduce the harmful consequences of synthetic chemical insecticides. To fulfill this main objective, we followed these specific objectives:

1. Evaluate essential genes for *B. germanica* and select the best candidate for RNAi experiments.
2. Study the selected candidate gene function in *B. germanica* oogenesis.
3. Find an effective oral delivery method that preserves the stability of the dsRNA as it passes through the gut.
4. Test antisense oligonucleotides as an alternative to RNAi to manage *B. germanica* pest.

1.3. Bibliography

- Araújo, M. F., Castanheira, E. M. S., & Sousa, S. F. (2023). The Buzz on Insecticides: A Review of Uses, Molecular Structures, Targets, Adverse Effects, and Alternatives. *Molecules*, 28, 3641. <https://doi.org/10.3390/molecules28083641>
- Bachman, P., Fischer, J., Song, Z., Urbanczyk-Wochniak, E., & Watson, G. (2020). Environmental Fate and Dissipation of Applied dsRNA in Soil, Aquatic Systems, and Plants. *Frontiers in Plant Science*, 11(21). <https://doi.org/10.3389/fpls.2020.00021>
- Bayer Crop Science. (2022). *SmartStax[®] PRO with RNAi Technology*. <https://www.cropscience.bayer.us/traits/corn/smartstax-pro>
- Bellés, X. (1988). *Insecticidas biorracionales*. Consejo Superior de Investigaciones Científicas.
- Bellés, X. (2010). Beyond *Drosophila*: RNAi *in vivo* and functional genomics in insects. *Annual Review of Entomology*, 55, 111–128. <https://doi.org/10.1146/annurev-ento-112408-085301>
- Bellés, X., Maestro, J. L., & Piulachs, M. D. (2024). The German cockroach as a model in insect development and reproduction in an endocrine context. *Advances in Insect Physiology*, 66, 1–47.

- <https://doi.org/https://doi.org/10.1016/bs.aiip.2024.03.001>
- Blacquièrè, T., Smagghe, G., van Gestel, C. A. M., & Mommaerts, V. (2012). Neonicotinoids in bees: A review on concentrations, side-effects and risk assessment. *Ecotoxicology*, *21*, 973–992. <https://doi.org/10.1007/s10646-012-0863-x>
- Bonina, V., & Arpaia, S. (2023). The use of RNA interference for the management of arthropod pests in livestock farms. *Medical and Veterinary Entomology*, *37*, 631–646. <https://doi.org/10.1111/mve.12677>
- Bonnefoy, X., Kampen, H., Sweeney, K., & World Health Organization. (2008). *Public health significance of urban pests*. WHO Regional Office for Europe. <https://iris.who.int/handle/10665/107363>
- Brader, L. (1979). Integrated Pest Control in the Developing World. *Annual Review of Entomology*, *24*, 225–254. <https://doi.org/10.1146/annurev.en.24.010179.001301>
- Christiaens, O., Niu, J., & Taning, C. N. T. (2020). RNAi in insects: A revolution in fundamental research and pest control applications. *Insects*, *11*(7), 415. <https://doi.org/10.3390/insects11070415>
- Cooper, A. M. W., Silver, K., Zhang, J., Park, Y., & Zhu, K. Y. (2019). Molecular mechanisms influencing efficiency of RNA interference in insects. *Pest Management Science*, *75*(1), 18–28. <https://doi.org/10.1002/ps.5126>
- Cornwell, P. B. (1968). *The cockroach: A laboratory insect and an industrial pest*. Hutchinson.
- Davies, T. G. E., Field, L. M., Usherwood, P. N. R., & Williamson, M. S. (2007). DDT, pyrethrins, pyrethroids and insect sodium channels. *IUBMB Life*, *59*(3), 151–162. <https://doi.org/10.1080/15216540701352042>
- Dharmadhikari, S. (2024). *Cockroach Control Market Report 2024*. <https://www.cognitivemarketresearch.com/cockroach-control-market-report>
- Dingha, B. N., O’Neal, J., Appel, A. G., & Jackai, L. E. N. (2016). Integrated Pest Management of the German Cockroach (Blattodea: Blattellidae) in Manufactured Homes in Rural North Carolina. *Florida Entomologist*, *99*(4), 587–592. <https://doi.org/10.1653/024.099.0401>
- Regulation 2018/783. *Regulation (EU) 2018/783 of 29 May 2018 Amending Implementing Regulation (EU) No 540/2011 as Regards the Conditions of Approval of the Active Substance Imidacloprid*.

- https://eur-lex.europa.eu/eli/reg_impl/2018/783/oj
- Fardisi, M., Gondhalekar, A. D., Ashbrook, A. R., & Scharf, M. E. (2019). Rapid evolutionary responses to insecticide resistance management interventions by the German cockroach (*Blattella germanica* L.). *Scientific Reports*, 9, 8292. <https://doi.org/10.1038/s41598-019-44296-y>
- Fire, A., Xu, S., Montgomery, M. K., Kostas, S. A., Driver, S. E., & Mello, C. C. (1998). Potent and specific genetic interference by double-stranded RNA in *Caenorhabditis elegans*. *Nature*, 391, 806–811. <https://www.nature.com/articles/35888.pdf>
- Fotedar, R., Shriniwas, U. B., & Verma, A. (1991). Cockroaches (*Blattella germanica*) as carriers of microorganisms of medical importance in hospitals. *Epidemiology & Infection*, 107(1), 181–187. <https://doi.org/10.1017/S0950268800048809>
- GreenLight Biosciencies. (2024). *Introducing Calantha™*. <https://calanthaag.com/>
- Grimaldi, D., & Engel, M. S. (2005). *Evolution of the insects*. Cambridge University Press.
- Hannon, G. J. (2002). RNA interference. *Nature*, 418, 244–251. <https://doi.org/10.4155/9781909453432.EBO.13.318>
- Harrison, M. C., Jongepier, E., Robertson, H. M., Arning, N., Bitard-feildel, T., Chao, H., Childers, C. P., Dinh, H., Dugan, S., Gowin, J., Greiner, C., Han, Y., Hughes, D. S. T., Huylmans, A., Kemena, C., Kremer, L. P. M., Lee, S. L., Lopez-ezquerria, A., Mallet, L., ... Bornberg-bauer, E. (2018). Hemimetabolous genomes reveal molecular basis of termite eusociality. *Nature Ecology & Evolution*, 2, 557–566. <https://doi.org/10.1038/s41559-017-0459-1>
- Hill, D. S. (1997). Pest Definitions. In *The Economic Importance of Insects*. Springer. https://doi.org/10.1007/978-94-011-5348-5_3
- Ihara, M., & Matsuda, K. (2018). Neonicotinoids: molecular mechanisms of action, insights into resistance and impact on pollinators. *Current Opinion in Insect Science*, 30, 86–92. <https://doi.org/10.1016/j.cois.2018.09.009>
- Khoobdel, M., Dehghan, H., Oshaghi, M. A., Saman, E. A. G., Asadi, A., & Yusuf, M. A. (2022). The different aspects of attractive toxic baits containing fipronil for control of the German cockroach (*Blattella germanica*). *Environmental Analysis Health and Toxicology*, 37(4), e2022032. <https://doi.org/10.5620/eaht.2022032>
- Koehler, P. G., & Patterson, R. S. (1991). Incorporation of pyriproxyfen in

- a German cockroach (Dictyoptera: Blattellidae) management program. *Journal of Economic Entomology*, 84(3), 917–921. <https://doi.org/10.1093/jee/84.3.917>
- Kramer, R. D., Koehler, P. G., & Patterson, R. S. (1990). Effects of hydroprene exposure on the physiology and insecticide susceptibility of German cockroaches (Orthoptera: Blattellidae). *Journal of Economic Entomology*, 83(6), 2310–2316. <https://doi.org/10.1093/jee/83.6.2310>
- Montañés, J. C., Rojano, C., Ylla, G., Piulachs, M. D., & Maestro, J. L. (2021). siRNA enrichment in Argonaute 2-depleted *Blattella germanica*. *Biochimica et Biophysica Acta - Gene Regulatory Mechanisms*, 1864(6–7), 194704. <https://doi.org/10.1016/j.bbagr.2021.194704>
- Mota-Sanchez, D., & Wise, J. (2024). *Arthropods Resistant to Pesticides Database (ARPD)*. <https://www.pesticideresistance.org/>
- Mukha, D., Wiegmann, B. M., & Schal, C. (2002). Evolution and phylogenetic information content of the ribosomal DNA repeat unit in the Blattodea (Insecta). *Insect Biochemistry and Molecular Biology*, 32(9), 951–960. [https://doi.org/10.1016/S0965-1748\(01\)00164-3](https://doi.org/10.1016/S0965-1748(01)00164-3)
- Obbard, D. J., Gordon, K. H. J., Buck, A. H., & Jiggins, F. M. (2009). The evolution of RNAi as a defence against viruses and transposable elements. *Philosophical Transactions of the Royal Society B*, 364(1513), 99–115. <https://doi.org/10.1098/rstb.2008.0168>
- Oberemok, V. V., Laikova, K. V., Repetskaya, A. I., Kenyo, I. M., Gorlov, M. V., Kasich, I. N., Krasnodubets, A. M., Gal'chinsky, N. V., Fomochkina, I. I., Zaitsev, A. S., Bekirova, V. V., Seidosmanova, E. E., Dydik, K. I., Meshcheryakova, A. O., Nazarov, S. A., Smagliy, N. N., Chelengerova, E. L., Kulanova, A. A., Deri, K., ... Kubyshkin, A. V. (2018). A half-century history of applications of antisense oligonucleotides in medicine, agriculture and forestry: we should continue the journey. *Molecules*, 23(6), 1302. <https://doi.org/10.3390/molecules23061302>
- Pan, X. Y., & Zhang, F. (2020). Advances in biological control of the German cockroach, *Blattella germanica* (L.). *Biological Control*, 142, 104104. <https://doi.org/10.1016/j.biocontrol.2019.104104>
- Reid, B. L., Appel, A. G., Demark, J. J., & Bennett, G. W. (1992). Oral toxicity, formulation effects, and field performance of flufenoxuron against the German cockroach (Dictyoptera: Blattellidae). *Journal of Economic Entomology*, 85(4), 1194–1200.

- <https://doi.org/10.1093/jee/85.4.1194>
- Roth, L. M. (1985). *A taxonomic revision of the genus Blattella Caudell (Dictyoptera, Blattaria: Blattellidae)*. Entomologica Scandinavica Supplement.
- Roth, L. M., & Willis, E. R. (1954). *The Reproduction of Cockroaches*. Smithsonian Miscellaneous Collections.
- Sohn, M. H., & Kim, K. E. (2012). The cockroach and allergic diseases. *Allergy, Asthma and Immunology Research*, 4(5), 264–269. <https://doi.org/10.4168/aaair.2012.4.5.264>
- Tang, Q., Bourguignon, T., Willenmse, L., De Coninck, E., & Evans, T. (2019). Global spread of the German cockroach, *Blattella germanica*. *Biological Invasions*, 21(3), 693–707. <https://doi.org/10.1007/s10530-018-1865-2>
- Tang, Q., Vargo, E. L., Ahmad, I., Jiang, H., Kotyková, Z., Dovih, P., Kim, D., & Bourguignon, T. (2024). Solving the 250-year-old mystery of the origin and global spread of the German cockroach, *Blattella germanica*. *PNAS*, 121(22), e2401185121. <https://doi.org/10.1073/pnas>
- Thuy, T. T. (2015). Effects of DDT on environment and human health. *Journal of Education and Social Sciences*, 2, 108–114.
- Toukhsati, S. R., & Scanes, C. G. (2018). Pest animals. In *Animals and Human Society*. Elsevier. <https://doi.org/10.1016/B978-0-12-805247-1.00022-8>
- Wada-Katsumata, A., Silverman, J., & Schal, C. (2013). Changes in taste neurons support the emergence of an adaptive behavior in cockroaches. *Science*, 340(6135), 972–975. <https://doi.org/10.1126/science.1234854>
- Wang, C., Lee, C., & Rust, M. (2021). German cockroach infestations in the world and their social and economic impacts. In *Biology and Management of the German Cockroach*. CABI.
- World Health Organization. (2006). *Pesticides and their application. For the control of vectors and pests of public health importance*. World Health Organization.
- Zhu, K. Y., & Palli, S. R. (2020). Mechanisms, applications, and challenges of insect RNA interference. *Annual Review of Entomology*, 65, 293–311. <https://doi.org/10.1146/annurev-ento-011019-025224>

2. DEPLETION OF ESSENTIAL GENES IN *Blattella germanica* USING RNA INTERFERENCE

2. DEPLETION OF ESSENTIAL GENES IN *Blattella germanica* USING RNA INTERFERENCE

2.1. Introduction

2.1.1. Selection of essential genes

The possible use of RNA interference (RNAi) for pest control involves the selection of some genes for which the reduction of their mRNA levels will determine the death of the individual. These are considered essential genes, and are the ones indispensable to support cellular life, most of them being highly conserved across species. Knockout (KO) of essential genes using gene editing strategies as CRISPR-Cas9 or downregulation of gene expression by RNAi is lethal for the organism (Rancati et al., 2018). Taking advantage of the small interfering RNA (siRNA) pathway, we selected four essential genes to be depleted based on previous literature about the effectiveness of their reduction in causing mortality in other insect species such as the African sweet potato weevil *Cylas puncticollis* (Boheman, 1833) (Coleoptera: Brentidae) (Prentice et al., 2017) and the southern green stinkbug *Nezara viridula* (Linnaeus, 1758) (Hemiptera: Pentatomidae) (Sharma, Christiaens, et al., 2021). These genes,

[REDACTED]
[REDACTED]

[REDACTED] are associated with distinct biological processes, essential for the organism.

[REDACTED]
[REDACTED]
[REDACTED]
[REDACTED]
[REDACTED]
[REDACTED]
[REDACTED]
[REDACTED]
[REDACTED]
[REDACTED]
[REDACTED]
[REDACTED]
[REDACTED]
[REDACTED]

Several scientific papers were published demonstrating insect mortality after feeding double-stranded RNA (dsRNA) against [REDACTED]

[REDACTED]

[REDACTED] From all these data, we considered these four genes as interesting target genes to be tested in *Blattella germanica* as plausible candidates to control this pest.

[REDACTED]

2.2. Materials and methods

2.2.1. Cockroach colony and tissues sampling

Specimens of the cockroach *B. germanica* were obtained from a colony fed on dog chow and water *ad libitum*, kept in the dark at 29 ± 1 °C and 60-70% relative humidity. Dissections were performed under Ringer's saline on carbon dioxide-anaesthetized specimens. After dissection, tissue samples were immediately frozen in liquid nitrogen and stored at -80 °C.

2.2.2. RNA extraction, cDNA synthesis and quantitative real-time PCR analysis

Total RNA from midgut, fat body, *corpora cardiaca-corpora allata* (CC-CA) and ovaries was extracted using HigherPurity™ Tissue Total RNA Purification kit (Canvax Biotech S.L.). The extracted RNA was treated with DNase (Thermo Fisher Scientific) and then retrotranscribed to cDNA using the Transcriptor First Strand cDNA Synthesis kit (Roche Diagnostics GmbH), following the manufacturer's instructions. The absence of genomic contamination was confirmed using a control without reverse transcription. The quantity of RNA retrotranscribed varied in each experiment, but comparisons were made between samples with the same amount of retrotranscribed RNA.

The expression levels of the different genes studied were analyzed by quantitative real-time PCR (qRT-PCR) using cDNA from tissues of 5-day-old adult females. Amplification reactions were carried out in a CFX Opus 384 Real-Time PCR System (BioRad) using the iTaq Universal SYBR Green Supermix (BioRad) following this program: (i) 95 °C for 3 min, (ii) 95 °C for 10 s; (iii) 57 °C for 1 min; (iv) steps (ii) and (iii) were repeated for 44 cycles. After the amplification phase, a dissociation curve was carried out to ensure that there was only one product amplified. Levels of mRNA were calculated relative to the reference gene, using the $2^{-\Delta Ct}$ method (Alborzi & Piulachs, 2023; Irls et al., 2009; Livak & Schmittgen, 2001). The PCR primers used in qRT-PCR expression studies were designed using the Primer3 v.4.1.0 software (Rozen & Skaletsky, 2000). The expression levels of *actin-5c*, [REDACTED] *Eukaryotic translation Initiation Factor 4aIII* (*eIF4aIII*), *juvenile hormone acid O-methyltransferase* (*jhamt*), [REDACTED] and *vitellogenin* (*Vg*) were quantified from 3 to 6 independent biological samples, making three technical replicates of each one, in a 10 µL of final volume. A control without template was included in all batches. *eIF4aIII* was used as reference gene. The sequence of the primers used, and the accession number of genes analyzed are detailed in Table S1 (See Annexes).

2.2.3. dsRNA synthesis and RNAi experiments by injection

To deplete the expression of essential genes, a dsRNA against each gene was designed [REDACTED]

[REDACTED] Furthermore, a heterologous 441 bp fragment from the Polyhedrin of the *Autographa californica* nucleopolyhedrovirus was used as negative control (dsPolyH) (Lozano & Bellés, 2011).

For dsRNA synthesis, RNA was extracted from *B. germanica* midgut using HigherPurity™ Tissue Total RNA Purification kit (Canvax Biotech S.L.) and then 1 µg was retrotranscribed to cDNA using the Transcriptor First Strand cDNA Synthesis kit (Roche Diagnostics GmbH), following the manufacturer's instructions. Then, cDNA was amplified by PCR using the specific primers. The PCR products were analyzed by agarose gel electrophoresis, cloned into the pSTBlue™-1 vector (Novagen), and then sequenced. Once obtained the sequences, dsRNAs were synthesized using MEGAscript™ RNAi kit (Invitrogen, Thermo Fisher Scientific), following manufacturer's instructions and stored at -20 °C until use. The sequence of the primers used is detailed in Table S1 (See Annexes).

For RNAi experiments, dsRNA was injected at a dose of 1 µg (1 µg/µL) into the abdomen of freshly emerged last (sixth)-instar female nymphs (N6D0) or newly emerged adult females (AdD0), using a 5 µL Hamilton® 75N microsyringe. Insects were kept in groups of 5-6 individuals which were monitored every day.

2.2.4. Statistical analysis

All data were expressed as mean ± standard error of the mean (S.E.M.). Data were evaluated for normality and homogeneity of variance using the Shapiro-Wilk test, which showed that no transformations were needed. All datasets passed normality test. Statistical analyses for mean comparison were performed employing Student's *t*-test. A *p* value < 0.05 was

considered statistically significant. Data were analyzed using GraphPad Prism version 8.1.0 for Windows, GraphPad Software.

For Kaplan-Meier (K-M) survival analysis, we used SPSS version 22 as statistical software. K-M survival curves illustrate the rate of survival after performing the different dsRNA treatments. We ran a log-rank test to explore overall differences among treatments, followed by pairwise comparisons to determine differences between specific pairs of treatments.

2.3. Results

[REDACTED]

[REDACTED]

[REDACTED]

[REDACTED]



2.5. Bibliography

- Alborzi, Z., & Piulachs, M. D. (2023). Dual function of the transcription factor Ftz-f1 on oviposition in the cockroach *Blattella germanica*. *Insect Molecular Biology*, 32(6), 689–702. <https://doi.org/10.1111/imb.12866>
- Amerik, A. Y., Nowak, J., Swaminathan, S., & Hochstrasser, M. (2000). The Doa4 deubiquitinating enzyme is functionally linked to the vacuolar protein-sorting and endocytic pathways. *Molecular Biology of the Cell*, 11(10), 3365–3380. <https://doi.org/10.1091/mbc.11.10.3365>
- Baum, J. A., Bogaert, T., Clinton, W., Heck, G. R., Feldmann, P., Ilagan, O., Johnson, S., Plaetinck, G., Munyikwa, T., Pleau, M., Vaughn, T., & Roberts, J. (2007). Control of coleopteran insect pests through RNA interference. *Nature Biotechnology*, 25, 1322–1326. <https://doi.org/10.1038/nbt1359>
- Beck, R., Ravet, M., Wieland, F. T., & Cassel, D. (2009). The COPI system: Molecular mechanisms and function. *FEBS Letters*, 583(17), 2701–2709. <https://doi.org/10.1016/j.febslet.2009.07.032>
- Bellés, X., Casas, J., Messeguer, A., & Piulachs, M. D. (1987). *In vitro* biosynthesis of JH III by the corpora allata of adult females of *Blattella germanica* (L). *Insect Biochemistry*, 17(7), 1007–1010. [https://doi.org/10.1016/0020-1790\(87\)90111-9](https://doi.org/10.1016/0020-1790(87)90111-9)

- Buysse, D., Pfitzner, A. K., West, M., Roux, A., & Odorizzi, G. (2020). The ubiquitin hydrolase Doa4 directly binds Snf7 to inhibit recruitment of ESCRT-III remodeling factors in *S. cerevisiae*. *Journal of Cell Science*, *133*(8), jcs241455. <https://doi.org/10.1242/jcs.241455>
- Carlton, J. G., & Martin-Serrano, J. (2007). Parallels between cytokinesis and retroviral budding: A role for the ESCRT machinery. *Science*, *316*(5833), 1908–1912. <https://doi.org/10.1126/science.1143422>
- Castellanos, N. L., Smagghe, G., Sharma, R., Oliveira, E. E., & Christiaens, O. (2019). Liposome encapsulation and EDTA formulation of dsRNA targeting essential genes increase oral RNAi-caused mortality in the Neotropical stink bug *Euschistus heros*. *Pest Management Science*, *75*(2), 537–548. <https://doi.org/10.1002/ps.5167>
- Comas, D., Piulachs, M. D., & Bellés, X. (1999). Fast induction of vitellogenin gene expression by juvenile hormone III in the cockroach *Blattella germanica* (L.) (Dictyoptera, Blattellidae). *Insect Biochemistry and Molecular Biology*, *29*(9), 821–827. [https://doi.org/10.1016/S0965-1748\(99\)00058-2](https://doi.org/10.1016/S0965-1748(99)00058-2)
- Dhandapani, R. K., Duan, J. J., & Palli, S. R. (2020). Orally delivered dsRNA induces knockdown of target genes and mortality in the Asian long-horned beetle, *Anoplophora glabripennis*. *Archives of Insect Biochemistry and Physiology*, *104*(4), e21679. <https://doi.org/10.1002/arch.21679>
- Dominguez, C. V., & Maestro, J. L. (2018). Expression of juvenile hormone acid O-methyltransferase and juvenile hormone synthesis in *Blattella germanica*. *Insect Science*, *25*(5), 787–796. <https://doi.org/10.1111/1744-7917.12467>
- Goodman, W. G., & Cusson, M. (2012). The juvenile hormones. In Gilbert L.I. (Ed.), *Insect Endocrinology* (pp. 310–365). American Press.
- Gurusamy, D., Howell, J. L., Cherreddy, S. C. R. R., Mogilicherla, K., & Palli, S. R. (2021). Improving RNA interference in the southern green stink bug, *Nezara viridula*. *Journal of Pest Science*, *94*, 1461–1472. <https://doi.org/10.1007/s10340-021-01358-3>
- Huvenne, H., & Smagghe, G. (2010). Mechanisms of dsRNA uptake in insects and potential of RNAi for pest control: A review. *Journal of Insect Physiology*, *56*(3), 227–235. <https://doi.org/10.1016/j.jinsphys.2009.10.004>
- Irls, P., Bellés, X., & Piulachs, M. D. (2009). Identifying genes related to choriogenesis in insect panoistic ovaries by Suppression Subtractive Hybridization. *BMC Genomics*, *10*, 206.

- <https://doi.org/10.1186/1471-2164-10-206>
- Irlles, P., & Piulachs, M. D. (2014). Unlike in *Drosophila* meroistic ovaries, Hippo represses Notch in *Blattella germanica* panoistic ovaries, triggering the mitosis-endocycle switch in the follicular cells. *PLOS ONE*, 9(11), e113850. <https://doi.org/10.1371/journal.pone.0113850>
- Johnson, N., West, M., & Odorizzi, G. (2017). Regulation of yeast ESCRT-III membrane scission activity by the Doa4 ubiquitin hydrolase. *Molecular Biology of the Cell*, 28(5), 661–672. <https://doi.org/10.1091/mbc.E16-11-0761>
- Katzmann, D. J., Odorizzi, G., & Emr, S. D. (2002). Receptor downregulation and multivesicular-body sorting. *Nature Reviews Molecular Cell Biology*, 3, 893–905. <https://doi.org/10.1038/nrm973>
- Koči, J., Ramaseshadri, P., Bolognesi, R., Segers, G., Flannagan, R., & Park, Y. (2014). Ultrastructural changes caused by Snf7 RNAi in larval enterocytes of western corn rootworm (*Diabrotica virgifera virgifera* Le Conte). *PLOS ONE*, 9(1), e83985. <https://doi.org/10.1371/journal.pone.0083985>
- Komander, D., Clague, M. J., & Urbé, S. (2009). Breaking the chains: Structure and function of the deubiquitinases. *Nature Reviews Molecular Cell Biology*, 10, 550–563. <https://doi.org/10.1038/nrm2731>
- Livak, K. J., & Schmittgen, T. D. (2001). Analysis of relative gene expression data using real-time quantitative PCR and the $2^{-\Delta\Delta CT}$ method. *Methods*, 25(4), 402–408. <https://doi.org/10.1006/meth.2001.1262>
- Low, P., Varga, Á., Pircs, K., Nagy, P., Szatmári, Z., Sass, M., & Juhász, G. (2013). Impaired proteasomal degradation enhances autophagy via hypoxia signaling in *Drosophila*. *BMC Cell Biology*, 14, 29. <https://doi.org/10.1186/1471-2121-14-29>
- Lozano, J., & Bellés, X. (2011). Conserved repressive function of Krüppel homolog 1 on insect metamorphosis in hemimetabolous and holometabolous species. *Scientific Reports*, 1, 163. <https://doi.org/10.1038/srep00163>
- Lü, J., Liu, Z., Guo, W., Guo, M., Chen, S., Li, H., Yang, C., Zhang, Y., & Pan, H. (2020). Feeding delivery of dsHvSnf7 is a promising method for management of the pest *Henosepilachna vigintioctopunctata* (Coleoptera: Coccinellidae). *Insects*, 11(1), 34. <https://doi.org/10.3390/insects11010034>
- Martín, D., Piulachs, M. D., Comas, D., & Bellés, X. (1998). Isolation and

- sequence of a partial vitellogenin cDNA from the cockroach, *Blattella germanica* (L.) (dictyoptera, blattellidae), and characterization of the vitellogenin gene expression. *Archives of Insect Biochemistry and Physiology*, 38(3), 137–146. [https://doi.org/10.1002/\(SICI\)1520-6327\(1998\)38:3<137::AID-ARCH4>3.0.CO;2-P](https://doi.org/10.1002/(SICI)1520-6327(1998)38:3<137::AID-ARCH4>3.0.CO;2-P)
- Nandi, D., Tahiliani, P., Kumar, A., & Chandu, D. (2006). The ubiquitin-proteasome system. *Journal of Biosciences*, 31, 137–155. <https://doi.org/https://doi.org/10.1007/BF02705243>
- Pinheiro, D. H., Taylor, C. E., Wu, K., & Siegfried, B. D. (2020). Delivery of gene-specific dsRNA by microinjection and feeding induces RNAi response in Sri Lanka weevil, *Mylocherus undecimpustulatus undatus* Marshall. *Pest Management Science*, 76(3), 936–943. <https://doi.org/10.1002/ps.5601>
- Prentice, K., Christiaens, O., Pertry, I., Bailey, A., Niblett, C., Ghislain, M., Gheysen, G., & Smagghe, G. (2017). RNAi-based gene silencing through dsRNA injection or ingestion against the African sweet potato weevil *Cylas puncticollis* (Coleoptera: Brentidae). *Pest Management Science*, 73, 44–52. <https://doi.org/10.1002/ps.4337>
- Ramaseshadri, P., Segers, G., Flannagan, R., Wiggins, E., Clinton, W., Ilagan, O., McNulty, B., Clark, T., & Bolognesi, R. (2013). Physiological and Cellular Responses Caused by RNAi-Mediated Suppression of Snf7 Orthologue in Western Corn Rootworm (*Diabrotica virgifera virgifera*) Larvae. *PLOS ONE*, 8(1), e54270. <https://doi.org/10.1371/journal.pone.0054270>
- Rancati, G., Moffat, J., Typas, A., & Pavelka, N. (2018). Emerging and evolving concepts in gene essentiality. *Nature Reviews Genetics*, 19, 34–49. <https://doi.org/10.1038/nrg.2017.74>
- Rozen, S., & Skaletsky, H. (2000). Primer3 on the WWW for General Users and for Biologist Programmers. In S. Misener & S. A. Krawetz (Eds.), *Bioinformatics Methods and Protocols*. Humana Press. <https://doi.org/10.1385/1-59259-192-2:365>
- Sarmah, N., Kaldis, A., Taning, C. N. T., Perdikis, D., Smagghe, G., & Voloudakis, A. (2021). dsRNA-mediated pest management of *Tuta absoluta* is compatible with its biological control agent *Nesidiocoris tenuis*. *Insects*, 12(4), 274. <https://doi.org/10.3390/insects12040274>
- Sharma, R., Christiaens, O., Taning, C. N. T., & Smagghe, G. (2021). RNAi-mediated mortality in southern green stinkbug *Nezara viridula* by oral delivery of dsRNA. *Pest Management Science*, 77(1), 77–84. <https://doi.org/10.1002/ps.6017>

- Sharma, R., Taning, C. N. T., Smagghe, G., & Christiaens, O. (2021). Silencing of double-stranded ribonuclease improves oral RNAi efficacy in southern green stinkbug *Nezara viridula*. *Insects*, *12*(2), 115. <https://doi.org/10.3390/insects12020115>
- Thakur, N., Upadhyay, S. K., Verma, P. C., Chandrashekar, K., Tuli, R., & Singh, P. K. (2014). Enhanced whitefly resistance in transgenic tobacco plants expressing double stranded RNA of v-ATPase a gene. *PLOS ONE*, *9*(3), e87235. <https://doi.org/10.1371/journal.pone.0087235>
- Vasanthakumar, T., & Rubinstein, J. L. (2020). Structure and Roles of V-type ATPases. *Trends in Biochemical Sciences*, *45*(4), 295–307. <https://doi.org/10.1016/j.tibs.2019.12.007>
- Willow, J., Soonvald, L., Sulg, S., Kaasik, R., Silva, A. I., Taning, C. N. T., Christiaens, O., Smagghe, G., & Veromann, E. (2021a). Anther-Feeding-Induced RNAi in *Brassicogethes aeneus* Larvae. *Frontiers in Agronomy*, *3*, 633120. <https://doi.org/10.3389/fagro.2021.633120>
- Willow, J., Soonvald, L., Sulg, S., Kaasik, R., Silva, A. I., Taning, C. N. T., Christiaens, O., Smagghe, G., & Veromann, E. (2021b). RNAi efficacy is enhanced by chronic dsRNA feeding in pollen beetle. *Communications Biology*, *4*, 444. <https://doi.org/10.1038/s42003-021-01975-9>
- Willow, J., Sulg, S., Taning, C. N. T., Silva, A. I., Christiaens, O., Kaasik, R., Prentice, K., Lövei, G. L., Smagghe, G., & Veromann, E. (2021). Targeting a coatomer protein complex-I gene via RNA interference results in effective lethality in the pollen beetle *Brassicogethes aeneus*. *Journal of Pest Science*, *94*, 703–712. <https://doi.org/10.1007/s10340-020-01288-6>

**3. CHMP4B CONTRIBUTES TO MAINTAINING
THE FOLLICULAR CELLS INTEGRITY IN THE
PANOISTIC OVARY OF THE COCKROACH**
Blattella germanica

3. CHMP4B CONTRIBUTES TO MAINTAINING THE FOLLICULAR CELLS INTEGRITY IN THE PANOISTIC OVARY OF THE COCKROACH *Blattella germanica*

Nuria Farrus¹, José Luis Maestro¹, Maria-Dolors Piulachs¹

¹ Institut de Biologia Evolutiva (CSIC-Universitat Pompeu Fabra),
Barcelona, Spain

Farrus, N., Maestro, J.L. & Piulachs, M.D. (2024)

[CHMP4B contributes to maintaining the follicular cells integrity in the panoistic ovary of the cockroach *Blattella germanica*](#). *Biology of the Cell*, 116(9), e2400010.

<https://doi.org/10.1111/boc.202400010>

Abstract

The Endosomal Sorting Complex Required for Transport (ESCRT) is a highly conserved cellular machinery essential for many cellular functions, including transmembrane protein sorting, endosomal trafficking, and membrane scission. CHMP4B is a key component of ESCRT-III subcomplex and has been thoroughly studied in the meroistic ovaries of *Drosophila melanogaster* showing its relevance in maintaining this reproductive organ during the life of the fly. However, the role of the CHMP4B in the most basal panoistic ovaries remains elusive. Using RNA interference (RNAi), we examined the function of CHMP4B in the ovary of *Blattella germanica* in two different physiological stages: in last instar nymphs, with proliferative follicular cells, and in vitellogenic adults when follicular cells enter in polyploidy and endoreplication.

In *Chmp4b*-depleted specimens, the actin fibers change their distribution, appearing accumulated in the basal pole of the follicular cells, resulting in an excess of actin bundles that surround the basal ovarian follicle and modifying their shape. Depletion of *Chmp4b* also determines an actin accumulation in follicular cell membranes, resulting in different cell morphologies and sizes. In the end, these changes disrupt the opening of intercellular spaces between the follicular cells (patency) impeding the incorporation of yolk proteins to the growing oocyte and resulting in female sterility. In addition, the nuclei of follicular cells appeared unusually elongated, suggesting an incomplete karyokinesis.

These results proved CHMP4B essential in preserving the proper expression of cytoskeleton proteins vital for basal ovarian follicle growth and maturation and for yolk protein incorporation. Moreover, the correct distribution of actin fibers in the basal ovarian follicle emerged as a critical factor for the successful completion of ovulation and oviposition. The overall results, obtained in two different proliferative stages, suggest that the requirement of CHMP4B in *B. germanica* follicular epithelium is not related to the proliferative stage of the tissue.

3.1. Introduction

The Endosomal Sorting Complex Required for Transport, also known as ESCRT, consists of five protein subcomplexes (ESCRT-0, -I, -II, -III, and VPS4, see Christ et al., 2017) highly conserved between yeast, humans, and insects (Li & Blissard, 2015). ESCRT subcomplexes are required for transmembrane protein sorting, endosomal trafficking, membrane remodeling, and membrane scission (Christ et al., 2017). CHMP4B (charged multivesicular body protein 4B) from humans (Peck et al., 2004), the orthologue of Snf7/VPS32 in yeast (Kranz et al., 2001) and of Shrb (Shrb) in *Drosophila melanogaster* (Sweeney et al., 2006), is a key component of ESCRT-III subcomplex. CHMP4B plays a crucial role in membrane protein trafficking and executes membrane scission during processes such as multivesicular body formation and cytokinesis, helping to separate the daughter cells (Carlton & Martin-Serrano, 2007; Christ et al., 2017).

In *D. melanogaster* ovaries, ESCRT complexes are not essential for global oocyte development (Vaccari et al., 2009). However, they are involved in the endosomal arrangement of membrane proteins, including the localization of Notch receptor, which signaling is essential for the development of the follicular cells and oocyte maturation (Klusza & Deng, 2010). Also, Shrb participates in the membrane abscission during cytokinesis of germinal stem cells, where it is recruited at the midbody, the thin intercellular membrane bridge that connects the two daughter cells. The interaction between Shrb and ALiX proteins ensures cytokinesis completion (Christ et al., 2017; Eikenes et al., 2015; Matias et al., 2015; Raiborg & Stenmark, 2009). On the other hand, deubiquitination of Shrb by USP8 prevents Shrb from being recruited to the fusome and allows the formation of germline cysts (Mathieu et al., 2022). Moreover, *D. melanogaster* ESCRT mutants lack the subcortical actin in germinal cells. In general, mutants for any of the ESCRT components show strong defects in actin and plasma membrane organization that can result in multinuclear cells (Vaccari et al., 2009). These actin flaws have led to the proposal that ESCRT complexes could directly regulate the actin cytoskeleton (Sevrioukov et al., 2005; Vaccari et al., 2009). The Shrb function was also analyzed in *D. melanogaster* males. It was observed that depletion of *shrb* mRNA in fly testes determines a significant increase in the expression of

certain cytoskeleton-associated genes. Results pointed to this increase as the responsible factor for the arrest of germ cell development, which led to the accumulation of early gametes that did not reach maturation (Chen et al., 2021).

The study of the function of Shrb in insect ovaries is limited to *D. melanogaster*, a species with a meroistic polytrophic ovary type, where the nurse cells (from germinal lineage) escort the oocytes during the egg chamber development. In the present work, we study the function of Shrb/CHMP4B in a basal ovary type, the panoistic ovary, using as an experimental model the cockroach *Blattella germanica*. The panoistic ovary lacks nurse cells and the oocyte is responsible for synthesizing the RNAs and proteins that will be necessary to determine future embryo development. After leaving the germarium, early differentiated oocytes are surrounded by a monolayer of somatic follicular cells (FC), forming an ovarian follicle (Rumbo et al., 2023; Figure 3.1A). In *B. germanica* oogenesis, only the basal oocyte in each ovariole matures in a gonadotropic cycle. The other ovarian follicles in the ovariole remain arrested in the vitellarium, waiting for the next cycle (Irles & Piulachs, 2014). The basal ovarian follicles (BOFs) become active in the sixth (last) nymphal instar when the oocyte is synthesizing RNAs and proteins that will be necessary for the oocyte to mature and for future embryo development (Elshaer & Piulachs, 2015; Irles & Piulachs, 2014). At the same time, the follicular epithelium in the BOF proliferates actively, producing an adequate number of cells distributed homogeneously to cover the oocyte surface. In 3-day-old adults, coinciding with the increase of juvenile hormone in the hemolymph and the beginning of the vitellogenic period, the follicular epithelium in the BOF reaches the maximum number of cells, changing their program and activating the mitosis-endocycle switch (Irles et al., 2016). In 5-day-old adults, all the FCs are binucleated, become polyploidy, and enter into endoreplication (Irles & Piulachs, 2014; Zhang & Kunkel, 1992). Then, the chorion synthesis starts.

During vitellogenesis, the oocytes in the BOFs take up proteins from the hemolymph to grow exponentially (Bellés et al., 1987). To allow these storage proteins to reach the oocyte membrane, the FCs contract their cytoplasm, leaving large intercellular spaces between them in a process called patency. This process, under juvenile hormone control, was first described in *Rhodnius prolixus* (Stål, 1859) (Hemiptera: Reduviidae)

(Davey, 1981; Davey & Huebner, 1974). Recently, the mechanism behind this process was studied in *D. melanogaster* (Isasti-Sanchez et al., 2021; Riechmann, 2021). According to these studies, the release of tension in the actin-myosin cytoskeleton and the removal of the adhesion proteins that participate in cell junctions determine a change in the number of connections between the FCs, which pass from tricellular junctions to bicellular junctions, leaving spaces between cells (Isasti-Sanchez et al., 2021). At the end of vitellogenesis, the FCs close these spaces, and the gonadotropic cycle ends with the chorion synthesis just before ovulation and oviposition.

B. germanica allow us to study the function of CHMP4B, the orthologue of Shrb (Sweeney et al., 2006), on the FCs in different situations: in the last instar nymphs, when FCs are actively proliferating, increasing their number as the BOF grows, and in adults, when the proliferative stage of FCs finishes, the cells become binucleated and enter into polyploidy and endoreplication. We found that Shrb/CHMP4B in the panoistic ovary of *B. germanica* regulates the actin cytoskeleton and associated genes involved in maintaining the follicular epithelium planar polarity. It is necessary to maintain the right levels of Shrb/CHMP4B in the ovary to correctly execute the changes of the FCs program in the BOF and thus ensure their correct growth.

3.2. Materials and methods

3.2.1. Insects sampling

Specimens of the cockroach *B. germanica* were obtained from a colony fed on dog chow and water *ad libitum*, kept in the dark at 29 ± 1 °C and 60-70% relative humidity. Dissections and ovarian tissue sampling were performed on carbon dioxide-anaesthetized specimens, held under Ringer's saline. After dissection, tissues were immediately frozen in liquid nitrogen and stored at -80 °C.

3.2.2. RNAi experiments

To deplete the expression of *shrb/Chmp4b* (from now *Chmp4b*), a dsRNA (ds*Chmp4b*; 461bp) was designed to target the conserved domain of the

Snf7 superfamily (Figure 3.S1). A heterologous 441 bp fragment from the gene sequence of the *Autographa californica* nucleopolyhedrovirus was used as negative control (dsMock) (Lozano & Bellés, 2011). The dsRNA was synthesized using MEGAscript™ RNAi kit (Invitrogen), following the manufacturer's instructions, and stored at -20 °C until its use. The dsRNA was injected at a dose of 1 µg (1 µg/µL) into the abdomen of freshly emerged last (sixth)-instar female nymphs (N6D0) or newly emerged adult females, using a Hamilton microsyringe (Teknokroma). Sixth nymphal instar ovaries were dissected on day six of the instar. Ovaries from adult individuals were dissected on day 0 or 5 of the first gonadotrophic cycle, depending on the experiment.

3.2.3. RNA extraction, cDNA synthesis, and quantitative real-time PCR analysis

Total RNA from the ovaries was extracted using HigherPurity™ Tissue Total RNA Purification kit (Canvax Biotech S.L.). A total of 500 ng of RNA was then retrotranscribed using the Transcriptor First Strand cDNA Synthesis kit (Roche LifeScience) as previously described (Montañés et al., 2021). The absence of genomic contamination was confirmed using a control without reverse transcription.

The expression levels of the different genes studied were analyzed by quantitative real-time PCR (qRT-PCR) using cDNA from ovaries. The schedule used for the amplifying reaction was as follows: (i) 95 °C for 3 min, (ii) 95 °C for 10 s; (iii) 57 °C for 1 min; (iv) steps (ii) and (iii) were repeated for 44 cycles. The expression of *actin-5c*, *armadillo* (*arm*), *Chmp4b*, *dachsous* (*ds*), *Eukaryotic translation Initiation Factor 4aIII* (*eIF4aIII*), *extracellular serine/threonine protein kinase four-jointed* (*ff*), *frizzled* (*fz*), *kugelei* (*kug*; *fat2* in *D. melanogaster*), *Myosin heavy chain* (*Mhc*) and protocadherin-like wing polarity protein *starry night* (*stan*) were quantified from 3-6 independent biological samples, making three technical replicates of each one, in a 10 µL of final volume. *actin-5c* was used as a reference gene to obtain the expression profile of *Chmp4b* in ovaries, and *eIF4aIII* was used as a reference gene to compare treated and control samples. The sequence of the primers used, and the accession number of genes analyzed are detailed in Table 3.S1.

3.2.4. Quantification of total ovarian proteins

For the quantification of total protein content, control and treated ovaries were homogenized in 0.4 M NaCl using an ultrasonic bath and centrifuged to eliminate cell debris (Martin et al., 1995). The protein concentration in the homogenate was determined with the Bradford's method, using bovine serum albumin as standard (Bradford, 1976).

3.2.5. Tissue staining and immunohistochemistry

Ovaries from 6-day-old last instar nymphs and 0-day- and 5-day-old adults were dissected and immediately fixed in paraformaldehyde (4% in PBS) for 2 h. Washing samples and antibody incubations were performed as previously described (Irls & Piulachs, 2014). The primary antibody employed was rabbit anti-Shrb (a gift from Dr. Thomas Klein; Bäumers et al., 2019) designed against the *D. melanogaster* Shrb. The high similarity between Shrub and CHMP4B from *B. germanica* (Figure 3.S1B) led us to use this antibody to detect CHMP4B in the ovaries of *B. germanica*. The primary antibody was used at dilution 1:50. The secondary antibody used was Alexa-Fluor 488 goat anti-rabbit IgG (Molecular Probes). In addition, ovaries were incubated at room temperature for 20 min in 300 ng/mL phalloidin-TRITC (Sigma) for F-actin staining and then, for 5 min in 1 µg/mL of DAPI (Sigma) for DNA staining. WGA (Sigma) was used to stain membranes (5 min in 1 µg/mL). Ovaries were mounted in Mowiol (Calbiochem) and observed using a Zeiss AxioImager Z1 microscope (Apotome) (Carl Zeiss MicroImaging).

3.2.6. Statistical analysis

All data were expressed as mean \pm standard error of the mean (S.E.M.) from at least three independent experiments. The data were evaluated for normality and homogeneity of variance using the Shapiro-Wilk test, which showed that no transformations were needed. All datasets passed the normality test. Statistical analyses were performed employing a Student's *t*-test. A *p*-value < 0.05 was considered statistically significant. Statistical analyses were performed using GraphPad Prism version 8.1.0 for Windows, GraphPad Software.

3.3. Results

3.3.1. *Chmp4b* expression in the ovaries of *Blattella germanica*

Chmp4b mRNA is highly expressed in ovaries during all the sixth nymphal instar, showing the highest values on the first day of the instar, just after the molt (Figure 3.1B). Then, its expression in ovaries begins to decline reaching the lowest values in 5-day-old nymphs, coinciding with the highest levels of ecdysteroids in the hemolymph. Just before the imaginal molt *Chmp4b* mRNA levels were recovered coinciding with the decrease of ecdysteroids (Figure 3.1B). After the molt to adult, expression of *Chmp4b* mRNA in ovaries quickly decreased until 3-day-old females, when the vitellogenic period started and FCs arrest cytokinesis to become binucleated. These relatively low levels of *Chmp4b* mRNA were maintained stable until the end of the gonadotropic cycle (Figure 3.1B).

Using a heterologous antibody against Shrb of *D. melanogaster* (Bäumers et al., 2019), we localized CHMP4B in the ovaries of *B. germanica* adults. In newly emerged females, labeling for CHMP4B was very faint, and an over-exposition was necessary to see the labeling in the cytoplasm of both, the basal oocyte and FCs from BOF (Figure 3.1C). The labeling, at this age, was absent from the FC nuclei (Figure 3.1D-D''). Later, in 5-day-old adult females, labeling for CHMP4B in ovaries was localized in the nuclei of the FCs from the BOFs (Figure 3.1E-E''), a translocation of the labeling that can be related to the change in the FCs program that occurs at this age. Due to the big oocyte size, we cannot observe the antibody labeling inside the basal oocyte of 5-day-old females.

3.3.2. Effects of *Chmp4b* depletion on the ovary of 5-day-old *Blattella germanica* adults

Chmp4b functions related to oocyte development in *B. germanica* were studied using RNAi. Newly emerged adult females were treated with ds*Chmp4b* or dsMock, and the expression levels of *Chmp4b* were analyzed in ovaries from 5-day-old adults (n = 3, for each treatment). The *Chmp4b* expression was significantly depleted (p < 0.01, Figure 3.2A), reaching a 49% reduction compared to dsMock. We measured *actin-5c* mRNA levels

which were significantly upregulated ($p < 0.01$, Figure 3.2B), showing a two-fold increase compared to dsMock-treated females indicating that also in *B. germanica* CHMP4B could regulate actin cytoskeleton expression.

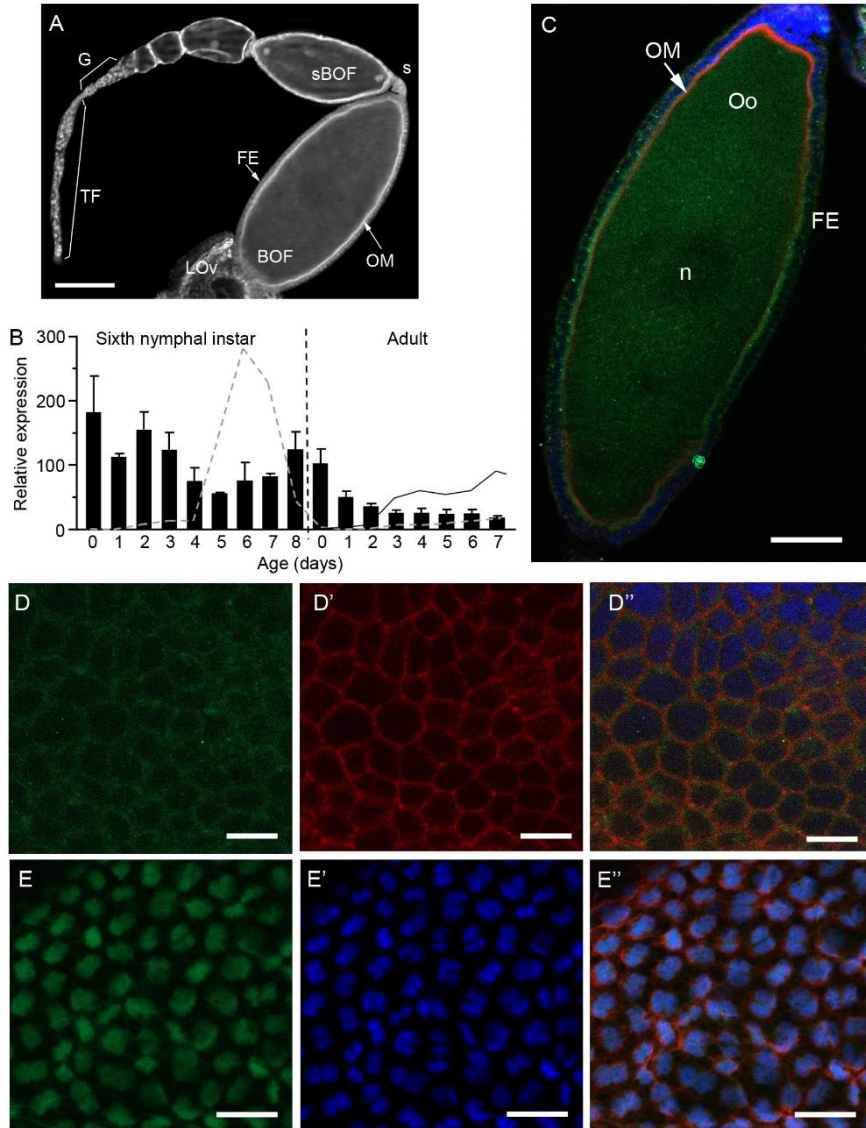


Figure 3.1. CHMP4B in *Blattella germanica* ovaries. (A) Panoistic ovariole from a 0-day-old adult female. Only the basal ovarian follicle (BOF) grows and matures in each gonadotrophic cycle. LOv, lateral oviduct; OM, oocyte membrane; FE, follicular epithelium; sBOF, sub-basal ovarian follicle; G, germarium; TF, terminal

The BOFs in 5-day-old *dsChmp4b*-treated females (Figure 3.2C), were significantly smaller ($p < 0.0001$; 0.933 ± 0.05 mm; $n = 19$) compared to *dsMock*-treated females (1.414 ± 0.03 mm; $n = 18$) (Figure 3.2D and E) and showed a fragile appearance. Moreover, *dsChmp4b*-treated females were not able to ovulate and oviposit. Labeling for CHMP4B in FCs of *dsChmp4b*-treated females was low (Figure 3.2F-F'), compared to the labeling in *dsMock*-treated females (Figure 3.2G-G'), and it was necessary to overexpose the images in the corresponding channel to detect some labeling in the nucleus of FCs from the treated ovaries (Figure 3.2F). Labeling of CHMP4B not only can be observed in the nuclei of FCs of *dsChmp4b*-treated insects but, it was also coincidental with some remains of DNA present in the cytoplasm after the depletion of CHMP4B (Figure 3.2F and F', arrows).

Figure 3.1. (continued) filament; s, stalk. Nuclei were stained with DAPI and F-actin with phalloidin-TRITC. The oocyte apical pole is at the top-right of the image. (B) mRNA expression pattern of *Chmp4b* in ovaries of sixth nymphal instar and adults during the first reproductive cycle. The black dashed line indicates the molt to adult. Profiles of ecdysteroid titer in hemolymph (grey dashed line) and ecdysteroid contents in the adult ovary (solid black line) are indicated (data from Cruz et al., 2003; Romaña et al., 1995). Data represent copies of *Chmp4b* mRNA per 1000 copies of *actin-5c* (relative expression), and is expressed as the mean \pm S.E.M. ($n = 3-4$). (C) Immunolocalization of CHMP4B (green) in the BOF from a 0-day-old adult, showing the labeling spread by the oocyte cytoplasm. The oocyte apical pole is at the top-right of the image. The image was overexposed (500 ms) to detect the fluorescence for CHMP4B in the corresponding channel. FE: Follicular epithelium; n: nucleus; OM, oocyte membrane; Oo: Oocyte. (D) Follicular epithelium in BOF from a 0-day-old adult showing CHMP4B (green) localized in the cytoplasm, close to cell membranes (340 ms of exposition). (D') F-actins from image D were stained with phalloidin-TRITC (red). (D'') Merge the image of D and D' including the DAPI staining (blue) to stain the nuclei. (E) Follicular epithelium in BOF from a 5-day-old adult showing CHMP4B (green) localized in the nuclei of FCs (360 ms of exposition). (E') DAPI (blue) staining of nuclei from image E. (E'') Merge image of E and E' showing the nuclear localization (blue) of CHMP4B at this age. F-actin microfilaments were stained with phalloidin-TRITC (red). Scale bar in A: 100 μ m, C: 50 μ m, D: 10 μ m and in E: 50 μ m.

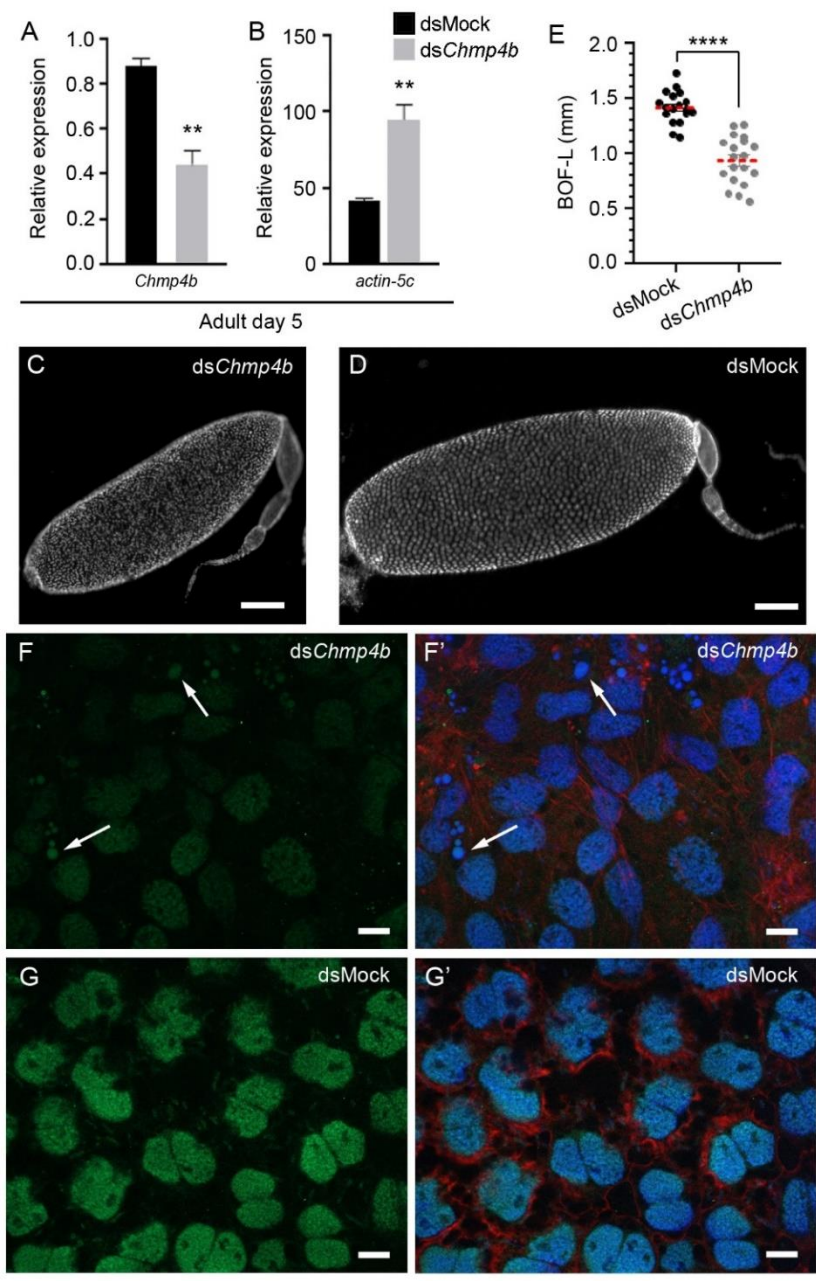


Figure 3.2. CHMP4B depletion in 5-day-old *Blattella germanica* ovaries. Newly emerged adult females were treated with ds*Chmp4b* or dsMock and dissected 5 days later. (A) Relative expression of *Chmp4b* in ovaries, showing the significant decrease of *Chmp4b* mRNA (n = 3; ** p = 0.0047). (B) Relative

In the BOF of 5-day-old *B. germanica* adults, the follicular epithelium is well-organized, with a uniform cell distribution, and all the FCs are binucleated since the cytokinesis was arrested (Figure 3.3A). At this age, the patency is very apparent. The contraction of cell membranes had occurred, leaving large intercellular spaces between the FCs (Figure 3.3A, arrows). During this process, the F-actin microfilaments in the cell membranes display lateral extensions that maintain the contact between cells through microfilament bridges (Figure 3.3A', arrowheads). The large endoreplicating nuclei (Figure 3.3A'') are located in the center of the cell, occupying almost all the cytoplasm (Figure 3.3A and A'').

In 5-day-old ds*Chmp4b*-treated females, the follicular epithelium shows clear disorganization compared to controls (Figure 3.3B and C). The FCs have lost their uniform distribution, showing a remarkable variation of size and shape (Figure 3.3C and F), affecting the overall follicular epithelia. Although many of the FCs are binucleated, they showed nuclei of bizarre shapes (Figure 3.3C', F and G).

Figure 3.2. (continued) expression of *actin-5c* in ovaries, showing the significant increase of *actin-5c* ($n = 3$; ** $p = 0.0093$). In A and B, data represent copies of mRNA per copy of *eIF4aIII* mRNA (relative expression), and data are expressed as the mean \pm S.E.M. (C) Ovariole from ds*Chmp4b*-treated adult. (D) Ovariole from dsMock-treated adult. In C and D, DNA was stained with DAPI (white). (E) Length of basal ovarian follicle (BOF-L; mm) in dsMock- and ds*Chmp4b*-treated females ($n = 18$ and 19 females, respectively; 3-5 ovarian follicles were measured per insect; **** $p < 0.0001$). The red dashed line indicates the mean. (F) Immunolocalization of CHMP4B in the nuclei of the follicular cells of ds*Chmp4b*-treated females (green). This image was overexposed until some signal was detected in the corresponding channel (500 ms of exposition). (F') Merged image showing the CHMP4B labelling, and the F-actin and DNA staining. The arrows in both images indicate vesicles containing rests of DNA. (G) Immunolocalization of CHMP4B in follicular cells of dsMock-treated females (320 ms of exposition). The labeling is limited to the nuclei of follicular cells (green). (G') Merged image showing the CHMP4B labeling, and the F-actin and DNA staining. CHMP4B was detected using a rabbit anti-Shrb antibody in a dilution of 1/50 (Bäumers et al., 2019). The F-actin microfilaments were stained with phalloidin-TRITC (red), and DNA with DAPI (blue). Scale bar in C and D: 200 μm , in F and G: 10 μm .

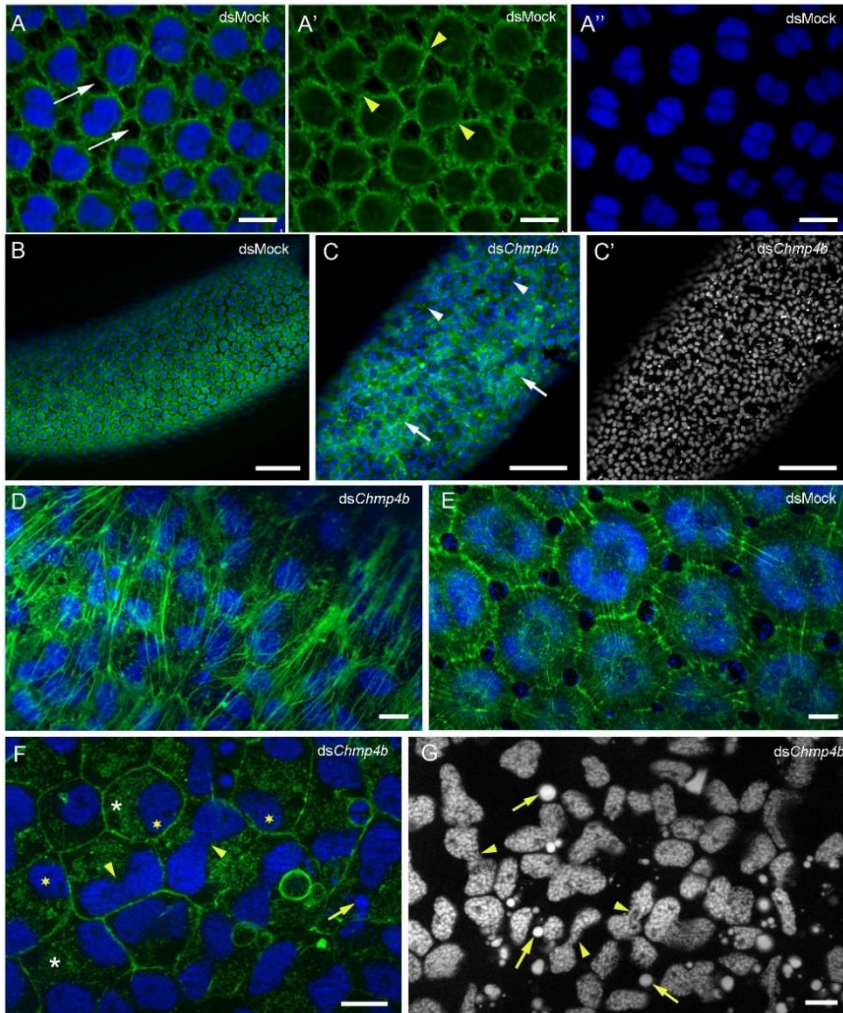


Figure 3.3. CHMP4B depletion in the basal ovarian follicle of 5-day-old adult *Blattella germanica*. (A) Follicular epithelium from a dsMock-treated female, showing the uniform distribution of the cells, the patency, and the binucleated FCs. Arrows show the intercellular spaces between the follicular cells. (A') F-actin fibers from A, show the big intercellular spaces and the bridges of actin connecting the cells (arrowheads). (A'') Paired nuclei in the FCs. (B) Basal ovarian follicle from a dsMock-treated female showing the uniform distribution of FCs. (C) Basal ovarian follicle from a dsChmp4b-treated female, showing the disorganization of F-actin cytoskeleton in the follicular epithelium. Arrows and arrowheads indicate rich and poor actin patches, respectively. (C') Nuclei from C, showing the variety of size and morphology. (D) Fibers of F-actin in dsChmp4b-treated insects

Along the oocyte surface, it is possible to visualize areas rich in F-actin microfilaments (Figure 3.3C, arrows) besides others with few F-actin fibers (Figure 3.3C, arrowheads).

In those actin-rich areas, the actin microfilaments appear like large bundles of fibers randomly distributed covering the FCs (Figure 3.3D), while in a 5-day-old dsMock adults, the F-actin fibers have a regular and orderly distribution, connecting cell to cell (Figure 3.3E). The FCs in BOF of ds*Chmp4b*-treated females maintained a narrow contact between them (Figure 3.3F) and did not show signs of patency as occurs in the controls of the same age (Figure 3.3A), not allowing the accumulation of storage proteins in the BOF ($1717.5 \pm 140.7 \mu\text{g}$ of total proteins in dsMock, versus $379.2 \pm 49.0 \mu\text{g}$ in ds*Chmp4b*-treated females; $n = 4$ each). In the FCs of ds*Chmp4b*-treated females, the F-actin fibers appeared concentrated in the cell membranes without showing expansions (Figure 3.3F). In addition, it is possible to detect staining for F-actin through the cytoplasm (Figure 3.3F, asterisks), as well as DNA remains that could suggest the beginning of apoptosis (Figure 3.3F and G, arrows). In these 5-day-old *B. germanica* ds*Chmp4b*-treated females, the FCs were smaller, with smaller nuclei than those of dsMock-treated insects and showing odd shapes (Figure 3.3C', D, and G), and the staining with WGA do not unveil the nuclear envelop (Figure 3.S2).

Figure 3.3. (continued) covering the follicular epithelia. (E) Fibers of F-actin in dsMock-treated insects, showing the regular distribution of F-actin fibers, connecting the FCs. (D) and (E) were obtained in a position close to the basal pole of the FCs. (F) FCs in a ds*Chmp4b*-treated female. The cells are stuck to each other, without signs of patency. Actin staining is abundant in the cytoplasm (asterisks). Remains of condensed DNA are visible (arrow). A high number of cells have nuclei with an hourglass shape (arrowheads). The nuclei appeared attached to cell membranes (yellow stars). (G) Nuclei from FCs in ds*Chmp4b*-treated females, showing odd shapes. It seems that the nuclei do not complete the karyokinesis and presented bridges connecting both nuclei (arrowheads). Remains of condensate DNA were abundant through cell cytoplasm (arrows). The F-actin microfilaments were stained with phalloidin-TRITC (green). DNA was stained with DAPI (blue, except in C' and G where appear in white). Scale bar in A: 20 μm , B and C: 100 μm , D-G: 10 μm .

Some of these FCs remained mononucleated (Figure 3.3F), while in others was possible to find two nuclei still attached one to the other with an elongated shape remembering an hourglass (Figure 3.3F and G, arrowheads), suggesting an incomplete karyokinesis process, as evidenced by visible bridges connecting them. In addition, most of the nuclei lost the central position in the cell and appeared bound to the cytoplasmic membrane (Figure 3.3F, yellow stars), suggesting changes in the polarity of the cells.

The disorganization of the F-actin cytoskeleton in the FCs of *dsChmp4b*-treated-adult females, together with the presence of remains of DNA in the cytoplasm and the changes in the FCs polarity and the morphology of the nuclei, suggested that these cells underwent apoptotic.

3.3.3. Expression of genes related to cell planar polarity in *dsChmp4b*-treated *Blattella germanica* adult ovaries

The morphological changes of FCs in the *dsChmp4b*-treated females, together with the increase of *actin-5c* expression and F-actin accumulation in the cytoplasm, suggest that the relaxation of the cytoskeleton at the gap junctions, which would allow the formation of patency and consequently the uptake of yolk proteins by the oocyte, has not occurred. As a result, cells appear tightly connected. All of that drove us to quantify the expression of the genes involved in the cell-cell adhesion that could determine the uniform distribution of cells in the follicular epithelium.

Based on *D. melanogaster* studies (Casal et al., 2006; Strutt & Strutt, 2021; Thomas & Strutt, 2012), we selected some genes involved in maintaining the epithelial planar polarity and the actin cytoskeleton organization. We measured two cadherins, *ds* and *kug*, and the extracellular serine/threonine protein kinase *ff*, all of them belonging to the *ds/fat* system. We also measured the main proteins from the *fz/stan* system, the protocadherin-like wing polarity protein *stan* and *fz*. In addition, we quantified the β -catenin *arm* and the actomyosin protein *Mhc*.

In the ovaries of 5-day-old *dsChmp4b*-treated females, the expression of those genes belonging to the *ds/fat* system was upregulated (Figure 3.4A).

The expression of *ds* was significantly increased by 45% ($p < 0.05$), *kug* expression increased by 99% ($p < 0.05$) while *ff* increased a 51% its expression, even though not significantly. The genes related to the *fz/stan* system showed a tendency to increase their expression (Figure 3.4B). The expression of *stan* increased a 15%, while *fz* increased a 24%. Similarly, the expression of the *arm* is significantly upregulated by 21% ($p < 0.01$, Figure 3.4C), while *Mhc* tends to be upregulated (29%, Figure 3.4D).

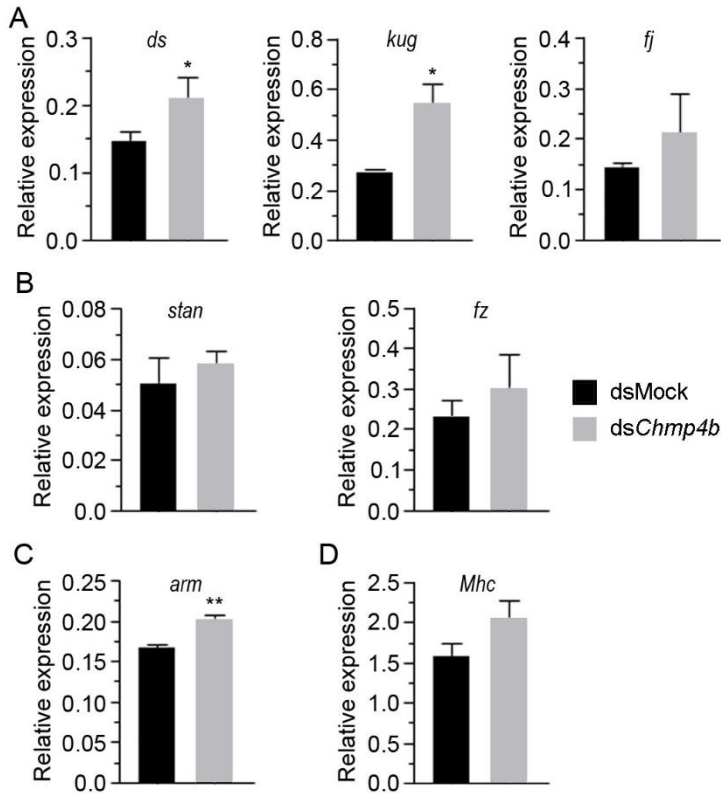


Figure 3.4. Expression of genes related to planar polarity in ovaries from 5-day-old dsChmp4b-treated adults of *Blattella germanica*. (A) Expression of *dachsous* (*ds*), *kugelei* (*kug*) and *four-jointed* (*ff*), belonging to *ds/fat* system. (B) Expression of *starry night* (*stan*) and *frizzled* (*fz*), from the *fz/stan* system. Expression of (C) the β -catenin *armadillo* (*arm*) and (D) *Myosin heavy chain* (*Mhc*). Data represent copies of mRNA per copy of *eIF4aIII* mRNA and are expressed as the mean \pm S.E.M. ($n = 3$). The asterisks indicate statistically significant differences respect to dsMock: * $p = 0.02$ (*ds*); * $p = 0.03$ (*kug*); ** $p = 0.0095$ (*arm*).

3.3.4. Effects of *Chmp4b* depletion on the basal ovarian follicle of *Blattella germanica* last instar nymphs

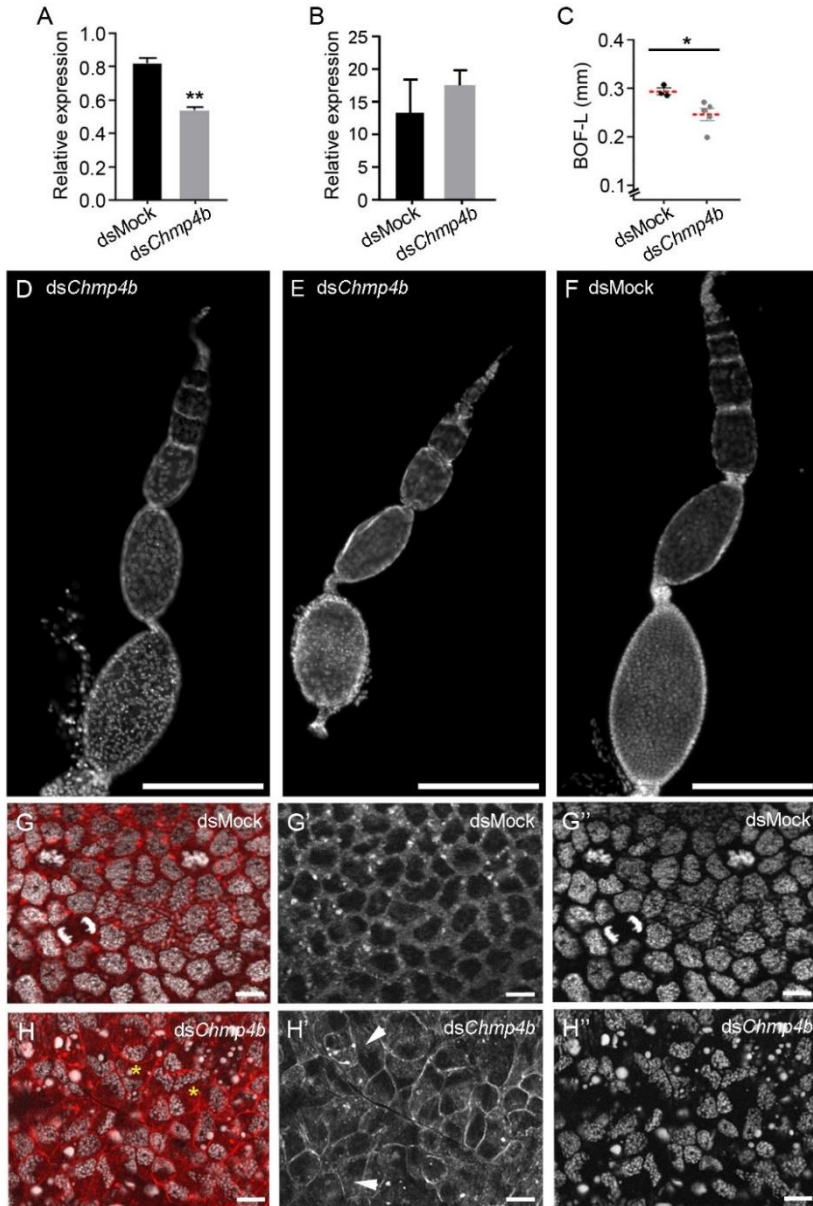


Figure 3.5. Depletion of CHMP4B in ovaries from 6-day-old sixth-instar nymphs of *Blattella germanica*. Newly emerged last instar nymphs were treated

In the first part of this work, we analyzed the effects of *Chmp4b* depletion in the FCs from ovaries of 5-day-old adult females when cytokinesis is arrested and the change to endoreplication occurs naturally (Irles and Piulachs, 2014). Then, we studied the function of CHMP4B in the ovaries of 6-day-old sixth instar nymphs when the FCs have a high mitotic activity (Irles and Piulachs, 2014).

Newly emerged sixth instar nymphs of *B. germanica* were treated with ds*Chmp4b* or dsMock, and the phenotypes produced were analyzed in nymphal ovaries six days later. The expression levels of *Chmp4b* were significantly depleted (34%, $p < 0.01$, Figure 3.5A), while the expression of *actin-5c* tended to be increased (32%; Figure 3.5B). In these ds*Chmp4b*-treated nymphs, the BOFs were significantly smaller ($p < 0.05$; 0.25 ± 0.01 mm; $n = 5$) compared with dsMock-treated nymphs (0.29 ± 0.01 mm; $n = 3$) (Figure 3.5C-F). In some ovarioles from ds*Chmp4b*, the BOFs even had a rounded shape (Figure 3.5E and 3.6B).

Figure 3.5. (continued) with ds*Chmp4b* or dsMock and analyzed six days later. (A) Relative expression of *Chmp4b*. (B) Relative expression of *actin-5c*. Data represent copies of mRNA per copy of *eIF4aIII* mRNA. Data are expressed as the mean \pm S.E.M. ($n = 3$). Asterisks indicate statistically significant differences concerning dsMock: ** $p = 0.0013$. (C) Length of BOF (BOF-L; mm) in dsMock- and ds*Chmp4b*-treated nymphs (10-20 ovarian follicles were measured per female, $n = 3$ and 5 females, respectively; * $p = 0.03$). The dashed line indicates the mean. (D) Ovariole from ds*Chmp4b*-treated nymph. (E) Ovariole from ds*Chmp4b*-treated nymph, showing the round shape (see also Figure 3.6B). (F) Ovariole from dsMock-treated nymph. (G) Follicular cells from dsMock-treated nymphs, showing the mitotic figures. (G') Channel corresponding to F-actin microfilaments of G. (G'') Channel corresponding to nuclei of FCs of G. (H) Follicular cells of ds*Chmp4b*-treated nymphs. The cell shapes and sizes are not uniform, there are no cells under division, and the nuclei of the FCs showed elongated shapes with a polarized position attached to cell membranes (see asterisks). (H') Channel corresponding to F-actin microfilaments of H, showing the great definition profile of the cell membranes due to the accumulation of F-actin there. The F-actin also appeared distributed by the cytoplasm (arrowheads). (H'') Channel corresponding to nuclei of H, showing the odd nuclei shape. The F-actin microfilaments were stained with phalloidin-TRITC (red in G and H and white in G' and H'). The DNA was stained with DAPI (white). Scale bar in D-F: 200 μ m; G and H: 10 μ m.

In the FCs of dsMock-treated *B. germanica* last instar nymphs, the mitotic figures were evident, and all cells were mononucleated, with nuclei of similar size occupying most of the cytoplasm of the cell (Figure 3.5G and G’). The F-actin cytoskeleton from the FCs maintained an organized and homogeneous distribution of the cells in a monolayer, without intercellular spaces between them (Figure 3.5G’). In 6-day-old ds*Chmp4b*-treated nymphs, no mitotic figures were visualized in the follicular epithelium. Although most of the FCs were mononucleated as in dsMock, unexpectedly a few binucleated cells appeared scattered throughout the follicular epithelia (Figure 3.5H, asterisks), a fact that never was observed in dsMock-treated nymphs. In these ds*Chmp4b*-treated nymphs, the nuclei of FCs had peculiar and elongated shapes (Figure 3.5H’), similar to the ones found in ds*Chmp4b*-treated adults (see Figure 3.3F-G). The nuclei, in general, were smaller than in dsMock-treated BOFs, and again, they appeared polarized on one side of the cells, losing their central position (Figure 3.5H).

Moreover, in 6-day-old ds*Chmp4b*-treated nymphs, the FCs showed different morphologies and sizes, indicating a loss of planar polarity (Figure 3.6). The labeling for actin marked sharply the profile of the FCs membranes and filled the cytoplasm not occupied by the nucleus (Figure 3.5H and H’ arrowheads). It was also possible to find remains of DNA in the cytoplasm of the FCs, suggesting cell apoptosis (Figure 3.5H and H’). Changes in F-actin were also evident in the oocyte membrane of the BOF, and also in the oocyte cytoplasm (Figure 3.6B). At this age, in BOF of control females, a huge concentration of F-actin is sporadically detected in the apical and basal poles of the oocyte attached to the oocyte membrane (Figure 3.6A, asterisks). Conversely, in 6-day-old ds*Chmp4b*-treated nymphs, these F-actin concentrations are common, do not appearing so close to the oocyte membrane (Figure 3.6B, asterisks), and the actin fibers connecting both actin accumulation points are clearly visible (Figure 3.6B’). In addition, some actin fibers seem to reach the oocyte membrane behind the actin center (Figure 3.6B’).

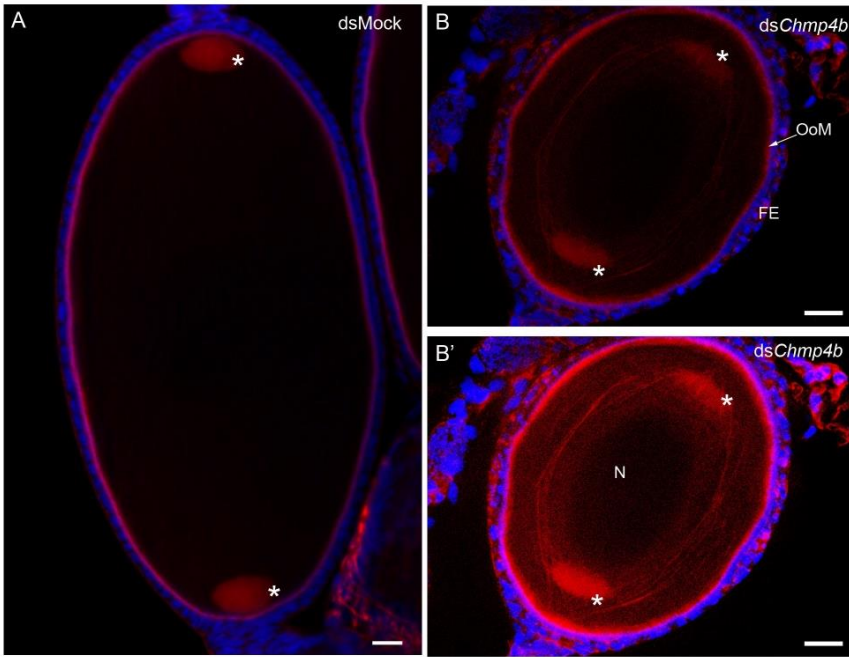


Figure 3.6. Organization of F-actin fibers in the basal ovarian follicles (BOFs) of 6-day-old sixth-instar nymphs of *Blattella germanica*. (A) BOF of dsMock-treated nymphs. The oocyte apical pole is positioned at the top in all images. The F-actin concentration in both poles is labelled by an *. (B) BOF of dsChmp4b-treated nymphs, showing both, the F-actin concentration (*) inside the oocyte and a thick oocyte membrane (OoM). Follicular epithelia (FE) display different morphologies and sizes of the follicular cells (FCs), indicative of loss of planar polarity. (B') Overlapping of Z-stack images of B, showing the actin fibers connecting the F-actin concentration in both poles. The F-actin microfilaments were stained with phalloidin-TRITC (red) and DNA with DAPI (blue). Scale bar: 20 μm .

3.4. Discussion

Insect oogenesis requires a sequential series of changes in the ovary to ensure oocyte maturation and egg formation. To accurately complete all these steps, the organization of cytoskeleton fibers is necessary, and as has been evidenced in *D. melanogaster*, the role of the ESCRT complex in regulating the actin cytoskeleton is essential (Vaccari et al., 2009). In this fly, mutations in any component of the ESCRT complex lead to flaws in actin and plasma membrane organization, resulting in multinucleated cells due to cytokinesis failures (Sevrioukov et al., 2005; Vaccari et al., 2009). The planar polarity of these cells was affected, and the disorganization of actin bundles determined spherical egg chambers (Cetera & Horne-Badovinac, 2015). These actin modifications were also described in the testis of ds*Shrb* *D. melanogaster*-treated adults, where an upregulation of genes related to the cytoskeleton was detected (Chen et al., 2021).

In *B. germanica*, similarly as it occurs in *D. melanogaster* (Cetera & Horne-Badovinac, 2015), depletion of *Chmp4b* provoked an increase in the expression of *actin-5c*. At the level of BOF, there are changes in the distribution of F-actin fibers. There is an excess of bundles covering the BOF that adopted, in some cases, a round shape (Figure 3.5E and 3.6). In *B. germanica*, this phenotype was more evident in previtellogenic ovaries from the last instar nymphs than in adults since the ovarian follicles begin to take their shape in the last nymphal instar.

In the BOF of *B. germanica* previtellogenic females, levels of *Chmp4b* are higher than in the vitellogenic period. These higher levels of *Chmp4b* coincides with the mitotically active FCs. Conversely, in adults during vitellogenesis, and coinciding with the decrease of *Chmp4b* expression levels, FCs arrest cytokinesis and become binucleated. The depletion of *Chmp4b* mRNA due to dsRNA treatments in both adult and last instar nymphs determine a loss of planar polarity in the ovarian follicular epithelium. The FCs loss their morphology and uniform distribution, appearing closely attached to each other. Furthermore, their nuclei exhibited a loss of polarity, deviating from their central position within the cell and instead becoming attached to the cytoplasmic membrane. The increased expression of proteins belonging *fat/ds* and *fz/stan* systems in adults, related with planar polarity and cell adhesion, would make

impossible to relax gap junctions to open spaces between the cells allowing patency to progress. In *D. melanogaster* it was demonstrated that patency requires a local loss of adhesion between FCs for the opening of cell junctions (Isasti-Sanchez et al., 2021). This process relies on the removal of adhesion proteins, including cadherins, from the plasma membrane through endocytic vesicles that requires the presence ESCRT-III complex, and therefore, CHMP4B.

In *B. germanica* last instar nymphs, the FCs in the BOF are mitotically active and mononucleated. Depletion of *Chmp4b* at this stage, leads to sporadically binucleated cells, similar to what happens in control adults that changes the cell program to become binucleated, coinciding with the natural decrease of *Chmp4b* expression during the vitellogenesis (Figure 3.1B). Low levels of *Chmp4b* mRNA in adult ovaries are coincident with the cytokinesis arrest in FCs that become binucleated, and undergo endoreplication programming (Irles et al., 2016; Irles & Piulachs, 2014). When depletion of *Chmp4b* mRNA is determined early in the adult stage by RNAi treatment, many cells arrest the mitotic program staying mononucleated and not changing their program. In both cases, in nymphs and adults, the FCs can exhibit abnormally elongated nuclei because the karyokinesis has not been completed. Results could be explained by the importance of CHMP4B in regulating the timing of membrane abscission (Eikenes et al., 2015; Matias et al., 2015), in a similar way as it was described for vertebrate cells, where depletion of the ESCRT-III components, including CHMP4B, produced aberrant nuclei with multiple lobes or micronuclei (Olmos et al., 2015). The consistent results observed in FCs of 6-day-old sixth-instar nymphs and 5-day-old adults of *B. germanica*, after the depletion of *Chmp4b*, characterized by the loss of planar polarity and an incorrect number of nuclei, as well as the presence of aberrant nuclei, suggest that the function of CHMP4B is not-related to the proliferative stage of the tissue. The changes determined by *Chmp4b* depletion in the FCs affect, in the end, the BOF development, causing female sterility.

In *B. germanica*, CHMP4B is necessary for maintaining the correct rate of FC proliferation, the planar polarity, and the nuclear count of FCs during the BOF growth. CHMP4B is needed to maintain the correct expression of cytoskeleton proteins to allow the BOF to grow and mature properly, incorporating yolk proteins. CHMP4B regulates the correct distribution of

actin fibers in the BOF, essential to complete ovulation and oviposition (Alborzi & Piulachs, 2023). All these data help to understand the oogenesis in a basal insect with panoistic ovaries. However, some studies on the other components of the ESCRT-III subcomplex and its regulation will be fundamental to understanding all these processes.

Acknowledgments

The authors thank Dr. Thomas Klein, Institut für Genetik, Heinrich-Heine-Universität for kindly supplying a sample of antibody against Shrub. We thank the financial support to the project PID2021-122316OB-I00 from the MCIN/AEI/10.13039/501100011033 and by ERDF, a way of making Europe. To the project PID2019-104483GB-I00, funded by MCIN/AEI/10.13039/501100011033 and to the Catalan Government (2021 SGR 00419). This work was also supported by Pla de Doctorats Industrials de la Secretaria d'Universitats i Recerca del Departament d'Empresa i Coneixement de la Generalitat de Catalunya (grant number 2021 DI 059). The authors acknowledge the support of the publication fee by CSIC Open Access Publication Support Initiative through its Unit of Information Resources for Research (URICI).

3.5. Bibliography

- Alborzi, Z., & Piulachs, M. D. (2023). Dual function of the transcription factor Ftz-f1 on oviposition in the cockroach *Blattella germanica*. *Insect Molecular Biology*, 32, 689–702. <https://doi.org/10.1111/imb.12866>
- Bäumers, M., Klose, S., Brüser, C., Haag, C., Hänsch, S., Pannen, H., Weidtkamp-Peters, S., Feldbrügge, M., Klein, T. (2019). The auxiliary ESCRT complexes provide robustness to cold in poikilothermic organisms. *Biology Open*, 8(9), 1–13. <https://doi.org/10.1242/bio.043422>
- Bellés, X., Casas, J., Messeguer, A., & Piulachs, M. D. (1987). *In vitro* biosynthesis of JH III by the corpora allata of adult females of *Blattella germanica* (L). *Insect Biochemistry*, 17, 1007–1010. [https://doi.org/10.1016/0020-1790\(87\)90111-9](https://doi.org/10.1016/0020-1790(87)90111-9)
- Bradford, M.M. (1976). A rapid and sensitive method for the quantitation

- of microgram quantities of protein utilizing the principle of protein-dye binding. *Analytical Biochemistry*, 72, 248-254. <https://doi.org/10.1006/abio.1976.9999>
- Carlton, J. G., & Martin-Serrano, J. (2007). Parallels between cytokinesis and retroviral budding: A role for the ESCRT machinery. *Science*, 316, 1908–1912. <https://doi.org/10.1126/science.1143422>
- Casal, J., Lawrence, P. A., & Struhl, G. (2006). Two separate molecular systems, Dachous/Fat and Starry night/Frizzled, act independently to confer planar star polarity. *Development*, 133, 4561–4572. <https://doi.org/10.1242/dev.02641>
- Cetera, M., & Horne-Badovinac, S. (2015). Round and round gets you somewhere: Collective cell migration and planar polarity in elongating *Drosophila* egg chambers. *Current Opinion in Genetics & Development*, 32, 10–15. <https://doi.org/10.1016/j.gde.2015.01.003>
- Chen, M. Y., Tayyeb, A., & Wang, Y. F. (2021). shrub is required for spermatogenesis of *Drosophila melanogaster*. *Archives of Insect Biochemistry and Physiology*, 106(4), 1–15. <https://doi.org/10.1002/arch.21779>
- Christ, L., Raiborg, C., Wenzel, E. M., Campsteijn, C., & Stenmark, H. (2017). Cellular Functions and Molecular Mechanisms of the ESCRT Membrane-Scission Machinery. *Trends in Biochemical Sciences*, 42, 42–56. <https://doi.org/10.1016/j.tibs.2016.08.016>
- Cruz, J., Martín, D., Pascual, N., Maestro, J. L., Piulachs, M. D., & Bellés, X. (2003). Quantity does matter. Juvenile hormone and the onset of vitellogenesis in the German cockroach. *Insect Biochemistry and Molecular Biology*, 33, 1219–1225. <https://doi.org/10.1016/j.ibmb.2003.06.004>
- Davey, K. G. (1981). Hormonal control of vitellogenin uptake in *Rhodnius prolixus* Stål. *American Zoologist*, 21, 701–705. <https://doi.org/10.1093/icb/21.3.701>
- Davey, K. G., & Huebner, E. (1974). The response of the follicle cells of *Rhodnius prolixus* to juvenile hormone and antigonadotropin *in vitro*. *Canadian Journal of Zoology*, 52, 1407–1412. <https://doi.org/10.1139/z74-178>
- Eikenes, Å. H., Malerød, L., Christensen, A. L., Steen, C. B., Mathieu, J., Nezis, I. P., Liestøl, K., Huynh, J.R., Stenmark, H., Haglund, K. (2015). ALIX and ESCRT-III Coordinately Control Cytokinetic Abscission during Germline Stem Cell Division *In Vivo*. *PLoS Genetics*, 11(1), 1–33. <https://doi.org/10.1371/journal.pgen.1004904>

- Elshaer, N., & Piulachs, M. D. (2015). Crosstalk of EGFR signalling with Notch and Hippo pathways to regulate cell specification, migration and proliferation in cockroach panoistic ovaries. *Biology of the Cell*, *107*, 273–285. <https://doi.org/10.1111/boc.201500003>
- Irles, P., & Piulachs, M. D. (2014). Unlike in *Drosophila* meroistic ovaries, Hippo represses Notch in *Blattella germanica* panoistic ovaries, triggering the mitosis-endocycle switch in the follicular cells. *PLoS ONE*, *9*(11), 1–19. <https://doi.org/10.1371/journal.pone.0113850>
- Irles, P., Elshaer, N., & Piulachs, M. D. (2016). The Notch pathway regulates both the proliferation and differentiation of follicular cells in the panoistic ovary of *Blattella germanica*. *Open Biology*, *6*(1), 1–13. <https://doi.org/10.1098/rsob.150197>
- Isasti-Sanchez, J., Münz-Zeise, F., Lancino, M., & Luschnig, S. (2021). Transient opening of tricellular vertices controls paracellular transport through the follicle epithelium during *Drosophila* oogenesis. *Developmental Cell*, *56*, 1083–1099. <https://doi.org/10.1016/j.devcel.2021.03.021>
- Klusza, S., & Deng, W. M. (2010). At the crossroads of differentiation and proliferation: Precise control of cell-cycle changes by multiple signaling pathways in *Drosophila* follicle cells. *BioEssays*, *33*, 124–134. <https://doi.org/10.1002/bies.201000089>
- Kranz, A., Kinner, A., & Kölling, R. (2001). A family of small coiled-coil-forming proteins functioning at the late endosome in yeast. *Molecular Biology of the Cell*, *12*, 711–723. <https://doi.org/10.1091/mbc.12.3.711>
- Li, Z., & Blissard, G. (2015). The vacuolar protein sorting genes in insects: A comparative genomeview. *Insect Biochemistry and Molecular Biology*, *62*, 211–225. <https://doi.org/10.1016/j.ibmb.2014.11.007>
- Lozano, J., & Bellés, X. (2011). Conserved repressive function of Kruppel homolog 1 on insect metamorphosis in hemimetabolous and holometabolous species, *Sci. Rep.* *1* (2011) 163. <https://doi.org/10.1038/srep00163>
- Martin, D., Piulachs, M.D., Bellés, X. (1995). Patterns of haemolymph vitellogenin and ovarian vitellin in the german cockroach, and the role of juvenile hormone. *Physiological entomology*, *20*: 59-65. <https://doi.org/10.1111/j.1365-3032.1995.tb00801.x>
- Matias, N. R., Mathieu, J., & Huynh, J. R. (2015). Abscission Is Regulated by the ESCRT-III Protein Shrub in *Drosophila* Germline Stem Cells. *PLoS Genetics*, *11*(2), 1–20.

- <https://doi.org/10.1371/journal.pgen.1004653>
- Mathieu, J., Michel-Hissier, P., Boucherit, V., Huynh, J.R. (2022). The deubiquitinase USP8 targets ESCRT-III to promote incomplete cell division. *Science*, 376, 818-823. <https://doi.org/10.1126/science.abg2653>
- Montañés, J. C., Rojano, C., Ylla, G., Piulachs, M. D., & Maestro, J. L. (2021). siRNA enrichment in Argonaute 2-depleted *Blattella germanica*. *Biochimica et Biophysica Acta - Gene Regulatory Mechanisms*, 1864(6-7), 1-8. <https://doi.org/10.1016/j.bbagr.2021.194704>
- Olmos, Y., Hodgson, L., Mantell, J., Verkade P., & Carlton J. G. (2015). ESCRT-III controls nuclear envelope reformation. *Nature*, 522, 236-239. <https://doi.org/10.1038/nature14503>
- Peck, J. W., Bowden, E. T., & Burbelo, P. D. (2004). Structure and function of human Vps20 and Snf7 proteins. *Biochemical Journal*, 377, 693-700. <https://doi.org/10.1042/bj20031347>
- Raiborg, C., & Stenmark, H. (2009). The ESCRT machinery in endosomal sorting of ubiquitylated membrane proteins. *Nature*, 458, 445-452. <https://doi.org/10.1038/nature07961>
- Riechmann, V. (2021). Paracellular transport: Opening the gates for growth. *Developmental Cell*, 56, 1075-1077. <https://doi.org/10.1016/j.devcel.2021.03.025>
- Romaña, I., Pascual, N., & Bellés, X. (1995). The ovary is a source of circulating ecdysteroids in *Blattella germanica*. *European Journal of Entomology*, 92, 93-103.
- Rumbo, M., Pagone, V., & Piulachs, M. D. (2023). Diverse functions of the ecdysone receptor (EcR) in the panoistic ovary of the German cockroach. *Insect Biochemistry and Molecular Biology*, 156, 103935. <https://doi.org/https://doi.org/10.1016/j.ibmb.2023.103935>
- Sevrioukov, E. A., Moghrabi, N., Kuhn, M., & Krämer, H. (2005). A mutation in dVps28 reveals a link between a subunit of the endosomal sorting complex required for transport-I complex and the actin cytoskeleton in *Drosophila*. *Molecular Biology of the Cell*, 16, 2301-2312. <https://doi.org/10.1091/mbc.E04-11-1013>
- Strutt, H., & Strutt, D. (2021). How do the Fat-Dachsous and core planar polarity pathways act together and independently to coordinate polarized cell behaviours? *Open Biology*, 11(2), 1-18. <https://doi.org/10.1098/rsob.200356>
- Sweeney, N. T., Brenman, J. E., Jan, Y. N., & Gao, F. B. (2006). The coiled-

- coil protein shrub controls neuronal morphogenesis in *Drosophila*. *Current Biology*, 16, 1006–1011. <https://doi.org/10.1016/j.cub.2006.03.067>
- Thomas, C., & Strutt, D. (2012). The roles of the cadherins Fat and Dachshous in planar polarity specification in *Drosophila*. *Developmental Dynamics*, 241, 27–39. <https://doi.org/10.1002/dvdy.22736>
- Vaccari, T., Rusten, T. E., Menut, L., Nezis, I. P., Brech, A., Stenmark, H., & Bilder, D. (2009). Comparative analysis of ESCRT-I, ESCRT-II and ESCRT-III function in *Drosophila* by efficient isolation of ESCRT mutants. *Journal of Cell Science*, 122, 2413–2423. <https://doi.org/10.1242/jcs.046391>
- Zhang, Y., & Kunkel, J. G. (1992). Program of F-actin in the follicular epithelium during oogenesis of the german cockroach, *Blattella germanica*. *Tissue and Cell*, 24, 905–917. [https://doi.org/10.1016/0040-8166\(92\)90025-3](https://doi.org/10.1016/0040-8166(92)90025-3)

3.6. Supplementary material

Table 3.S1. Primers used for transcript measurements, and for dsRNA synthesis. The length of the amplicon and the accession number of the sequence under study are indicated. F: forward and R: reverse primers

Primer set		primer 5'-3'	Amplicon length (bp)	Accession number
<i>actin-5c</i>	F R	AGCTTCCTGATGGTCAGGTGA ACCATGTACCCTGGAATTGCCGACA	213	AJ862721
<i>arm</i>	F R	CCTGTGTGAACCCTTGGTCT CACTCTGGAGCCACAACCTCA	100	PSN33457.1
<i>Chmp4b</i>	F R	ACTACAAAATGAGTTTCTTGGC GCATTTCCCTCAGTTTCTCTTAA	105	PSN45592.1
<i>ds</i>	F R	CGGTGAGAATGTTTCGTGTGG CATCGCGTGGGGTATTTTCA	110	PSN55018.1
<i>eIF4aIII</i>	F R	ATGGTGACATGCCACAAAAA GCAACACCTTTCCTTCCAAA	208	HF969254
<i>fj</i>	F R	ACAACAACAAGAGCGTCGT CTCACAACACTGCCACCTGA	91	PSN40108.1
<i>fz</i>	F R	CGCGTGTATGGGTTGGAGTT ATAGGTCGCTCTGGATATCG	109	PSN55438.1
<i>kug</i>	F R	TGCTATGATGCCAAGTCGCT TGCACCGACTCGTTCACCTT	90	PSN45660.1
<i>Mhc</i>	F R	ACACCAGGAAGAACCACCAG CTGAGTGCCTCAGCCTTACC	85	LT717632
<i>stan</i>	F R	ACGCACCGAGATTTTACACC ATGCTGAAACCAAGTGGGAAC	70	PSN41253.1
<u><i>dsChmp4b</i></u>	F R	CACAACCTGGTGAAGCTATTCAGAA CTTGTTCCAATTCTTCCAACCTCCT	461	PSN45592.1
<u><i>dsPolyH</i></u>	F R	CCTACGTGTACGACAACAAGT ATGAAGGCTCGACGATCCTA	441	K01149

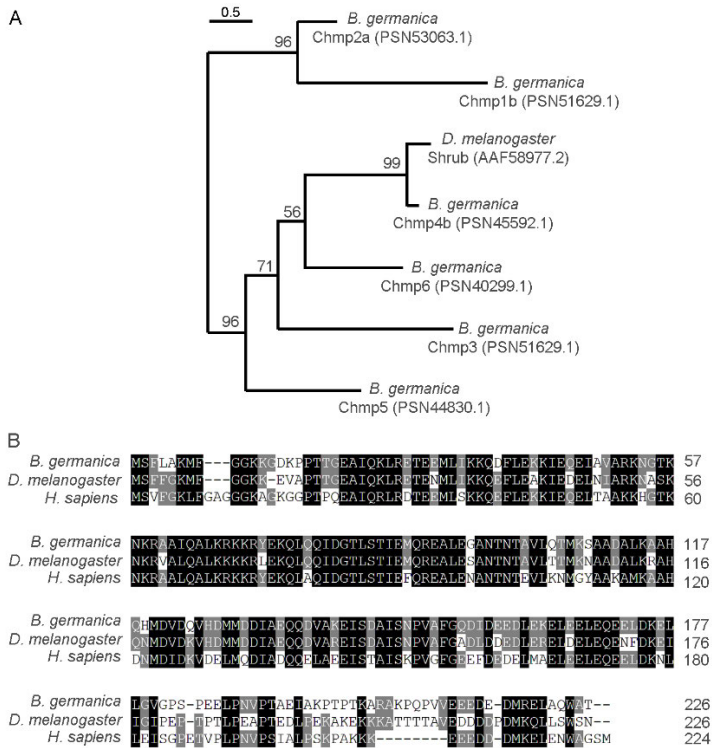


Figure 3.S1. (A) Phylogenetic analysis of *Blattella germanica* CHMP and *Drosophila melanogaster* Shrub proteins, using CHMP sequences annotated in *B. germanica* genome. Protein sequences were aligned using the online software MAFFT (Katoh & Standley, 2016). The resulting alignment was analyzed by PHYML 3.0. program (Guindon & Gascuel, 2003) based on maximum-likelihood principle with the amino acid substitution model. Data were bootstrapped for 100 replicates using PHYML 3.0 program. The accession numbers of the sequences are indicated in the tree, beside the protein name. Scale bar indicates the number of substitutions per site. (B) Alignment of *D. melanogaster* shrub (AAF58977.2), *B. germanica* CHMP4B (PSN45592.1) and *Homo sapiens* CHMP4B (NP_789782.1), showing the high degree of similarity between them. In the case of *D. melanogaster* shrub, and *B. germanica* CHMP4B there is 69% of similarity. Protein sequences were aligned using the online software MAFFT (<http://mafft.cbrc.jp/alignment/software/>) (Katoh & Standley, 2016).

Guindon, S., & Gascuel, O. (2003). A Simple, Fast, and Accurate Algorithm to Estimate Large Phylogenies by Maximum Likelihood. *Systematic Biology*, 52(5), 696–704. <https://doi.org/10.1080/10635150390235520>

Katoh, K., & Standley, D. M. (2016). A simple method to control over-alignment in the MAFFT multiple sequence alignment program. *Bioinformatics*, 32(13), 1933–1942. <https://doi.org/10.1093/bioinformatics/btw108>

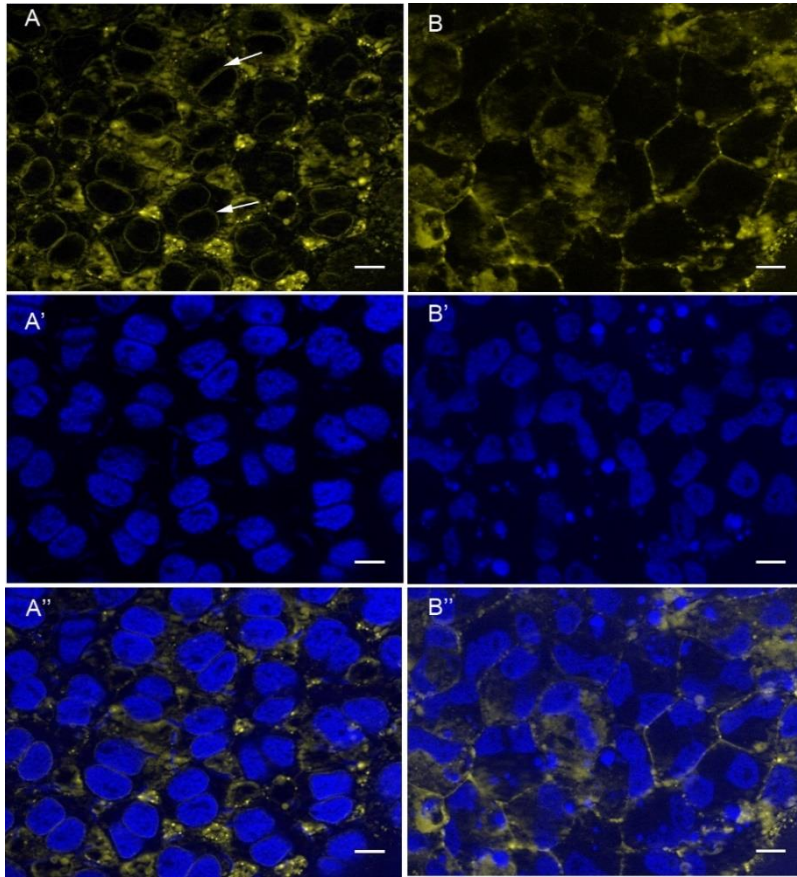


Figure 3.S2. CHMP4B depletion in 5-day-old adult *Blattella germanica* affects the nuclear envelope in the follicular cells of the basal ovarian follicle. (A) Follicular epithelium from a dsMock-treated insect stained with wheat germ agglutinin (WGA). The nuclei membranes (arrows), the cellular membranes and intercellular spaces between FCs appeared stained. (A') Paired nuclei of FCs from image A. (A'') Merged image of A and A', showing the localization of the membranes surrounding the nuclei. (B) Follicular epithelium from a ds*Chmp4b*-treated insect stained with WGA. The nuclear envelope is not stained with WGA. However, WGA staining is present in cytoplasmic membranes and in the cytoplasm of FCs. (B') Nuclei from B, showing variety of sizes and morphologies. (B'') Merged image of B and B' showing cytoplasmic membrane localization but not nuclear localization. DNA was stained with DAPI (blue) and glycoproteins with wheat germ agglutinin (WGA, yellow). After fixation, samples were incubated in PBS with 1 $\mu\text{g/ml}$ of WGA (Sigma) together with 1 $\mu\text{g/ml}$ of DAPI (Sigma) for 5 min. Scale bar: 10 μm .

4. CHARACTERIZATION OF [REDACTED] NANOPARTICLES

4. CHARACTERIZATION OF [REDACTED] NANOPARTICLES

4.1. Introduction

4.1.1. Nanoparticles for dsRNA oral delivery

Several delivery vectors, such as nanoparticles (NPs), have been developed to protect the double-stranded RNA (dsRNA) from the degradation by nucleases and to facilitate its cellular transfection, meaning dsRNA uptake and transport to the cytosol, where RNA interference (RNAi) machinery is located. RNAi-based NPs delivery, especially containing small interfering RNAs (siRNAs), has been extensively studied in the context of human therapy (Ali Zaidi et al., 2023; Setten et al., 2019) and it has been followed by exploitation of these nanomaterials in the area of crop protection (Adeyinka et al., 2020). In insects, various nanomaterials conjugated with dsRNA have successfully demonstrated mortality through oral delivery, improving the effects compared to using naked dsRNA (Pugsley et al., 2021).

The most common nanomaterials used for oral RNAi delivery in insects are the ones that are positively charged because they can form electrostatic interactions between the anionic phosphate backbone of the dsRNA and the cationic nanomaterial (Pugsley et al., 2021). These electrostatic interactions allow the nanomaterial to protect the dsRNA. Moreover, this interaction needs to be stable enough to protect the dsRNA during the transport to the midgut cells while releasing the dsRNA once it reaches the cytosol of the cells. Another important characteristic of nanomaterials is their biocompatibility, meaning low or non-toxicity, since the toxic effect will be achieved by the species-specific effect of the dsRNA (Kozielski et al., 2013).

Several classifications have been established for nucleic acid delivery vectors but, they can be predominantly grouped into two main complexes: liposome-based or lipoplexes and polymer-based or polyplexes (Rafael et al., 2015). Liposomes are spherical vesicles composed of a bilayer of phospholipids that have the ability to encapsulate dsRNA within their aqueous interior (Nitnavare et al., 2021). Liposomes often include neutral lipids in their composition, mainly dioleoyl phosphatidylethanolamine,

cholesterol and dioleoyl phosphatidylcholine (Rafael et al., 2015), which play an important role in improving cellular transfection (Hong et al., 1997). In contrast, polymers are chain-like molecules consisting of a large number of repeating structural units (Hagnauer, 1986). Unlike liposomes, polymers interact with dsRNA without encapsulating it. Polymers can be classified as natural, as chitosan, or synthetic, as polyamidoamine (PAMAM) or polyethylenimine (PEI) (Pugsley et al., 2021).

Even though liposomes and polymers are the most common RNAi-based NPs, other nanomaterials have been developed, known as inorganic and bio-inspired (Pugsley et al., 2021). Inorganic NPs include carbon nanotubes, quantum dots and metal NPs (Zhou et al., 2013). About bio-inspired materials, peptides are the most used in crop protection, especially Branched Amphiphilic Peptide Capsules, which have a similar structure to liposomes but contain lysine surface groups (Avila et al., 2018); and Cell-Penetrating Peptides which enhance cellular transfection of dsRNA (Gillet et al., 2017). Combinations of different nanomaterial types are also possible, such as liposomes with polymers (Su et al., 2023).

We selected four of the most common used cationic nanomaterials to prepare [REDACTED]-NPs. One of them is liposome-based and the other three are polymer-based, being chitosan, PAMAM and linear PEI the selected ones (Figure 4.1). Chitosan, liposomes and PEI have demonstrated effectiveness in causing mortality in insect species by oral delivery (Das et al., 2015; Lin et al., 2017; Ramesh Kumar et al., 2016; Vasquez et al., 2023; Zhang et al., 2015), while PAMAM just by injection (Edwards et al., 2020). Briefly, chitosan is the deacetylated product of chitin, derived from the exoskeleton of crustaceans, insects and fungal cell walls. It is a polysaccharide composed of glucosamine and *N*-acetyl glucosamine. It is low cost, biodegradable and non-toxic (El-banna et al., 2019; Mudo et al., 2022). PAMAM is a synthetic branched dendrimer that comprises a central core with at least two reactive groups; repeating units linked to the central core and distributed in concentric layers named generations; and a high number of terminal functional groups on their surface (Pugsley et al., 2021). Linear PEI is a polymer with C_2H_5N repeating units (Nimesh & Chandra, 2009).

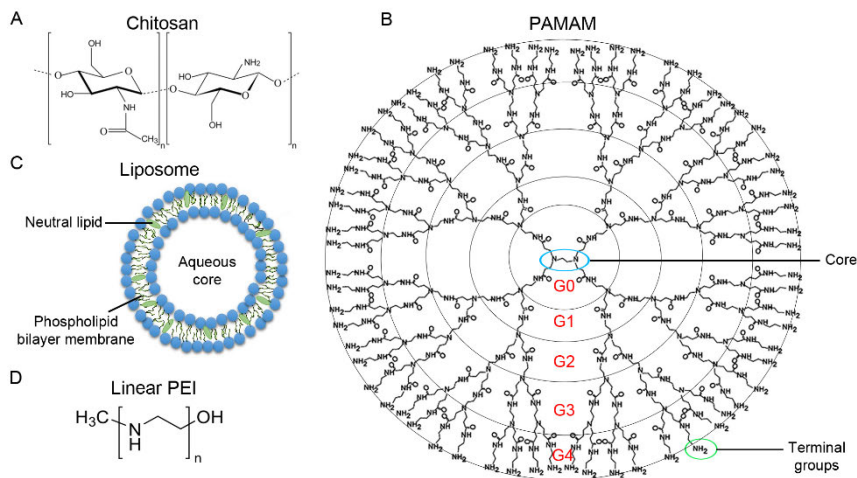


Figure 4.1. Chemical structure of the selected nanomaterials for complexing or encapsulating the dsRNA. (A) Monomers of chitosan, acetylated on the left and deacetylated on the right; (B) polyamidoamine (PAMAM) of 4 generations (G); (C) liposome; and (D) linear polyethylenimine (PEI). Modified from (A) Hamman (2010); (B) Kesharwani et al., (2015); (C) Nsairat et al., (2022); and (D) sigmaaldrich.com.

4.1.2. Selection criteria of nanomaterials for dsRNA oral delivery

The optimum ratio of complexation or encapsulation is a crucial factor for oral delivery. It determines the minimum nanomaterial needed to complex or encapsulate certain quantity of dsRNA, affecting nanoparticle size, NP-cell interaction, and transfection efficiency. An excess of nanomaterial can enhance cellular interaction but may bind dsRNA too tightly, preventing its release in the cytoplasm. Conversely, excess of dsRNA can cause nanoparticle aggregation, reducing transfection efficiency (Alameh et al., 2018; Cao et al., 2019).

The molecular weight (MW) is also a relevant factor for polymers selection. Higher MW chitosan is preferred due to their enhanced stability but it may delay transfection by restricting dsRNA release (Cao et al., 2019; Fernandes et al., 2012). The optimal MW range of chitosan to form NPs with siRNA is 65-170 kDa (Liu et al., 2007). However, in linear polymers, such as PEI, higher MW promotes an increased transfection efficiency due to an

elevated content of amines but, on the other hand, it increases the cytotoxicity (Rafael et al., 2015; Xu et al., 2014). Branched polymers, exemplified by PAMAM, were designed with the aim of reducing cytotoxicity effects of the linear polymers. The use of a higher generation or MW of branched polymers, which means an increase in the number of amine groups capable to interact with the dsRNA, enhances cellular uptake (Pugsley et al., 2021). Specifically for chitosan, the deacetylation degree is also important, since it determines the positive charge, solubility, binding capacity and transfection efficiency of chitosan NPs (Cao et al., 2019). High deacetylation degree (> 80%) is crucial for stable NP formation when complexing with siRNA (Liu et al., 2007).

[REDACTED]

4.2. Materials and methods

4.2.1. Cockroach colony

Specimens of the cockroach *B. germanica* were obtained from a colony fed on dog chow and water *ad libitum*, kept in the dark at 29 ± 1 °C and 60-70% relative humidity.

[REDACTED]

4.2.4. Efficiency of complexation or encapsulation of dsRNA using nanomaterials

The efficiency of complexation was measured maintaining a constant amount of dsRNA and varying the quantity of chitosan, PAMAM and PEI. However, since the concentration of liposomes was unknown, the efficiency of encapsulation was measured maintaining a constant amount of dsRNA, while varying the volume of liposomes. The ratio of complexation or encapsulation was based on the bibliography available with some modifications (Lin et al., 2017; Mudo et al., 2022; Navarro & Tros de Ilarduya, 2009; Vasquez et al., 2023). dsRNA-NPs were electrophoresed through a 1% agarose gel containing SYBR Safe (Invitrogen, Thermo Fisher Scientific) to stain the dsRNA and using 0.5X TBE buffer. The gel was run for 2 h at 80-100 V, and visualized under blue-light. The absence of any fast-migrating dsRNA band in the gel indicates that the dsRNA was efficiently complexed or encapsulated with the nanomaterial (Gurusamy et al., 2020; Lin et al., 2017). The dsRNA conjugated in the cationic nanomaterial becomes a neutral NP, losing its mobility on gel electrophoresis and remaining trapped in the loading well. In the case of CX, the samples were freeze-dried after its preparation to concentrate the sample, facilitating its visualization in the agarose gel. The same volume of each prepared dilution was run on agarose gel to facilitate its visualization in the agarose gel and sample comparisons.

4.2.5. Characterization of dsRNA-nanoparticles in the Scanning Electron Microscope

Samples were prepared at 0.025 $\mu\text{g}/\mu\text{L}$ of dsRNA complexed or encapsulated in chitosan, liposomes, PAMAM or PEI, at the optimum ratios of complexation or encapsulation (see 4.3. Results). Then, 10 μL of CX, PAX and PEIX was air-dried on a glass slide at room temperature. However, LX particles were not subjected to air-drying due to the potential collapse of their lipidic structure upon dehydration, which required the implementation of an alternative protocol explained below.

LX samples were fixed in 1% osmium tetroxide (Merck) while shaking (Thermomixer comfort; Eppendorf) at 600 rpm for 10 min, and then centrifuged 7,500 $\times g$ for 10 min at 4 $^{\circ}\text{C}$. Supernatant was discarded and

samples were incubated with glucose 5% for 10 min and centrifuged 7,500 x g at 4 °C, repeating these two steps for three times. A membrane filter Nuclepore track etched (Whatman, Avantor) with 0.8 µm pore size was hydrated with poly-L-lysine solution 0.01% (Merck) and then the filter was cleaned with water. The sample was then loaded in the filter which was carefully added inside a capsule and afterwards, the sample was dehydrated using a sequence of ethanol solutions of increasing concentration (20%, 40%, 60%, 80%, 95% and 100% ethanol), 5 min each. Subsequently, ethanol was replaced for acetone using an increasing concentration series (25%, 50%, 75% and 100%), 5 min each. The sample was kept in anhydrous acetone and then, it was critical-point dried using dryer CPD 300 (Leica Microsystems).

Once NPs were air-dried or critical point dried, they were placed on stubs and covered with iridium to improve conductivity using a Q150T ES Plus sputter coater (Quorum Technologies). dsRNA-NPs morphology was observed by FE-SEM HITACHI SU8600 Scanning Electron Microscope (SEM) (Hitachi High-Tech). The electron beam energy used was 3 kV. Observations were done at the Microscopy Service of the Institut de Ciències del Mar (CSIC).

4.2.6. Determination of particle size by Dynamic Light Scattering

Nanoparticle size was determined by Dynamic Light Scattering (DLS) measurements using a Photon Correlation Spectrometer 3D (LS Instruments) at the Institut de Química Avançada de Catalunya (CSIC). Polydispersity Index (PDI) was measured together with the nanoparticle size, as an indicator of size distribution of the nanoparticles in the sample, specifying the uniformity of the nanoparticles. A PDI between 0.1-0.25 indicates a narrow size distribution of NPs, meaning homogeneity, while a PDI greater than 0.5 indicates a broad size distribution of NPs, indicative of size heterogeneity (Hoseini et al., 2023). Samples were measured for 50 s at 90° scattering angle at 25°C by a decalin thermostatic bath, which matches the refractive index of glass and does not interfere with the measurement. The particle size was estimated by the Cumulants method, which assumes a single particle size population and applies a single exponential fit to the autocorrelation function (Figure S1, see Annexes).

[REDACTED]

[REDACTED]

4.5. Bibliography

- Adeyinka, O. S., Riaz, S., Toufiq, N., Yousaf, I., Bhatti, M. U., Batcho, A., Olajide, A. A., Nasir, I. A., & Tabassum, B. (2020). Advances in exogenous RNA delivery techniques for RNAi-mediated pest control. *Molecular Biology Reports*, *47*, 6309–6319. <https://doi.org/10.1007/s11033-020-05666-2>
- Alameh, M., Lavertu, M., Tran-Khanh, N., Chang, C. Y., Lesage, F., Bail, M., Darras, V., Chevrier, A., & Buschmann, M. D. (2018). siRNA delivery with chitosan: Influence of chitosan Molecular Weight, Degree of Deacetylation, and Amine to Phosphate Ratio on *in vitro* silencing efficiency, hemocompatibility, biodistribution, and *in vivo* efficacy. *Biomacromolecules*, *19*(1), 112–131. <https://doi.org/10.1021/acs.biomac.7b01297>
- Ali Zaidi, S. S., Fatima, F., Ali Zaidi, S. A., Zhou, D., Deng, W., & Liu, S. (2023). Engineering siRNA therapeutics: challenges and strategies. *Journal of Nanobiotechnology*, *21*, 381. <https://doi.org/10.1186/s12951-023-02147-z>
- Avila, L. A., Chandrasekar, R., Wilkinson, K. E., Balthazor, J., Heerman, M., Bechard, J., Brown, S., Park, Y., Dhar, S., Reeck, G. R., & Tomich, J. M. (2018). Delivery of lethal dsRNAs in insect diets by branched amphiphilic peptide capsules. *Journal of Controlled Release*, *273*, 139–146. <https://doi.org/10.1016/j.jconrel.2018.01.010>



- Cao, Y., Tan, Y. F., Wong, Y. S., Liew, M. W. J., & Venkatraman, S. (2019). Recent advances in chitosan-based carriers for gene delivery. *Marine Drugs*, *17*(6), 381. <https://doi.org/10.3390/md17060381>
- Das, S., Debnath, N., Cui, Y., Unrine, J., & Palli, S. R. (2015). Chitosan, Carbon Quantum Dot, and Silica Nanoparticle mediated dsRNA delivery for gene silencing in *Aedes aegypti*: A comparative analysis. *ACS Applied Materials and Interfaces*, *7*(35), 19530–19535. <https://doi.org/10.1021/acsami.5b05232>
- Edwards, C. H., Christie, C. R., Masotti, A., Celluzzi, A., Caporali, A., & Campbell, E. M. (2020). Dendrimer-coated carbon nanotubes deliver dsRNA and increase the efficacy of gene knockdown in the red flour beetle *Tribolium castaneum*. *Scientific Reports*, *10*, 12422. <https://doi.org/10.1038/s41598-020-69068-x>
- El-banna, F. S., Mahfouz, M. E., Leporatti, S., El-Kemary, M., & Hanafy, N. A. N. (2019). Chitosan as a natural copolymer with unique properties for the development of hydrogels. *Applied Sciences*, *9*(11), 2193. <https://doi.org/10.3390/app9112193>
- Fernandes, J. C., Qiu, X., Winnik, F. M., Benderdour, M., Zhang, X., Dai, K., & Shi, Q. (2012). Low molecular weight chitosan conjugated with folate for siRNA delivery *in vitro*: Optimization studies. *International Journal of Nanomedicine*, *7*, 5833–5845. <https://doi.org/10.2147/IJN.S35567>
- Gillet, F. X., Garcia, R. A., Macedo, L. L. P., Albuquerque, E. V. S., Silva, M. C. M., & Grossi-de-Sa, M. F. (2017). Investigating engineered ribonucleoprotein particles to improve oral RNAi delivery in crop insect pests. *Frontiers in Physiology*, *8*, 256. <https://doi.org/10.3389/fphys.2017.00256>
- Godbey, W. T., Wu, K. K., & Mikos, A. G. (2001). Poly(ethylenimine)-mediated gene delivery affects endothelial cell function and viability. *Biomaterials*, *22*(5), 471–480. [https://doi.org/10.1016/S0142-9612\(00\)00203-9](https://doi.org/10.1016/S0142-9612(00)00203-9)
- Gurusamy, D., Mogilicherla, K., & Palli, S. R. (2020). Chitosan nanoparticles help double-stranded RNA escape from endosomes and improve RNA interference in the fall armyworm, *Spodoptera frugiperda*. *Archives of Insect Biochemistry and Physiology*, *104*(4), e21677. <https://doi.org/10.1002/arch.21677>
- Hagnauer, G. L. (1986). Polymers and Polymer Precursor Characterization. In J. W. McCauley & V. Weiss (Eds.), *Materials Characterization for Systems Performance and Reliability* (pp. 189–243). Springer.

- Hamman, J. H. (2010). Chitosan based polyelectrolyte complexes as potential carrier materials in drug delivery systems. *Marine Drugs*, 8(4), 1305–1322. <https://doi.org/10.3390/md8041305>
- Hoang, N. H., Thanh, T. Le, Sangpueak, R., Treekoon, J., Saengchan, C., Thepbandit, W., Papatoti, N. K., Kamkaew, A., & Buensanteai, N. (2022). Chitosan Nanoparticles-Based Ionic Gelation Method: A promising candidate for Plant Disease Management. *Polymers*, 14(4), 662. <https://doi.org/10.3390/polym14040662>
- Hong, K., Zheng, W., Baker, A., & Papahadjopoulos, D. (1997). Stabilization of cationic liposome-plasmid DNA complexes by polyamines and poly(ethylene glycol)-phospholipid conjugates for efficient *in vivo* gene delivery. *FEBS Letters*, 400(2), 233–237. [https://doi.org/10.1016/S0014-5793\(96\)01397-X](https://doi.org/10.1016/S0014-5793(96)01397-X)
- Hoseini, B., Jaafari, M. R., Golabpour, A., Momtazi-Borojeni, A. A., Karimi, M., & Eslami, S. (2023). Application of ensemble machine learning approach to assess the factors affecting size and polydispersity index of liposomal nanoparticles. *Scientific Reports*, 13, 18012. <https://doi.org/10.1038/s41598-023-43689-4>
- Kesharwani, P., Banerjee, S., Gupta, U., Mohd Amin, M. C. I., Padhye, S., Sarkar, F. H., & Iyer, A. K. (2015). PAMAM dendrimers as promising nanocarriers for RNAi therapeutics. *Materials Today*, 18(10), 565–572. <https://doi.org/10.1016/j.mattod.2015.06.003>
- Kozielski, K. L., Tzeng, S. Y., & Green, J. J. (2013). Bioengineered nanoparticles for siRNA delivery. *WIREs Nanomedicine and Nanobiotechnology*, 5, 449–468. <https://doi.org/10.1002/wnan.1233>
- Lin, Y. H., Huang, J. H., Liu, Y., Bellés, X., & Lee, H. J. (2017). Oral delivery of dsRNA lipoplexes to German cockroach protects dsRNA from degradation and induces RNAi response. *Pest Management Science*, 73(5), 960–966. <https://doi.org/10.1002/ps.4407>
- Liu, X., Howard, K. A., Dong, M., Andersen, M., Rahbek, U. L., Johnsen, M. G., Hansen, O. C., Besenbacher, F., & Kjems, J. (2007). The influence of polymeric properties on chitosan/siRNA nanoparticle formulation and gene silencing. *Biomaterials*, 28(6), 1280–1288. <https://doi.org/10.1016/j.biomaterials.2006.11.004>
- Mudo, L. M. D., Queiroz, A. F. S., de Melo, N. F., Barbosa, M. A. G., de Andrade, E. C., & de Britto, D. (2022). Stability evaluation of dsRNA and DNA encapsulated in chitosan nanoparticles. *BioNanoScience*, 12, 774–784. <https://doi.org/10.1007/s12668-022-01003-y>
- Navarro, G., & Tros de Ilarduya, C. (2009). Activated and non-activated

- PAMAM dendrimers for gene delivery *in vitro* and *in vivo*. *Nanomedicine: Nanotechnology, Biology, and Medicine*, 5(3), 287–297. <https://doi.org/10.1016/j.nano.2008.12.007>
- Nimesh, S., & Chandra, R. (2009). Polyethylenimine nanoparticles as an efficient *in vitro* siRNA delivery system. *European Journal of Pharmaceutics and Biopharmaceutics*, 73(1), 43–49. <https://doi.org/10.1016/j.ejpb.2009.04.001>
- Nitnavare, R. B., Bhattacharya, J., Singh, S., Kour, A., Hawkesford, M. J., & Arora, N. (2021). Next Generation dsRNA-Based Insect Control: Success So Far and Challenges. *Frontiers in Plant Science*, 12, 673576. <https://doi.org/10.3389/fpls.2021.673576>
- Nsairat, H., Khater, D., Sayed, U., Odeh, F., Al Bawab, A., & Alshaer, W. (2022). Liposomes: structure, composition, types, and clinical applications. *Heliyon*, 8(5), e09394. <https://doi.org/10.1016/j.heliyon.2022.e09394>
- Pugsley, C. E., Isaac, R. E., Warren, N. J., & Cayre, O. J. (2021). Recent Advances in Engineered Nanoparticles for RNAi-Mediated Crop Protection Against Insect Pests. *Frontiers in Agronomy*, 3, 652981. <https://doi.org/10.3389/fagro.2021.652981>
- Rafael, D., Andrade, F., Arranja, A., Luís, S., & Videira, M. (2015). Lipoplexes and Polyplexes: Gene Therapy. In M. K. Mishra (Ed.), *Encyclopedia of Biomedical Polymers and Polymeric Biomaterials* (pp. 4335–4347). <https://doi.org/10.1081/e-ebpp-120050058>
- Rahdar, A., Amini, N., Askari, F., Bin, M. A., & Susan, H. (2019). Dynamic light scattering: A useful technique to characterize nanoparticles. *J. Nanoanalysis*, 6(2), 80–89. <https://doi.org/10.22034/JNA.2019.667079>
- Ramesh Kumar, D., Saravana Kumar, P., Gandhi, M. R., Al-Dhabi, N. A., Paulraj, M. G., & Ignacimuthu, S. (2016). Delivery of chitosan/dsRNA nanoparticles for silencing of wing development vestigial (vg) gene in *Aedes aegypti* mosquitoes. *International Journal of Biological Macromolecules*, 86, 89–95. <https://doi.org/10.1016/j.ijbiomac.2016.01.030>
- Setten, R. L., Rossi, J. J., & Han, S. ping. (2019). The current state and future directions of RNAi-based therapeutics. *Nature Reviews Drug Discovery*, 18, 421–446. <https://doi.org/10.1038/s41573-019-0017-4>
- Su, C., Liu, S., Sun, M., Yu, Q., Li, C., Graham, R. I., Wang, X., Wang, X., Xu, P., & Ren, G. (2023). Delivery of Methoprene-Tolerant dsRNA to Improve RNAi Efficiency by Modified Liposomes for Pest Control.

- ACS Applied Materials and Interfaces*, 15(10), 13576–13588. <https://doi.org/10.1021/acsami.2c20151>
- Vasquez, D. D. N., Pinheiro, D. H., Teixeira, L. A., Moreira-Pinto, C. E., Macedo, L. L. P., Salles-Filho, A. L. O., Silva, M. C. M., Lourenço-Tessutti, I. T., Morgante, C. V., Silva, L. P., & Grossi-de-Sa, M. F. (2023). Simultaneous silencing of juvenile hormone metabolism genes through RNAi interrupts metamorphosis in the cotton boll weevil. *Frontiers in Molecular Biosciences*, 10, 1073721. <https://doi.org/10.3389/fmolb.2023.1073721>
- Xu, Z., He, B., Wei, W., Liu, K., Yin, M., Yang, W., & Shen, J. (2014). Highly water-soluble perylenediimide-cored poly(amido amine) vector for efficient gene transfection. *Journal of Materials Chemistry B*, 2(20), 3079–3086. <https://doi.org/10.1039/c4tb00195h>
- Zhang, X., Mysore, K., Flannery, E., Michel, K., Severson, D. W., Zhu, K. Y., & Duman-Scheel, M. (2015). Chitosan/interfering RNA nanoparticle mediated gene silencing in disease vector mosquito larvae. *Journal of Visualized Experiments*, 2015(97), 1–2. <https://doi.org/10.3791/52523>
- Zhou, J., Shum, K. T., Burnett, J. C., & Rossi, J. J. (2013). Nanoparticle-based delivery of RNAi therapeutics: Progress and challenges. *Pharmaceuticals*, 6(1), 85–107. <https://doi.org/10.3390/ph6010085>

**5. dsRNA ORALLY DELIVERED TO ADULT
FEMALES**

5. dsRNA ORALLY DELIVERED TO ADULT FEMALES

5.1. Introduction

5.1.1. The insect gut

Throughout evolution, the insect gut has undergone various modifications in response to the food requirements and insect habitats. In cockroaches, which are omnivorous, the mouthparts facilitate them to bite and chew hard materials, consume soft foods and lap up liquids. Mouthparts together with the enzymes secreted by the salivary glands initiate the digestion of food (Miall & Denny, 1886). Processed food travels to the insect gut, a tube that goes from mouth to anus, and is divided into three parts: foregut, midgut, and hindgut (Figure 5.1).

The foregut is concerned with ingesting the food, continuing its digestion and transferring it to the midgut; these activities involve the pharynx and the oesophagus. The foregut often forms a storage organ, known as the crop, and sometimes also a grinding organ called the gizzard (Figure 5.1). The midgut epithelium is involved in the synthesis and secretion of digestive enzymes into the lumen of the ventriculus, as well as the absorption of nutrients by specialized epithelial cells with microvilli. In many species, a peritrophic membrane delimits food from the epithelial cells (Kerkut & Gilbert, 1985). Additionally, some insects have gastric caeca in the midgut (Figure 5.1), a structure that also contributes to the secretion of enzymes and the absorption of food and water. Moreover, in the junction between midgut and hindgut, there are located the Malpighian tubules, which have excretory and osmoregulatory functions (Figure 5.1) (Klowden, 2008). Finally, the hindgut is divided into three parts: the pylorus, the ileum, sometimes the posterior part of it is referred as colon, and the rectum (Figure 5.1). The cells of the rectum are often involved in the absorption of water and salts, and with defecation (Kerkut & Gilbert, 1985; Miall & Denny, 1886).

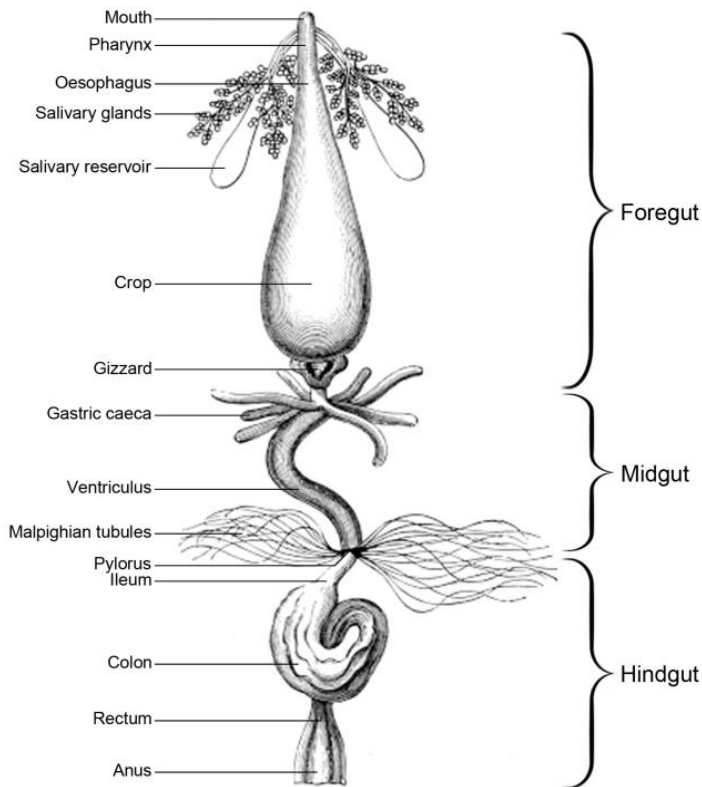


Figure 5.1. Illustration indicating the three main divisions of the gut and their structures in the cockroach *Periplaneta americana*. Modified from Miall & Denny, (1886).

5.1.2. dsRNA feeding and the barriers that limit its efficiency

The discovery that double-stranded RNA (dsRNA) could be effectively delivered orally was first demonstrated in the nematode *C. elegans*, in which feeding of *Escherichia coli* bacteria expressing dsRNA resulted in the same phenotype as injected dsRNA (Lisa et al., 2001; Timmons & Fire, 1998). This method quickly garnered the attention for its potential in agricultural pest protection, mainly because it offered a practical alternative to injection techniques (Yu et al., 2013).

Successful gene silencing through oral delivery has been reported in many insect species (Kunte et al., 2020). However, the efficiency of dsRNA when

provided by ingestion is variable and differs notably between orders and species (Nitnavare et al., 2021). This variability is attributed to the barriers that dsRNA needs to overcome to reach the cytoplasm of the midgut cells (Figure 5.2). In the ideal case, once dsRNA is ingested, specialized epithelial cells of the midgut take up the dsRNA in their apical pole and transport it to the basolateral side, which will produce the later systemically spread of the dsRNA effect to other tissues in the body (Caccia et al., 2019; Kunte et al., 2020). In addition, the different tissues could exhibit different susceptibility to the dsRNA effect (Wynant et al., 2012), exacerbating the variability of dsRNA efficiency across insect species.

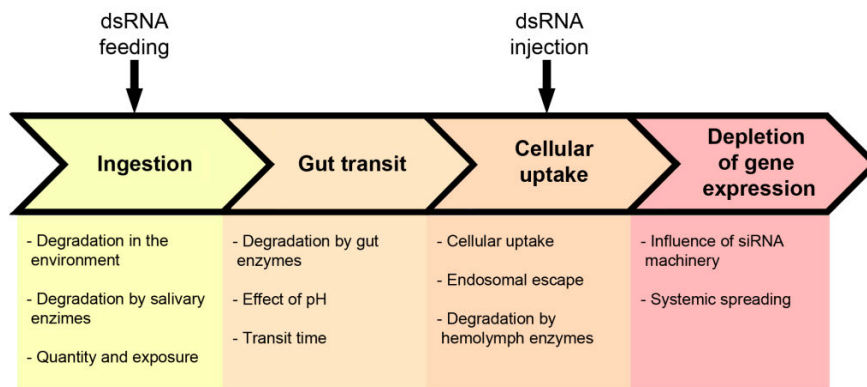


Figure 5.2. Schema underlining the main barriers that dsRNA has to overcome during ingestion, gut transition, cellular uptake and depletion of gene expression, through oral delivery compared to the barriers that dsRNA could find when injected.

5.1.2.1. Degradation of dsRNA by RNases and effect of pH

To be effective by oral delivery, dsRNA must be stable enough to prevent degradation before ingestion. Environmental factors such as UV light and microorganisms can degrade dsRNA, whereas rain can hydrate dsRNA, making it less stable (Christiaens et al., 2020). Therefore, all these factors must be considered when dsRNA is used in pest control.

Moreover, once ingested, the dsRNA could be degraded by RNases from salivary glands and midgut secretions (Christiaens et al., 2020). The physiological pH of the gut significantly influences enzymatic activity, with evidences suggesting its optimal function in alkaline conditions (Luo et al.,

2013). Diptera, Hymenoptera, Orthoptera, and Lepidoptera have alkaline midguts (Cooper et al., 2019), enhancing dsRNA degradation due to phosphodiester bonds hydrolysis (Zhang et al., 2021). Conversely, Hemiptera and Coleoptera have slightly acidic midguts (Cooper et al., 2019), in which dsRNA degradation would be at slower rates than in alkaline conditions (Järvinen et al., 1991).

5.1.2.2. Cellular uptake of dsRNA and systemic spreading of the dsRNA effect

Two mechanisms facilitate the internalization of orally administered dsRNA into midgut cells of insects: endocytosis and the involvement of Sid-1-like receptors (Huvenne & Smagghe, 2010). Among these, the main cellular dsRNA uptake mechanism in insects is the receptor-mediated endocytosis, with clathrin vesicles as the most documented pathway (Wytinck et al., 2020), first described *in vitro* in *Drosophila melanogaster* S2 cells (Saleh et al., 2006; Ulvila et al., 2006).

In the nematode *C. elegans*, dsRNA cellular uptake occurs by the transmembrane channels Sid-1, expressed in almost all tissues, together with Sid-2, exclusive of the gut (Winston et al., 2007). Once in the cytoplasm, the RNA interference (RNAi) machinery generates siRNAs, which are amplified by an RNA-dependent RNA polymerase (RdRP), transported to closer cells and systemically spread to other tissues through Sid-1 channels (Adeyinka et al., 2020; Joga et al., 2016). In insects, no RdRP or *sid-2* homologs have been found (Firmino et al., 2013; Tomoyasu et al., 2008; Vélez & Fishilevich, 2018), but *sid-1*-like genes have been identified, with unclear functional homology (Cooper et al., 2019; Tomoyasu et al., 2008).

Whether the form of the signal that produces the RNAi effect in close and distant cells is dsRNA or siRNA remains uncertain in insects (Vélez & Fishilevich, 2018). Additionally, the spreading mechanism used by the dsRNA or siRNA has not been deeply studied in insects (Santos et al., 2021). In some insect species, it was observed that siRNA or dsRNA molecules were transported to distant tissues via extracellular vesicles or by interaction with RNA-binding proteins (Mingels et al., 2020; Tassetto et al., 2017; Wynant, et al., 2014b; Yoon et al., 2020). In addition, nanotube-like

structures were proposed for the transport between close cells (Karlikow et al., 2016).

5.1.2.3. Endosomal escape of dsRNA

One of the major bottlenecks for dsRNA efficiency is the endosomal barrier (Figure 5.3) (Dominska & Dykxhoorn, 2010). As previously explained, receptor-mediated endocytosis is the most common mechanism of dsRNA cellular uptake. Once dsRNA is trapped inside endocytic vesicles, dsRNA is delivered to the early endosomes that gradually mature into late endosomes (Figure 5.3) (Casey et al., 2010). During the maturation, endosomes are acidified by membrane-bound proton-pump ATPases (V-ATPases), being the late endosomes more acidic than the early ones (Dominska & Dykxhoorn, 2010). Finally, the late endosome fuses with the lysosome for degradation (Figure 5.3). If the dsRNA does not escape from the endosomes, it will be trafficked toward the lysosomes, where digestive enzymes would degrade it (Ohkuma & Poole, 1978). Therefore, to knockdown gene expression, dsRNA must escape from the endosomes to the cytoplasm, where the RNAi machinery is located (Gurusamy et al., 2020; Yoon et al., 2017). The differences in the efficiency of endosomal escape of dsRNA between species are explained by the variations in the time window of endosomal maturation and fusion of lysosomes (Cooper et al., 2019).

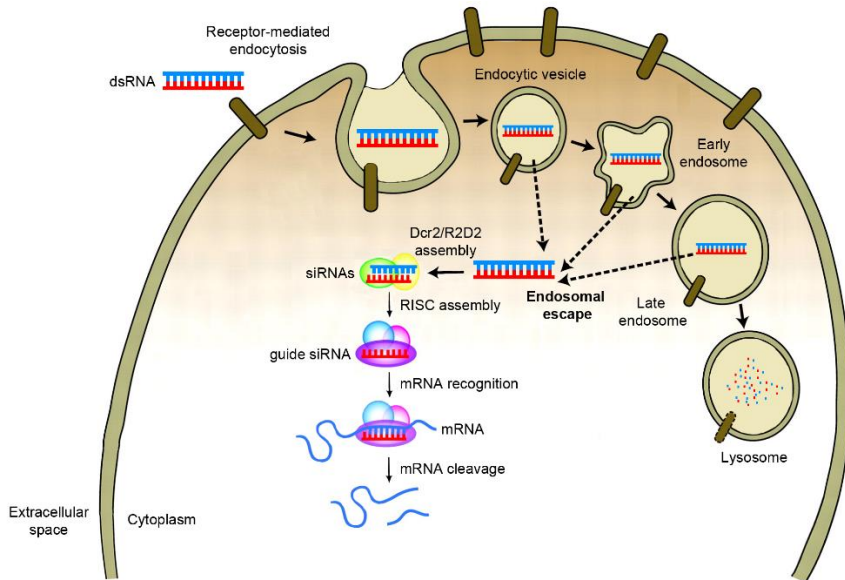


Figure 5.3. Endosomal escape of dsRNA. dsRNA is internalized by receptor-mediated endocytosis. The endocytic vesicles fuse to form the early endosome that matures to a late endosome while decreasing its pH. dsRNA has to escape from the endosomes to prevent being incorporated into the lysosome, which contains enzymes and low pH able to degrade the dsRNA. dsRNA in the cytoplasm interacts with the RNAi machinery to direct the cleavage of the complementary mRNA. Modified from Dominska & Dykxhoorn et al. (2010).

5.1.2.4. Other factors influencing dsRNA efficiency

Once dsRNA reaches the cytoplasm, the gene copy number and the expression rate of enzymes involved in siRNA production could contribute to differences in the dsRNA efficiency among insects (Singh et al., 2017). The components of the siRNA pathway in insects have undergone various gene duplications and deletions during evolution (Dowling et al., 2016). However, it has been speculated that the expression of enzymes involved in siRNA production is more important than the number of gene copies (Cooper et al., 2019; Swevers et al., 2011). In addition, the expression of these enzymes could be affected by the repeated exposure to dsRNA, infection by virus, starvation, or environmental factors such as temperature. Also, the biochemical kinetics of the enzymes involved in siRNA production, meaning the strong binding to the dsRNA or siRNA strands, is also an important factor (Cooper et al., 2019).

The dsRNA efficiency could also be affected by the quantity of dsRNA provided and its transit through the gut. Since dsRNA delivered by ingestion has to overcome several barriers, the amount of dsRNA that ultimately reaches the siRNA machinery of the midgut cells can be reduced in each step. Consequently, large amounts of dsRNA need to be fed to trigger its effects (Kunte et al., 2020). Alternatively, the continuous administration of dsRNA increases the efficacy of the treatment (Prentice et al., 2017). In addition, the gut transit varies among species (Chapman, 2013): while in the American cockroach *Periplaneta americana* lasts 20 hours to empty the gut (Bignell, 1981), in the case of *Blattella germanica*, the food lasts approximately 10 min to reach the midgut and 5 hours to arrive the rectum (Day & Powning, 1949). In general, rapid transit could reduce dsRNA uptake, while slow transit could facilitate its cellular uptake due to prolonged exposure time.

5.1.3. Enhancing dsRNA efficiency using nanoparticles

Nanoparticles (NPs) can act as delivery vectors designed to overcome the barriers that limit dsRNA efficiency, mainly protecting dsRNA from degradation by nucleases and facilitating cellular transfection of dsRNA, including cellular uptake and endosomal escape. The mechanisms of escape from endosomes differ from lipoplexes to polyplexes, and are based on the transient pore model or the proton-sponge effect, respectively (Yan et al., 2021). These mechanisms, explained below, are based on the most recent knowledge about endosomal escape. However, there is still lack of understanding of the endosomal escape process that must be addressed to precise engineering of the NPs (Vermeulen et al., 2018; Xu et al., 2021).

5.1.3.1. The transient pore model

The transient pore model used by lipoplexes to escape endosomes, involves a localized destabilization of the endosomal membrane induced by the close proximity of the lipoplex (Figure 5.4). This perturbation is possible due to the fact that endosomes in their inner membrane are enriched with anionic lipids, such as lysobisphosphatidic acid, which can interact with the cationic liposome. This electrostatic interaction led to the mixing, dispersal, or degradation of some lipid molecules of the endosome membrane resulting in the formation of transient pores on it, facilitating the gradual passage of dsRNA into the cytosol (Figure 5.4). Subsequently, the initially membrane-

dispersed lipids are reintegrated in that specific region, closing the pore (Figure 5.4) (Degors et al., 2019; Rehman et al., 2013).

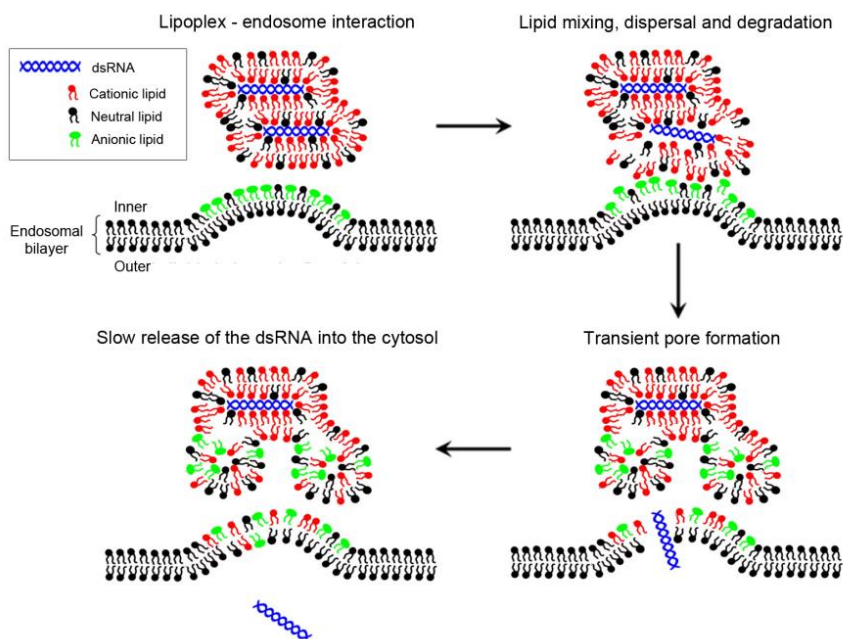


Figure 5.4. The transient pore model for endosomal escape of lipoplexes. Electrostatic interactions between cationic lipoplexes and anionic lipids of the inner endosomal membrane can induce a localized destabilization of the endosome. This leads to mixing, dispersal and degradation of lipids, promoting the formation of transient pores. dsRNA could gradually pass through these pores to the cytosol before their closure. Modified from Degors et al. (2019).

5.1.3.2. The proton-sponge effect model

The proton-sponge effect used by polyplexes to escape endosomes, is based on the combination of three factors: 1) the osmotic pressure inside the endosome, 2) polymer extension and 3) destabilization of the endosomal membrane, leading altogether to the release of its content into the cytosol of the cell (Vermeulen et al., 2018).

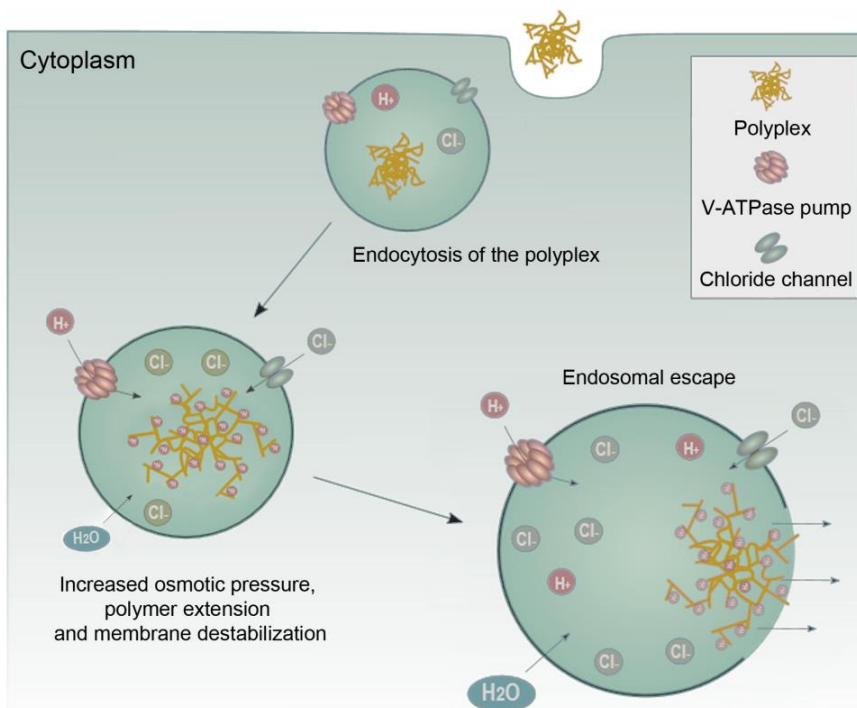
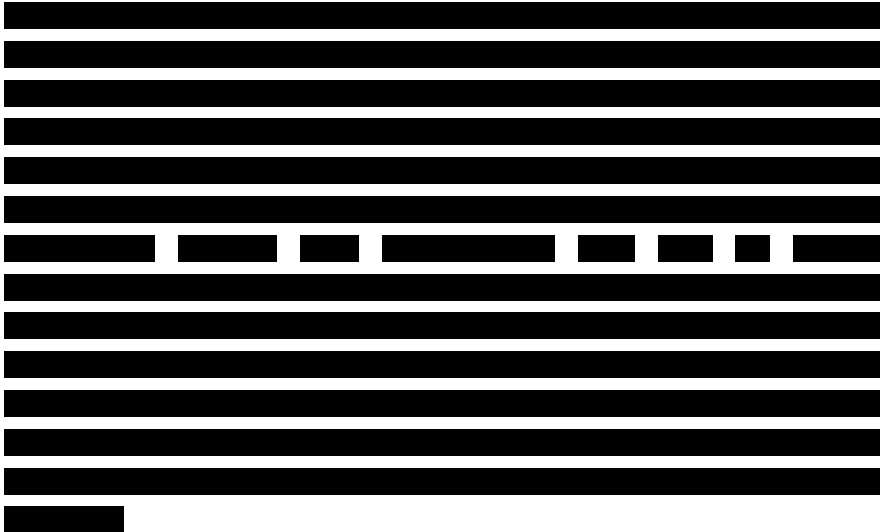


Figure 5.5. Proton-sponge effect model for endosomal escape of polyplexes. Local endosomal rupture is due to the combination of increased osmotic pressure, because of the buffer capacity of the polymer, to polymer extension due to charge repulsion upon protonation, and membrane destabilization because of the interaction between the protonated polymer and the endosomal membrane. Modified from Vermeulen et al. (2018).

Inside the acidic endosomes, polymers act as buffers by binding protons. This buffering capacity limits the acidification of the endosome and as a consequence, the V-ATPase proton pumps will translocate more protons inside the endosome to lower the pH. The translocation of the protons is accompanied by the entry of chloride ions to maintain the charge balance, increasing the ionic concentration inside the endosome. Then, an influx of water molecules will enter to maintain the osmolarity, increasing osmotic pressure. Protonated polyplex undergo conformational extension due to electrostatic repulsion between their charges, interacting with the endosomal membrane and causing its destabilization (Vermeulen et al., 2018). Finally, membrane destabilization leads to localized endosomal rupture, promoting polyplex release into the cytosol without complete lysis

or cytotoxicity (Rehman et al., 2013). Once in the cytosol, dsRNA must unbind sufficiently from the polymer to become available for RNAi machinery (Kozielski et al., 2013). This process differs from lipoplexes, where dsRNA is directly released into the cytosol (Tros de Ilarduya et al., 2010).



5.2. Materials and methods

5.2.1. Cockroach colony and tissues sampling

Specimens of the cockroach *B. germanica* were obtained from a colony fed on dog chow and water *ad libitum*, kept in the dark at 29 ± 1 °C and 60-70% relative humidity. Dissections were performed on carbon dioxide-anaesthetized specimens, held under Ringer's saline. After dissection, tissue samples were immediately frozen in liquid nitrogen and stored at -80 °C.

5.2.2. RNA extraction, cDNA synthesis and quantitative real-time PCR analysis

Total RNA from midgut was extracted using HigherPurity™ Tissue Total RNA Purification kit (Canvax Biotech S.L.). The extracted RNA was treated with DNase (Thermo Fisher Scientific) and then retrotranscribed to

cDNA using the Transcriptor First Strand cDNA Synthesis kit (Roche Diagnostics GmbH), following the manufacturer's instructions. The absence of genomic contamination was confirmed using a control without reverse transcription. The quantity of RNA retrotranscribed varied in each experiment, but comparisons were made between samples with the same amount of retrotranscribed RNA.

The expression levels of the different genes studied were analyzed by quantitative real-time PCR (qRT-PCR) using cDNA from the midgut of 4-day-old or 6-day-old adult females. Amplification reactions were carried out in a CFX Opus 384 Real-Time PCR System (BioRad) using the iTaq Universal SYBR Green Supermix (BioRad) following this program: (i) 95 °C for 3 min, (ii) 95 °C for 10 s; (iii) 57 °C for 1 min; (iv) steps (ii) and (iii) were repeated for 44 cycles. After the amplification phase, a dissociation curve was carried out to ensure that only one product was amplified. Levels of mRNA were calculated relative to the reference gene, using the $2^{-\Delta C_t}$ method (Alborzi & Piulachs, 2023; Irls et al., 2009; Livak & Schmittgen, 2001). The PCR primers used in qRT-PCR expression studies were designed using the Primer3 v.4.1.0 software (Rozen & Skaletsky, 2000). The *Eukaryotic translation Initiation Factor 4aIII (eIF4aIII)* was used as reference gene. The expression levels of [REDACTED] and *eIF4aIII* were quantified from 2 to 3 independent biological samples, making 3 technical replicates of each one, in a final volume of 10 µL. A control without template was included in all batches. The sequence of the primers used, and the accession number of genes analyzed are detailed in Table S1 (See Annexes).

[REDACTED]

[REDACTED]
[REDACTED]
[REDACTED]
[REDACTED]
[REDACTED]
[REDACTED]

5.2.4. [REDACTED] and dsPolyH synthesis

[REDACTED]
[REDACTED]
[REDACTED] As a negative control, a heterologous 441 bp fragment from polyhedrin of the *Autographa californica* nucleopolyhedrovirus was used (dsPolyH) (Lozano & Bellés, 2011). dsRNAs were synthesized using MEGAscript™ RNAi kit (Invitrogen), as detailed in Chapter 2, and stored at -20 °C until its use. The sequence and the accession number of the selected genes are detailed in Data S1 (See Annexes).

[REDACTED]

[REDACTED]
[REDACTED]
[REDACTED]
[REDACTED] [REDACTED] [REDACTED] [REDACTED] [REDACTED] [REDACTED]
[REDACTED]

[REDACTED]

[REDACTED]
[REDACTED]
[REDACTED]

[REDACTED]

[REDACTED]
[REDACTED]
[REDACTED]
[REDACTED]
[REDACTED]
[REDACTED]
[REDACTED]
[REDACTED]

[REDACTED]
[REDACTED]
[REDACTED]
[REDACTED]

[REDACTED]

[REDACTED]

[REDACTED]

[REDACTED]

[REDACTED]

5.2.7. Statistical analysis

All data were expressed as mean ± standard error of the mean (S.E.M.). Data were evaluated for normality and homogeneity of variance using the

Shapiro-Wilk test, which showed that no transformations were needed. All datasets passed the normality test. Statistical analyses for mean comparison were performed employing Student's *t*-test. A *p*-value < 0.05 was considered statistically significant. Data were analyzed using GraphPad Prism version 8.1.0 for Windows, GraphPad Software.

[REDACTED]

[REDACTED]

[REDACTED]

[REDACTED]

[REDACTED]

[REDACTED]

[REDACTED]

[REDACTED]

[REDACTED]

[REDACTED]

[REDACTED]

[REDACTED]

[REDACTED]

[REDACTED]

[REDACTED]


[REDACTED]

[REDACTED]

[REDACTED]



5.5. Bibliography

- Adeyinka, O. S., Riaz, S., Toufiq, N., Yousaf, I., Bhatti, M. U., Batcho, A., Olajide, A. A., Nasir, I. A., & Tabassum, B. (2020). Advances in exogenous RNA delivery techniques for RNAi-mediated pest control. *Molecular Biology Reports*, *47*, 6309–6319. <https://doi.org/10.1007/s11033-020-05666-2>
- Alborzi, Z., & Piulachs, M. D. (2023). Dual function of the transcription factor Ftz-f1 on oviposition in the cockroach *Blattella germanica*. *Insect Molecular Biology*, *32*(6), 689–702. <https://doi.org/10.1111/imb.12866>
- Arjunan, N., Thiruvengadam, V., & Sushil, S. N. (2024). Nanoparticle-mediated dsRNA delivery for precision insect pest control: a comprehensive review. *Molecular Biology Reports*, *51*, 355. <https://doi.org/10.1007/s11033-023-09187-6>
- Biggnell, D. (1981). Nutrition and digestion. In W. J. Bell & K. G. Adiyodi (Eds.), *The American Cockroach*. Springer. https://doi.org/https://doi.org/10.1007/978-94-009-5827-2_4
- Caccia, S., Casartelli, M., & Tettamanti, G. (2019). The amazing complexity of insect midgut cells: types, peculiarities, and functions. *Cell and Tissue Research*, *377*, 505–525. <https://doi.org/10.1007/s00441-019-03076-w>
- Casey, J. R., Grinstein, S., & Orlowski, J. (2010). Sensors and regulators of intracellular pH. *Nature Reviews Molecular Cell Biology*, *11*, 50–61. <https://doi.org/10.1038/nrm2820>
- Chapman, R. F. (2013). The head, ingestion, utilization and distribution of food. In S. J. Simpson & E. Douglas (Eds.), *The Insects. Structure and function*. Cambridge University Press. <https://doi.org/10.1017/cbo9780511818202.007>
- 

- Christiaens, O., Whyard, S., Vélez, A. M., & Smagghe, G. (2020). Double-Stranded RNA Technology to Control Insect Pests: Current Status and Challenges. *Frontiers in Plant Science*, *11*, 451. <https://doi.org/10.3389/fpls.2020.00451>
- Cooper, A. M. W., Silver, K., Zhang, J., Park, Y., & Zhu, K. Y. (2019). Molecular mechanisms influencing efficiency of RNA interference in insects. *Pest Management Science*, *75*(1), 18–28. <https://doi.org/10.1002/ps.5126>
- Day, M., & Powning, R. (1949). A study of the processes of digestion in certain insects. *Australian Journal of Biological Sciences*, *2*(2), 175–215. <https://doi.org/10.1071/BI9490175>
- Degors, I. M. S., Wang, C., Rehman, Z. U., & Zuhorn, I. S. (2019). Carriers break barriers in drug delivery: endocytosis and endosomal escape of gene delivery vectors. *Accounts of Chemical Research*, *52*(7), 1750–1760. <https://doi.org/10.1021/acs.accounts.9b00177>
- Dominska, M., & Dykxhoorn, D. M. (2010). Breaking down the barriers: siRNA delivery and endosome escape. *Journal of Cell Science*, *123*(8), 1183–1189. <https://doi.org/10.1242/jcs.066399>
- Dowling, D., Pauli, T., Donath, A., Meusemann, K., Podsiadlowski, L., Petersen, M., Peters, R. S., Mayer, C., Liu, S., Zhou, X., Misof, B., & Niehuis, O. (2016). Phylogenetic origin and diversification of RNAi pathway genes in insects. *Genome Biology and Evolution*, *8*(12), 3784–3793. <https://doi.org/10.1093/gbe/evw281>
- Firmino, A. A. P., De Fonseca, F. C. A., De Macedo, L. L. P., Coelho, R. R., De, J. D. A. S., Togawa, R. C., Silva-Junior, O. B., Pappas-Jr, G. J., Silva, M. C. M. Da, Engler, G., & Grossi-de-Sa, M. F. (2013). Transcriptome analysis in cotton boll weevil (*Anthonomus grandis*) and RNA interference in insect pests. *PLOS ONE*, *8*(12), e85079. <https://doi.org/10.1371/journal.pone.0085079>
- Gurusamy, D., Mogilicherla, K., Shukla, J. N., & Palli, S. R. (2020). Lipids help double-stranded RNA in endosomal escape and improve RNA interference in the fall armyworm, *Spodoptera frugiperda*. *Archives of Insect Biochemistry and Physiology*, *104*(4), 1–19. <https://doi.org/10.1002/arch.21678>
- Huvenne, H., & Smagghe, G. (2010). Mechanisms of dsRNA uptake in insects and potential of RNAi for pest control: A review. *Journal of Insect Physiology*, *56*(3), 227–235. <https://doi.org/10.1016/j.jinsphys.2009.10.004>
- Irles, P., Bellés, X., & Piulachs, M. D. (2009). Identifying genes related to

- choriogenesis in insect panoistic ovaries by Suppression Subtractive Hybridization. *BMC Genomics*, *10*, 206. <https://doi.org/10.1186/1471-2164-10-206>
- Järvinen, P., Oivanen, M., & Lönnberg, H. (1991). Interconversion and phosphoester hydrolysis of 2',5'- and 3',5'-dinucleosidemonophosphates: kinetics and mechanisms. *The Journal of Organic Chemistry*, *56*, 5396–5401.
- Joga, M. R., Zotti, M. J., Smagghe, G., & Christiaens, O. (2016). RNAi efficiency, systemic properties, and novel delivery methods for pest insect control: What we know so far. *Frontiers in Physiology*, *7*, 553. <https://doi.org/10.3389/fphys.2016.00553>
- Karlikow, M., Goic, B., Mongelli, V., Salles, A., Schmitt, C., Bonne, I., Zurzolo, C., & Saleh, M. C. (2016). *Drosophila* cells use nanotube-like structures to transfer dsRNA and RNAi machinery between cells. *Scientific Reports*, *6*, 27085. <https://doi.org/10.1038/srep27085>
- Kerkut, G., & Gilbert, L. (1985). Regulation: Digestion, Nutrition, Excretion. In *Comprehensive Insect Physiology, Biochemistry and Pharmacology*. Pergamon Press.
- Klowden, M. J. (2008). Metabolic Systems. In *Physiological Systems in Insects* (pp. 293–355). Academic Press. <https://doi.org/10.1016/b978-0-12-415819-1.00006-4>
- Kozielski, K. L., Tzeng, S. Y., & Green, J. J. (2013). Bioengineered nanoparticles for siRNA delivery. *WIREs Nanomedicine and Nanobiotechnology*, *5*, 449–468. <https://doi.org/10.1002/wnan.1233>
- Kunte, N., McGraw, E., Bell, S., Held, D., & Avila, L. A. (2020). Prospects, challenges and current status of RNAi through insect feeding. *Pest Management Science*, *76*(1), 26–41. <https://doi.org/10.1002/ps.5588>
- Lin, Y. H., Huang, J. H., Liu, Y., Bellés, X., & Lee, H. J. (2017). Oral delivery of dsRNA lipoplexes to German cockroach protects dsRNA from degradation and induces RNAi response. *Pest Management Science*, *73*(5), 960–966. <https://doi.org/10.1002/ps.4407>
- Lisa, T., Donald, L. C., & Andrew, F. (2001). Ingestion of bacterially expressed dsRNAs can produce specific and potent genetic interference in *Caenorhabditis elegans*. *Gene*, *263*, 103–112. www.elsevier.com/locate/gene
- Livak, K. J., & Schmittgen, T. D. (2001). Analysis of relative gene expression data using real-time quantitative PCR and the $2^{-\Delta\Delta CT}$ method. *Methods*, *25*(4), 402–408. <https://doi.org/10.1006/meth.2001.1262>

- Long, G. J., Liu, X. Z., Guo, H., Zhang, M. Q., Gong, L. L., Ma, Y. F., Dewar, Y., Mo, W. J., Ding, L. W., Wang, Q., He, M., & He, P. (2023). Oral-based nanoparticle-wrapped dsRNA delivery system: a promising approach for controlling an urban pest, *Blattella germanica*. *Journal of Pest Science*, *97*, 739–755. <https://doi.org/10.1007/s10340-023-01677-7>
- Lozano, J., & Bellés, X. (2011). Conserved repressive function of Krüppel homolog 1 on insect metamorphosis in hemimetabolous and holometabolous species. *Scientific Reports*, *1*, 163. <https://doi.org/10.1038/srep00163>
- Luo, Y., Wang, X., Wang, X., Yu, D., Chen, B., & Kang, L. (2013). Differential responses of migratory locusts to systemic RNA interference via double-stranded RNA injection and feeding. *Insect Molecular Biology*, *22*(5), 574–583. <https://doi.org/10.1111/imb.12046>
- Miall, L., & Denny, A. (1886). *The Structure and Life-history of the Cockroach (Periplaneta orientalis)*. Lovell Reeve.
- Mingels, L., Wynant, N., Santos, D., Peeters, P., Gansemans, Y., Billen, J., Van Nieuwerburgh, F., & Vanden Broeck, J. (2020). Extracellular vesicles spread the RNA interference signal of *Tribolium castaneum* TcA cells. *Insect Biochemistry and Molecular Biology*, *122*, 103377. <https://doi.org/10.1016/j.ibmb.2020.103377>
- Nitnavare, R. B., Bhattacharya, J., Singh, S., Kour, A., Hawkesford, M. J., & Arora, N. (2021). Next Generation dsRNA-Based Insect Control: Success So Far and Challenges. *Frontiers in Plant Science*, *12*, 673576. <https://doi.org/10.3389/fpls.2021.673576>
- Ohkuma, S., & Poole, B. (1978). Fluorescence probe measurement of the intralysosomal pH in living cells and the perturbation of pH by various agents. *Proceedings of the National Academy of Sciences of the United States of America*, *75*(7), 3327–3331. <https://doi.org/10.1073/pnas.75.7.3327>
- Prentice, K., Christiaens, O., Pertry, I., Bailey, A., Niblett, C., Ghislain, M., Gheysen, G., & Smagghe, G. (2017). RNAi-based gene silencing through dsRNA injection or ingestion against the African sweet potato weevil *Cylas puncticollis* (Coleoptera: Brentidae). *Pest Management Science*, *73*, 44–52. <https://doi.org/10.1002/ps.4337>
- Pugsley, C. E., Isaac, R. E., Warren, N. J., & Cayre, O. J. (2021). Recent Advances in Engineered Nanoparticles for RNAi-Mediated Crop Protection Against Insect Pests. *Frontiers in Agronomy*, *3*, 652981.

- <https://doi.org/10.3389/fagro.2021.652981>
- Rehman, Z. U., Hoekstra, D., & Zuhorn, I. S. (2013). On the mechanism of polyplex- and lipoplex-mediated delivery of nucleic acids: Real-time visualization of transient membrane destabilization without endosomal lysis. *ACS Nano*, 7(5), 3767–3777. <https://doi.org/10.1021/nn3049494>
- Rozen, S., & Skaletsky, H. (2000). Primer3 on the WWW for General Users and for Biologist Programmers. In S. Misener & S. A. Krawetz (Eds.), *Bioinformatics Methods and Protocols*. Humana Press. <https://doi.org/10.1385/1-59259-192-2:365>
- Saleh, M.-C., Rij, R. P. van, Hekele, A., Gillis, A., Foley, E., O'Farrell, P. H., & Andino, R. (2006). The endocytic pathway mediates cell entry of dsRNA to induce RNAi silencing. *Nature Cell Biology*, 8(8), 793–802. <https://doi.org/10.1038/ncb1439>
- Santos, D., Remans, S., Van den Brande, S., & Broeck, J. Vanden. (2021). RNAs on the go: Extracellular transfer in insects with promising prospects for pest management. *Plants*, 10(3), 484. <https://doi.org/10.3390/plants10030484>
- Singh, I. K., Singh, S., Mogilicherla, K., Shukla, J. N., & Palli, S. R. (2017). Comparative analysis of double-stranded RNA degradation and processing in insects. *Scientific Reports*, 7, 17059. <https://doi.org/10.1038/s41598-017-17134-2>
- Swevers, L., Liu, J., Huvenne, H., & Smagghe, G. (2011). Search for limiting factors in the RNAi pathway in silkmoth tissues and the Bm5 cell line: The RNA-binding proteins R2D2 and translin. *PLOS ONE*, 6(5), e20250. <https://doi.org/10.1371/journal.pone.0020250>
- Tassetto, M., Kunitomi, M., & Andino, R. (2017). Circulating Immune Cells Mediate a Systemic RNAi-Based Adaptive Antiviral Response in *Drosophila*. *Cell*, 169(2), 314-325.e13. <https://doi.org/10.1016/j.cell.2017.03.033>
- Timmons, L., & Fire, A. (1998). Specific interference by ingested dsRNA. *Nature*, 395, 854. <https://doi.org/10.1038/27579>
- Tomoyasu, Y., Miller, S. C., Tomita, S., Schoppmeier, M., Grossmann, D., & Bucher, G. (2008). Exploring systemic RNA interference in insects: A genome-wide survey for RNAi genes in *Tribolium*. *Genome Biology*, 9(1), 1–22. <https://doi.org/10.1186/gb-2008-9-1-r10>
- Tros de Ilarduya, C., Sun, Y., & Düzgüneş, N. (2010). Gene delivery by lipoplexes and polyplexes. *European Journal of Pharmaceutical Sciences*, 40(3), 159–170. <https://doi.org/10.1016/j.ejps.2010.03.019>

- Ulvila, J., Parikka, M., Kleino, A., Sormunen, R., Ezekowitz, R. A., Kocks, C., & Rämetsä, M. (2006). Double-stranded RNA is internalized by scavenger receptor-mediated endocytosis in *Drosophila* S2 cells. *Journal of Biological Chemistry*, *281*(20), 14370–14375. <https://doi.org/10.1074/jbc.M513868200>
- Vélez, A. M., & Fishilevich, E. (2018). The mysteries of insect RNAi: A focus on dsRNA uptake and transport. *Pesticide Biochemistry and Physiology*, *151*, 25–31. <https://doi.org/10.1016/j.pestbp.2018.08.005>
- Vermeulen, L. M. P., De Smedt, S. C., Remaut, K., & Braeckmans, K. (2018). The proton sponge hypothesis: Fable or fact? *European Journal of Pharmaceutics and Biopharmaceutics*, *129*, 184–190. <https://doi.org/10.1016/j.ejpb.2018.05.034>
- Wang, K., Peng, Y., Pu, J., Fu, W., Wang, J., & Han, Z. (2016). Variation in RNAi efficacy among insect species is attributable to dsRNA degradation in vivo. *Insect Biochemistry and Molecular Biology*, *77*, 1–9. <https://doi.org/10.1016/j.ibmb.2016.07.007>
- Winston, W. M., Sutherlin, M., Wright, A. J., Feinberg, E. H., & Hunter, C. P. (2007). *Caenorhabditis elegans* SID-2 is required for environmental RNA interference. *Proceedings of the National Academy of Sciences of the United States of America*, *104*(25), 10565–10570. <https://doi.org/10.1073/pnas.0611282104>
- Wynant, N., Duressa, T. F., Santos, D., Van Duppen, J., Proost, P., Huybrechts, R., & Vanden Broeck, J. (2014b). Lipophorins can adhere to dsRNA, bacteria and fungi present in the hemolymph of the desert locust: A role as general scavenger for pathogens in the open body cavity. *Journal of Insect Physiology*, *64*, 7–13. <https://doi.org/10.1016/j.jinsphys.2014.02.010>
- Wynant, N., Santos, D., Verdonck, R., Spit, J., Van Wielendaele, P., & Vanden Broeck, J. (2014a). Identification, functional characterization and phylogenetic analysis of double stranded RNA degrading enzymes present in the gut of the desert locust, *Schistocerca gregaria*. *Insect Biochemistry and Molecular Biology*, *46*(1), 1–8. <https://doi.org/10.1016/j.ibmb.2013.12.008>
- Wynant, N., Verlinden, H., Breugelmans, B., Simonet, G., & Vanden Broeck, J. (2012). Tissue-dependence and sensitivity of the systemic RNA interference response in the desert locust, *Schistocerca gregaria*. *Insect Biochemistry and Molecular Biology*, *42*(12), 911–917. <https://doi.org/10.1016/j.ibmb.2012.09.004>
- Wytinck, N., Manchur, C. L., Li, V. H., Whyard, S., & Belmonte, M. F.

- (2020). DsRNA uptake in plant pests and pathogens: Insights into RNAi-based insect and fungal control technology. *Plants*, 9(12), 1780. <https://doi.org/10.3390/plants9121780>
- Xu, E., Saltzman, W. M., & Piotrowski-Daspit, A. S. (2021). Escaping the endosome: assessing cellular trafficking mechanisms of non-viral vehicles. *Journal of Controlled Release*, 335, 465–480. <https://doi.org/10.1016/j.jconrel.2021.05.038>
- Yan, S., Ren, B. Y., & Shen, J. (2021). Nanoparticle-mediated double-stranded RNA delivery system: A promising approach for sustainable pest management. *Insect Science*, 28(1), 21–34. <https://doi.org/10.1111/1744-7917.12822>
- Yoon, J. S., Gurusamy, D., & Palli, S. R. (2017). Accumulation of dsRNA in endosomes contributes to inefficient RNA interference in the fall armyworm, *Spodoptera frugiperda*. *Insect Biochemistry and Molecular Biology*, 90, 53–60. <https://doi.org/10.1016/j.ibmb.2017.09.011>
- Yoon, J. S., Kim, K., & Palli, S. R. (2020). Double-stranded RNA in exosomes: Potential systemic RNA interference pathway in the Colorado potato beetle, *Leptinotarsa decemlineata*. *Journal of Asia-Pacific Entomology*, 23(4), 1160–1164. <https://doi.org/10.1016/j.aspen.2020.09.012>
- Yu, N., Christiaens, O., Liu, J., Niu, J., Cappelle, K., Caccia, S., Huvenne, H., & Smagghe, G. (2013). Delivery of dsRNA for RNAi in insects: An overview and future directions. *Insect Science*, 20(1), 4–14. <https://doi.org/10.1111/j.1744-7917.2012.01534.x>
- Zhang, K., Hodge, J., Chatterjee, A., Moon, T. S., & Parker, K. M. (2021). Duplex structure of double-stranded RNA provides stability against hydrolysis relative to single-stranded RNA. *Environmental Science and Technology*, 55(12), 8045–8053. <https://doi.org/10.1021/acs.est.1c01255>

6. UNRAVELING THE ABSENCE OF MORTALITY IN THE dsRNA-NPs FEEDING EXPERIMENTS

6. UNRAVELING THE ABSENCE OF MORTALITY IN THE dsRNA-NPs FEEDING EXPERIMENTS

6.1. Introduction

Nanomaterials have successfully demonstrated their potential to enhance double-stranded RNA (dsRNA) efficiency in oral delivery assays in many insect species (Arjunan et al., 2024; Pugsley et al., 2021). However, nanoparticles (NPs) conjugated with dsRNA must be carefully designed to successfully reach the midgut epithelial cells by ingestion, with different aspects that need to be considered when designing these NPs.

One important aspect is the binding between dsRNA and the nanomaterial, that has to be stable enough to protect the dsRNA until it reaches the midgut epithelial cells, yet weak enough to release the dsRNA inside the cytosol of these cells. This initial protection is necessary to avoid the degradation of dsRNA by midgut enzymes. Previous studies have identified midgut enzymes as a crucial barrier for the efficiency of orally delivered dsRNA in insects (Christiaens et al., 2020; Peng et al., 2018), also in *Blattella germanica* (Lin et al., 2017). In orally RNA interference (RNAi)-refractory insects, such as *Locusta migratoria*, it has also been identified a gut-specific dsRNase (*RNase2*) responsible for the low RNAi oral efficiency (Song et al., 2017).

Another important factor, frequently ignored in dsRNA-NPs oral delivery assays, is the anatomy of the insect gut. Inside the midgut of certain arthropods, such as insects, there is the peritrophic membrane (PM), a non-cellular, and semi-permeable porous structure that encloses the food. The PM compartmentalizes the midgut lumen in two spaces: the ectoperitrophic space, between the midgut epithelium and the peritrophic membrane, and the endoperitrophic space, which is the lumen of the PM and where the food mass is enclosed (Kerkut & Gilbert, 1985). The PM in *B. germanica* is composed of multiple layers of chitin, synthesized by the midgut epithelial cells. Its formation is induced after food ingestion (Peters, 1992; Wigglesworth, 1930). The porous structure of the PM is created by these fibrils of chitin, and also includes various proteins, predominantly glycoproteins (Peters, 1992). The roles of the PM include spatial separation of the digestive process (Terra, 2001), prevention of mechanical injuries

(Peters, 1992; Sudha & Muthu, 1988) and protection against the entry of pathogens and harmful molecules due to the selectivity conferred by its pores (Barbehenn, 2001; Lehane, 1997; J. Peng et al., 1999), probably complicating the passage of dsRNA-NPs to the midgut epithelial cells.

[REDACTED]

6.2. Materials and methods

6.2.1. Cockroach colony and tissues sampling

Specimens of the cockroach *B. germanica* were obtained from a colony fed on dog chow and water *ad libitum*, kept in the dark at 29 ± 1 °C and 60-70% relative humidity. Dissections were performed on carbon dioxide-anaesthetized specimens, held under Ringer's saline.

[REDACTED]

[REDACTED]

[REDACTED]

[REDACTED]

6.2.4. Collection of midgut juice and hemolymph

Midgut juice and hemolymph were collected from freshly adult *B. germanica* females following the protocol by Lin et al., (2017).

Briefly, midguts were explanted and directly transferred into 100 μL of phosphate buffered saline (PBS) 1X. Midguts in PBS were kept on ice while the dissection of all the tissues. The sample was gently vortexed to extract the midgut juice from the midguts and then, centrifuged at 3,000 rpm for 10 min at 4 $^{\circ}\text{C}$ to precipitate the tissue. The supernatant containing the diluted midgut juice was transferred into a new tube.

Hemolymph was collected cutting the coxa of the hind legs and collecting the hemolymph using a micropipette. The maximum hemolymph obtained per insect was 2-3 μL . Hemolymph was maintained on ice while the collection of the fluid. Then, 5 μL of PBS 1X was added per microliter of hemolymph. Samples were centrifuged at 3,000 rpm for 10 min at 4 $^{\circ}\text{C}$ to precipitate the hemocytes. The supernatant containing the diluted hemolymph was transferred into a new tube.

The absorbances of the resulting supernatants from midgut juice or hemolymph samples were measured by spectrophotometry at 280 nm wavelength and adjusted to a protein concentration of 6 $\mu\text{g}/\mu\text{L}$ as in Lin et al., (2017).

6.2.5. *Ex vivo* dsRNA degradation assay

The protection conferred by the nanomaterials conjugated with [REDACTED] was studied *ex vivo* using midgut juice and hemolymph, adjusting the protein concentration to 6 $\mu\text{g}/\mu\text{L}$. For the dsRNA degradation assay using midgut juice, 50 ng of naked [REDACTED] (4 μL) or 50 ng of [REDACTED] conjugated with nanomaterials (4 μL) were added into microtubes containing 10 μL of diluted midgut juice. Samples were kept for 4 or 18 h in this solution. Moreover, samples without incubation, named 0 h, were used as controls of the experiment. After the incubation time, the enzymatic activity of the midgut juice was inhibited by adding 1.4 μL of ethylenediaminetetraacetic acid (EDTA) and heating the samples in a water bath for 10 min at 75 $^{\circ}\text{C}$. EDTA was also added to 0 h samples. After the 10 min, samples were kept 5 min on ice and stored at -80 $^{\circ}\text{C}$ until their use.

Following exactly the same protocol, 50 ng of naked [REDACTED] were added into microtubes containing 10 μL of diluted hemolymph at protein concentration of 6 $\mu\text{g}/\mu\text{L}$ and incubated for 4 h. Samples without incubation, named 0 h, were used as controls of the experiment. This experiment was done to validate the previous explained methodology, as it is reported that dsRNA could be detected 24 h after the incubation in *B. germanica* hemolymph (Garbutt et al., 2013; Lin et al., 2017).

Samples were then processed using QIAzol[®] lysis reagent (Qiagen) to isolate dsRNA. In each sample, 200 μL of QIAzol[®] was added and vortexed for 1 minute. Then, samples were centrifuged at 12,000 $\times g$ for 10 min at 4 $^{\circ}\text{C}$ and, the supernatant was transferred into a new tube and placed 5 min at room temperature. Then, 40 μL of chloroform was pipetted into the tube and vortexed for 15 s. The tube with the homogenate was kept for 3 min at room temperature. Following this step, samples were centrifuged at 12,000 $\times g$ for 15 min at 4 $^{\circ}\text{C}$. The upper aqueous phase, which contained the dsRNA, was transferred into a new tube. 150 μL of isopropanol was added to the tube and the sample was placed 10 min at room temperature. Then, samples were centrifuged at 12,000 $\times g$ for 15 min at 4 $^{\circ}\text{C}$ and the supernatant was discarded. Next, 500 μL of 75% of ethanol was added and centrifuged at 7,500 $\times g$ for 5 min at 4 $^{\circ}\text{C}$. The supernatant was discarded, and the pellet containing the dsRNA was air-dried. Finally, the pellet that contained the dsRNA was resuspended in 50 μL of nuclease-free water.

25 μL of the sample was freeze-dried and resuspended with 7 μL of nuclease-free water. These samples were then treated with DNase (Thermo Fisher Scientific), followed by retrotranscription to cDNA using the Transcriptor First Strand cDNA Synthesis kit (Roche Diagnostics GmbH), adding some modifications to the manufacturer instructions. For retrotranscribing [REDACTED] the forward primer at the extreme of the dsRNA sequence was used (Data S1, see Annexes), together with the RNase inhibitor, dNTPs, reverse transcriptase enzyme and the buffer. Due to the addition of a specific primer to retrotranscribe [REDACTED] neither random hexamers nor OligodT were used. Retrotranscription reaction was done following the program: (i) 75 $^{\circ}\text{C}$ for 10 min, (ii) 55 $^{\circ}\text{C}$ for 30 min, and (iii) 85 $^{\circ}\text{C}$ for 5 min. This first step of heating was added to the protocol to separate both strands of dsRNA, allowing the access of the reverse transcriptase to the sequence, which will act at the next step of 55 $^{\circ}\text{C}$. It has

been demonstrated that 75 °C is enough temperature to separate the strands of dsRNA (Garbutt et al., 2013).

To study the *ex vivo* degradation of dsRNA, cDNA levels of the sequence corresponding to [REDACTED] were analyzed by quantitative real-time PCR (qRT-PCR). Amplification reactions were carried out in a CFX Opus 384 Real-Time PCR System (BioRad) using the iTaq Universal SYBR Green Supermix (BioRad) following this program: (i) 95 °C for 3 min, (ii) 95 °C for 10 s; (iii) 57 °C for 1 min; (iv) steps (ii) and (iii) were repeated for 44 cycles. After the amplification phase, a dissociation curve was carried out to ensure that there was only one amplified product. The PCR primers used in qRT-PCR expression studies were designed inside the [REDACTED] sequence (Data S1, see Annexes) using the Primer3 v.4.1.0 software (Rozen & Skaletsky, 2000). The cDNA levels of [REDACTED] were quantified from 3 to 11 independent biological samples, making three technical replicates of each one, in a 10 µL of final volume. A control without template was included in all batches.

Results of qRT-PCR were expressed as cycle threshold (Ct), a value defined as the PCR cycle at which the fluorescent signal of the reporter dye (SYBR in our case) crosses an arbitrarily placed threshold. Hence, lower the concentration of cDNA, higher is the Ct value, indicating more degradation by the midgut enzymes. A difference of 3.3 Cts represents 10-fold dsRNA amount difference (Higuchi et al., 1993). The naked dsRNA at 0 h served as a reference of the optimum dsRNA extraction and was compared against all dsRNA-NPs at 0 h. Moreover, samples of naked dsRNA or dsRNA-NPs at 0 h were used as controls of non-degradation of dsRNA, and its values were compared with the same samples over the time.

6.2.6. Characterization of Peritrophic Membrane in the Scanning Electron Microscope

Midguts were dissected from 5-day-old adult *B. germanica* females. The dissected PMs were fixed in 4% paraformaldehyde overnight at 4 °C. After fixation, the samples were post-fixed in 1% osmium tetroxide for 2 h, and then rinsed three times for 30 min with distilled water. Further, dehydration was accomplished with a sequence of ethanol solutions of increasing concentration (20%, 40%, 60%, 80%, 95% and 100% ethanol) for 15 min

each. The last washes, 95% and 100%, were repeated twice. Subsequently, ethanol was replaced with acetone using an increasing concentration series (25%, 50%, 75% and 100%), each for 15 min. The samples were kept in anhydrous acetone overnight at 4 °C before being subjected to critical-point drying, in order to complete the dehydration process, by using a CPD300 dryer (Leica).

Samples were placed on stubs and covered with iridium to improve their conductivity using a QUORUM 150T ES Plus sputter coater (JEOL). Peritrophic membrane structure was observed by FE-SEM HITACHI SU8600 scanning electron microscope (SEM) (Hitachi High-Technologies Corporation). The electron beam energy used was 2 kV. Observations were done at the Microscopy Service of the Institut de Ciències del Mar (CSIC).


6.2.7. Statistical analysis

For relative cDNA quantification, qRT-PCR data were evaluated for normality and homogeneity of variance using the Shapiro-Wilk test, which showed that no transformations were needed. All datasets passed normality test. Statistical analyses for mean comparison were performed employing Student's *t*-test. A *p* value < 0.05 was considered statistically significant. Data were analyzed using GraphPad Prism version 8.1.0 for Windows, GraphPad Software.

For the PM pore size calculation, the longer pore axis was measured in 7 pictures of 5 different samples (10-30 pores/picture, *n* = 150). For microvilli diameter calculation, 2 pictures of 2 samples were measured (25 microvilli/picture, *n* = 50). Data were presented as mean ± standard error of the mean (S.E.M.). The size of the PM pores and microvilli was analyzed in ImageJ (version 1.54g).



6.5. Bibliography

- Arjunan, N., Thiruvengadam, V., & Sushil, S. N. (2024). Nanoparticle-mediated dsRNA delivery for precision insect pest control: a comprehensive review. *Molecular Biology Reports*, *51*, 355. <https://doi.org/10.1007/s11033-023-09187-6>
- Barbehenn, R. V. (2001). Roles of peritrophic membranes in protecting herbivorous insects from ingested plant allelochemicals. *Archives of Insect Biochemistry and Physiology*, *47*(2), 86–99. <https://doi.org/10.1002/arch.1039>
- Christiaens, O., Whyard, S., Vélez, A. M., & Smagghe, G. (2020). Double-Stranded RNA Technology to Control Insect Pests: Current Status and Challenges. *Frontiers in Plant Science*, *11*, 451. <https://doi.org/10.3389/fpls.2020.00451>
- Garbutt, J. S., Bellés, X., Richards, E. H., & Reynolds, S. E. (2013). Persistence of double-stranded RNA in insect hemolymph as a potential determiner of RNA interference success: Evidence from *Manduca sexta* and *Blattella germanica*. *Journal of Insect Physiology*, *59*(2), 171–178. <https://doi.org/10.1016/j.jinsphys.2012.05.013>
- Higuchi, R., Fockler, C., Dollinger, G., & Watson, R. (1993). Kinetic PCR analysis: real-time monitoring of DNA amplification reactions. *Biotechnology*, *11*(9), 1026–1030. <https://doi.org/10.1038/nbt0993-1026>
- Kerkut, G., & Gilbert, L. (1985). Regulation: Digestion, Nutrition, Excretion. In *Comprehensive Insect Physiology, Biochemistry and Pharmacology*. Pergamon Press.
- Lehane, M. J. (1997). Peritrophic matrix structure and function. *Annual*
- 

- Review of Entomology*, 42, 525–550.
<https://doi.org/10.1146/annurev.ento.42.1.525>
- Lin, Y. H., Huang, J. H., Liu, Y., Bellés, X., & Lee, H. J. (2017). Oral delivery of dsRNA lipoplexes to German cockroach protects dsRNA from degradation and induces RNAi response. *Pest Management Science*, 73(5), 960–966. <https://doi.org/10.1002/ps.4407>
- Peng, J., Zhong, J., & Granados, R. R. (1999). A baculovirus enhancin alters the permeability of a mucosal midgut peritrophic matrix from lepidopteran larvae. *Journal of Insect Physiology*, 45(2), 159–166. [https://doi.org/10.1016/S0022-1910\(98\)00110-3](https://doi.org/10.1016/S0022-1910(98)00110-3)
- Peng, Y., Wang, K., Fu, W., Sheng, C., & Han, Z. (2018). Biochemical comparison of dsRNA degrading nucleases in four different insects. *Frontiers in Physiology*, 9, 624. <https://doi.org/10.3389/fphys.2018.00624>
- Peters, W. (1992). *Peritrophic membranes*. Springer-Verlag. <https://doi.org/10.1007/978-3-642-84414-0>
- Pugsley, C. E., Isaac, R. E., Warren, N. J., & Cayre, O. J. (2021). Recent Advances in Engineered Nanoparticles for RNAi-Mediated Crop Protection Against Insect Pests. *Frontiers in Agronomy*, 3, 652981. <https://doi.org/10.3389/fagro.2021.652981>
- Rozen, S., & Skaletsky, H. (2000). Primer3 on the WWW for General Users and for Biologist Programmers. In S. Misener & S. A. Krawetz (Eds.), *Bioinformatics Methods and Protocols*. Humana Press. <https://doi.org/10.1385/1-59259-192-2:365>
- Santos, C. D., & Terra, W. R. (1986). Distribution and characterization of oligomeric digestive enzymes from *Erinnyis ello* larvae and inferences concerning secretory mechanisms and the permeability of the peritrophic membrane. *Insect Biochemistry*, 16(4), 691–700. [https://doi.org/10.1016/0020-1790\(86\)90013-2](https://doi.org/10.1016/0020-1790(86)90013-2)
- Skaer, R. J. (1981). Cellular sieving by a natural, high-flux membrane: I. The separation of platelets from plasma. *Journal of Microscopy*, 124(3), 331–333. <https://doi.org/10.1111/j.1365-2818.1981.tb02498.x>
- Song, H., Zhang, J., Li, D., Cooper, A. M. W., Silver, K., Li, T., Liu, X., Ma, E., Zhu, K. Y., & Zhang, J. (2017). A double-stranded RNA degrading enzyme reduces the efficiency of oral RNA interference in migratory locust. *Insect Biochemistry and Molecular Biology*, 86, 68–80. <https://doi.org/10.1016/j.ibmb.2017.05.008>
- Sudha, P. M., & Muthu, S. P. (1988). Damage to the midgut epithelium

- caused by food in the absence of peritrophic membrane. *Current Science*, 57(11), 624–625.
- Terra, W. R. (2001). The origin and functions of the insect peritrophic membrane and peritrophic gel. *Archives of Insect Biochemistry and Physiology*, 47(2), 47–61. <https://doi.org/10.1002/arch.1036>
- Wigglesworth, V. B. (1930). The formation of the Peritrophic Membrane in insects, with special reference to the larvae of mosquitoes. *Journal of Cell Science*, S2-73(292), 593–616. <https://doi.org/10.1242/jcs.s2-73.292.593>

7. A piRNA REGULATING OOGENESIS AND EMBRYO DEVELOPMENT IN COCKROACHES

7. A piRNA REGULATING OOGENESIS AND EMBRYO DEVELOPMENT IN COCKROACHES

Judit Gonzalvo^{1*}, Nuria Farrus^{1*}, Jorge Escudero^{1*}, David Pujal¹, Josep Bau², Maria-Dolors Piulachs¹

¹ Institut de Biologia Evolutiva (CSIC-Universitat Pompeu Fabra), Barcelona, Spain

² Department of Biosciences, Universitat de Vic-Universitat Central de Catalunya. Barcelona, Spain

* These authors contributed equally to this work.

Gonzalvo, J., Farrus, N., Escudero, J., Pujal, D., Bau, J., & Piulachs, M.D. (2024)

[A piRNA regulating oogenesis and embryo development in cockroaches. *bioRxiv*, 10.10.617606.](https://doi.org/10.1101/2024.10.10.617606)

<https://doi.org/10.1101/2024.10.10.617606>

Abstract

PIWI-interacting RNAs (piRNAs) are small non-coding RNAs, typically 26 to 31 nucleotides long. Initially known for repressing transposable elements to maintain genomic stability, recent research has revealed their additional regulatory roles. We studied the piRNA-83679, a highly expressed piRNA in the ovaries of the cockroach *Blattella germanica*, focusing on its role in oogenesis and embryo development. piRNA-83679 is found in both germinal and somatic cells during the gonadotropic cycle and is maternally provided to the egg. Using antisense oligonucleotides (ASOs) to reduce piRNA-83679 levels in adult females, we observed altered expression of ecdysone and chorion-related genes, along with disrupted F-actin organization in follicle cells. These changes led to improper egg encapsulation, delayed oviposition, and significant effects on early embryo development.

7.1. Introduction

The piwi-interacting RNAs (piRNAs) are small non-coding RNAs (sncRNAs) ranging from 26 to 31 nt in length, whose biogenesis is associated with PIWI proteins subfamily (Hirakata and Siomi, 2016; Le Thomas et al., 2014). In terms of sequence, piRNAs are poorly conserved even among closely related species, suggesting their function is highly species-specific (Aravin et al., 2007; O'Donnell and Boeke, 2007; Wang et al., 2019). In *Drosophila melanogaster*, two pathways of piRNA biogenesis have been described: the primary pathway active in somatic cells and the secondary, or "ping-pong" pathway, operative in germ cells. Altogether, these pathways silence transposons through both transcriptional and post-transcriptional (Gleason et al., 2018; Hirakata and Siomi, 2016). However, evidence from other arthropods indicates that the two piRNA pathways operate in somatic and germinal tissues (Cerqueira de Araujo et al., 2022; Yamashita et al., 2024).

The first function associated with piRNAs was the repression of transposable elements (TEs), as part of an evolutionarily conserved mechanism that ensures genomic stability in germ cells (Aravin et al., 2007; Senti et al., 2015). However, recent studies have shown that piRNAs can

also originate from coding sequences, intergenic regions unrelated to TEs, and 5' and 3' untranslated regions (UTRs) of mRNAs, which suggest that piRNAs regulate gene expression (Iki et al., 2023; Jensen et al., 2020; Lambert et al., 2019; Rojas-Ríos et al., 2018). In this context, piRNA have been implicated in diverse functions, including embryogenesis, germ cell specification, primary sex determination and the establishment of epigenetic states (Gleason et al., 2018; Gou et al., 2014; Iki et al., 2023; Kiuchi et al., 2014).

In a previous study on the cockroach *Blattella germanica*, we identified a significant number of piRNAs maternally provided to the zygote, which are abundant in early embryo stages (Bellés et al., 2024; Llonga et al., 2018). In the present work, we approached the functional study of one of these piRNAs by reducing its expression with an antisense oligonucleotide (ASO). ASOs are short (18-30 nt) single-stranded DNA molecules that bind specifically RNA to modulate gene expression (Roberts et al., 2020). Since the late 1970s, ASOs have been used as therapeutics against different illnesses, as they can be designed with high specificity against their mRNA targets (Crooke et al., 2021). ASOs bind to the corresponding mRNA target by Watson-Crick base pairing, forming RNA-DNA heteroduplexes that recruit RNase-H endonuclease leading to cleavage and degradation of the target RNA. Despite their proven potential, ASOs have barely been used to regulate insect gene expression (Oberemok et al., 2018).

B. germanica has the panoistic ovary type, in which all germline stem cells are converted into functional oocytes, with transcriptionally active nuclei (Büning, 1994). During *B. germanica* oogenesis, only the basal oocyte of each ovariole matures in every gonadotropic cycle, while the rest of oocytes present in the vitellarium remain arrested until the next cycle begins (Irles and Piulachs, 2014; Rumbo et al., 2023). Once released from the germarium, the oocyte is surrounded by a monolayer of follicular cells (FCs), thus establishing an ovarian follicle (Rumbo et al., 2023). The FCs mature and change their characteristics in parallel to oocyte growth. In the sixth (last) nymphal instar, when the basal ovarian follicle (BOF) begins to mature, the FCs proliferate, increasing their number until they completely cover the oocyte (Irles and Piulachs, 2014). Later, in 3-day-old adult, cytokinesis in FCs is arrested, and cells become binucleated. Under the control of the juvenile hormone circulating in the hemolymph, the FCs contract their cytoplasm thus leaving large intercellular spaces (Davey,

1981; Davey and Huebner, 1974), which facilitate the access of vitellogenin to the oocyte membrane. Henceforth, the oocytes in the BOFs grow exponentially. At the end of the gonadotropic cycle, the FCs close the intercellular spaces definitively (Bellés et al., 2024) and chorion synthesis begins, triggered by the ecdysone production in the ovary (Bellés et al., 1993; Pascual et al., 1992), a process that takes just a few hours (Irles et al., 2009b).

Several genes involved in ecdysone biosynthesis have been characterized in the ovaries of *B. germanica*, namely *neverland (nvd)*, *spook (spo)*, *spookiest (spot)*, *phantom (phm)*, *disembodied (dib)*, *shadow (sad)* and *shade (shd)* (Bellés et al., 2024). The action of ecdysone is mediated by *E75*, an early gene in the ecdysone signaling cascade, and *fushi tarazu- fl (ftz-fl)*, a late gene that also regulates the expression of ecdysteroidogenic genes, and helps to maintain the correct cytoskeleton organization in the BOF at the end of the gonadotropic cycle (Alborzi and Piulachs, 2023). Regarding chorion formation, two genes have been thoroughly characterized in *B. germanica*: *citrus* (Irles and Piulachs, 2011) and *brownie (brw)* (Irles et al., 2009a). At the end of choriogenesis, the cytoskeleton of the follicular epithelium in the BOFs is rearranged, thus facilitating the release of the egg into the oviduct (Alborzi and Piulachs, 2023). The eggs are then oviposited into a hardened egg capsule or ootheca. In *B. germanica*, the female carries the ootheca attached to the genital atrium throughout embryogenesis, which lasts 18 days under our laboratory conditions (Bellés et al., 2024).

7.2. Materials and methods

7.2.1. *Blattella germanica* colony and tissue sampling

Newly emerged *B. germanica* adult females, were obtained from a colony fed *ad libitum* on Panlab 125 dog food and water, maintained in darkness at 29 ± 1 °C and 60-70% relative humidity (Bellés et al., 1987). All dissections were performed on CO₂ anesthetized specimens. In adult females, the length of the BOF was used to establish chronological age. Females were maintained with males and, at the end of each experiment, the presence of spermatozoa in the spermatheca was assessed to confirm fertility.

7.2.2. Small RNA library processing

B. germanica piRNA sequences were obtained from small RNA libraries previously prepared in our laboratory (Ylla et al., 2017), publicly available at GEO, under accession number GSE87031. These sequences correspond to various developmental stages, including ovaries from 7-day-old adults, non-fertilized eggs, embryos (days 0, 1, 2, 6 and 13) and nymphs (instars 1, 3, 5 and 6). The small RNA libraries were preprocessed to remove sequencing adapters using Trimmomatic (v 0.39; relevant parameters used were: ILLUMINACLIP TruSeq2-PE.fa:2:15:10 LEADING:20 MINLEN:18) (Bolger et al., 2014). Reads ranging from 26 to 31 nucleotides were selected using Cutadapt (v 3.5) (Martin, 2011) and aligned to the *B. germanica* genome assembly (v 1.1) (Harrison et al., 2018) with Bowtie2 (v 2.4.4; relevant parameters used were: -a --end-to-end --score-min L,0,0) (Langmead and Salzberg, 2012), resulting in 2,534,205 aligned putative piRNA sequences. Infrequent sequences were filtered out by applying a cut-off of 17 reads across the whole dataset, reducing the number of sequences to 128,653. Finally, the sequences that shared the same genomic 5' start position and only differed in their length at the 3' end were collapsed. The counts of each of the collapsed variants were attributed to the most expressed one and normalized using the median-of-ratios method from DESeq2 (Love et al., 2014). The resulting data were used to select the piRNA candidate for functional studies.

7.2.3. RNA extraction and expression studies

The extraction of ovarian small RNAs was carried out at different ages using the miRNAeasy Mini Kit (Qiagen), following the manufacturer's protocol. The quantity and quality of the extracted small RNAs were estimated by spectrophotometric absorption at 260/280 nm using a Nanodrop spectrophotometer (MicroDigital Co, Ltd). A total of 400 ng from each RNA extraction was reverse transcribed with the 1st Strand cDNA synthesis Kit (Agilent Technologies) to obtain cDNA. The forward primer used in qRT-PCR was designed using the full piRNA sequence, while the universal primer from the Agilent 1st Strand cDNA synthesis Kit was used as the reverse primer. The efficiency of the primers used in qRT-PCR was first validated by constructing a standard curve based on three serial dilutions of cDNA from ovaries (Figure 7.S1). The *U6* small nuclear RNA was used as a reference for expression studies (Tanaka and Piulachs,

2012). qRT-PCR reactions were performed with iTaq Universal SYBR Green Supermix (Bio-Rad Laboratories). Amplification reactions were performed at 95 °C for 5 min, 44 cycles of 95 °C for 10 s plus 62 °C for 40 s, followed by 95 °C for 1 min and finally, the melting curve: from 60 °C to 95 °C with a measurement every 0.5 °C increase. After the amplification phase, a dissociation curve was carried out to ensure the presence of only a single product in the amplification (Figure 7.S1).

Total RNA extraction from 7-day-old adult *B. germanica* ovaries was carried out using Tissue Total RNA purification Kit (Canvax Biotech), following the manufacturer's protocol. The quantity and quality of the extracted RNAs were estimated by spectrophotometric absorption at 260/280 nm using a Nanodrop spectrophotometer (MicroDigital Co, Ltd). A total of 200 ng of each RNA extraction was reverse-transcribed using the Transcriptor First Strand cDNA Synthesis Kit (Roche) to obtain the corresponding cDNAs. The expression of selected mRNAs related to the studied processes was determined by qRT-PCR, using iTaq Universal SYBR Green Supermix (Bio-Rad Laboratories), and *actin-5c* mRNA expression as a reference. The amplification reactions were performed at 95 °C for 3 min, 44 cycles of 95 °C for 10 s plus 57 °C for 1 min, followed by 95 °C for 10 s and finally, the melting curve: from 57 °C to 95 °C with a measurement at each 0.5 °C increase.

Expression levels of small RNAs and mRNAs were calculated relative to their respective reference gene, using the $2^{-\Delta C_t}$ method (Irlles et al., 2009b; Livak and Schmittgen, 2001). Results are given as copies of small RNA per 1000 copies of *U6*, or copies of mRNA per 1000 copies of *actin-5c* mRNA and correspond to three biological replicates. The primer sequences are detailed in Table 7.S1.

7.2.4. Treatments with antisense oligonucleotides

The piRNA-83679 levels were reduced using a chemically unmodified antisense oligonucleotide (ASO: 5'-GGAGGTCCCCAGACCGGCACAGACCGAA-3') designed to encompass the entire piRNA sequence. Newly emerged adult females were treated with 1 μ L of a solution containing 15 μ g/ μ L of ASO in water (hereafter referred to as ASO-treated). As negative control, the same dose of a custom-designed oligonucleotide (ASO-Control) was administered.

The sequence of ASO-Control corresponds to the concatenated recognition sites of four restriction enzymes (XbaI, HindIII, KpnI, BamHI), and four additional nucleotides to reach the length of the ASO (5'-TCTAGAAAGCTTGGTACCGGATCCCAGGT-3'). Alternatively, both water and ASO-Control were used in control animals since no significant differences were observed in oviposition rates or the number of emerged nymphs (ASO: 40.27 ± 1.16 nymphs, $n = 15$; Water: 42.25 ± 0.75 nymphs, $n = 12$; $p = 0.187$), henceforth referred to as Mock-treated.

7.2.5. Microscopy methodologies

7.2.5.1. *In situ* hybridization

The piRNA-83679 was localized in ovaries from *B. germanica* adults using an antisense LNA (locked nucleic acid) probe conjugated to Digoxigenin (DIG) at the 5' and 3' ends (5'-DIG-GGAGGTCCCCAGACCGGCACAGACCGAA-DIG-3', Merck). Ovaries were dissected in Ringer's saline, and immediately fixed in paraformaldehyde (4% in PBS 0.2 M; pH 6.8) overnight. Subsequent hybridization and washing reactions were carried out as previously reported (Irls et al., 2009b). The DIG hapten was detected by incubating the samples in a 1:4,000 dilution of anti-DIG-rhodamine antibody (Roche, Basel, Switzerland) in PBS-T for 90 min at room temperature. Ovaries were washed again and incubated in DAPI (4',6-diamidino-2-phenylindole, 1 $\mu\text{g}/\text{mL}$, Merck) for 5 min at room temperature.

7.2.5.2. DAPI-TRITC-Phalloidin staining

Ovaries from 7-day-old *B. germanica* adults, were dissected under Ringer's saline, and immediately fixed in paraformaldehyde (4% in PBS 0.2 M; pH 6.8) for 2 h. Subsequently, they were washed with PBT (PBS 0.2 M; pH 6.8 + 0.2% Tween-20) (Irls and Piulachs, 2014). The ovaries were incubated for 20 min in 300 ng/mL of TRITC-phalloidin (tetramethyl rhodamine isocyanate-phalloidin, Merck) prepared in PBT, and after washing with PBT, were incubated for 5 min in 1 $\mu\text{g}/\text{mL}$ of DAPI, and washed again with PBT.

Samples were mounted with Mowiol (Calbiochem) and analyzed by epifluorescence using a Zeiss Axiomager.Z1 microscope (Apotome) (Carl Zeiss MicroImaging).

7.2.5.3. Embryo observations

Fifteen-day-old oothecae were removed from the female abdomen by gentle pressure, to observe the embryo development. The oothecae were incubated during 5 min in water at 95 °C to facilitate the individualization of the embryos. Images of the embryos were obtained using a Zeiss DiscoveryV8 stereomicroscope (Carl Zeiss MicroImaging).

7.2.6. Statistical analysis

The data are expressed as mean \pm standard error of the mean (S.E.M.). Statistical analyses were performed using GraphPad Prism version 8.1.0 for Windows, GraphPad Software. Significant differences between control and treated groups were calculated using the Student's *t*-test. Data were evaluated for normality and homogeneity of variance using the Shapiro-Wilk test, which indicated that no transformations were needed. All datasets passed normality test.

7.3. Results

7.3.1. piRNA-83679 in the ovary

B. germanica piRNAs were ranked according to their levels in the transcriptomes of both 7-day old adult ovaries and non-fertilized eggs. We selected as a candidate for functional studies the piRNA-83679 (5'-UUCGGUCUGUGCCGGUCUGGGGGACCUCC-3'), one of the most abundant piRNAs in ovaries of 7-day-old adults, and with quite high levels in non-fertilized eggs, which suggests that it is maternally transmitted (Figure 7.1A).

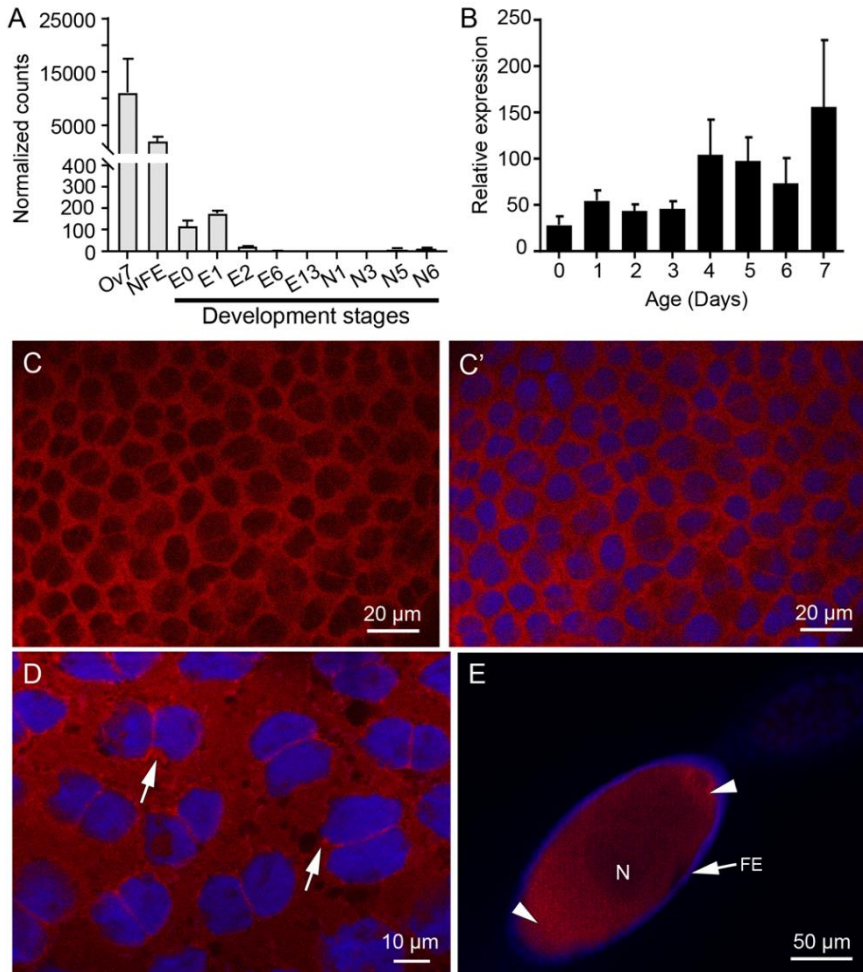


Figure 7.1. piRNA-83679 in ovaries of adult *Blattella germanica*. (A) Levels of piRNA-83679 in the small RNA libraries from different developmental stages, including embryos of different ages (days 0, 1, 2, 6 and 13 (E0, E1, E2, E6, E13)), nymphs from first (N1), third (N3), fifth (N5) and sixth (N6) instars. Data from transcriptomes from 7-day-old adult ovaries (Ov7) and non-fertilized eggs (NFE) were also included (Ylla et al., 2017). Each value represents the average of normalized counts, conducted using the median-of-ratios method from DESeq2. Data are shown as mean \pm S.E.M. ($n = 2$). (B) Expression profile of piRNA-83679 in adult ovaries during the first gonadotropic cycle. Data represent copies of piRNA per 1000 copies of *U6*, and are expressed as the mean \pm S.E.M. ($n = 3$). (C) *In situ* hybridization in late 3-day-old adult ovaries showing the piRNA-83679 localization in the cytoplasm of follicular cells of a BOF; (C') shows the merged images with the nuclei stained with DAPI. (D) *In situ* hybridization in follicular

The piRNA-83679 continues to be detectable during early embryonic stages (days 0 to 2), but it becomes undetectable in later embryonic stages and early nymphal instars (Figure 7.1A). Its levels reappear, albeit low, in the last nymphal instars (Figure 7.1A).

In *B. germanica* adult ovaries, piRNA-83679 increase gradually as the BOF grows and matures. In the transition from 3- to 4-day-old females, piRNA-83679 levels double (Figure 7.1B), coinciding with changes in the program of FCs in the BOF, which become binucleated at this period (Irles and Piulachs, 2014). From day 4, piRNA-83679 levels tend to decrease, increasing again on day 7 and reaching the highest levels, concurrently with the synthesis of the chorion proteins by the FCs (Figure 7.1B) (Irles et al., 2009b). *In situ* hybridization revealed the localization of piRNA-83679 in the FCs of the adult female BOF. Labeling appeared to accumulate in the cytoplasm of FCs early in the gonadotropic cycle (Figure 7.1C). In 5-day-old females, piRNA labeling remains present in the cytoplasm of the FCs (Figure 7.1D), with an increase of the signal next to the nuclei membrane (Figure 7.1D, white arrow).

Although the large size of the BOF in 5-day-old females prevented the observation of labeling inside the basal oocyte, the piRNA-83679 labeling was detected in the oocyte cytoplasm and nucleus of subbasal ovarian follicles, with stronger signals towards the anterior and posterior oocyte poles (Figure 7.1E, arrowheads).

Figure 7.1. (continued) cells from 5-day-old adult ovaries. piRNA-83679 labeling accumulates close to the nucleus membrane (arrows). (E) Subbasal ovarian follicle from a 5-day-old adult, showing the piRNA-83679 labelling in the ooplasm, with increasing labelling towards the oocyte poles (arrowheads); FE: follicular epithelia. N: nucleus. The apical pole is in the top-right. An antisense LNA probe with the piRNA sequence was used, labeled with DIG at both ends. In C-E, the probe was revealed with a rhodamine-labeled anti-DIG antibody (red). The DNA in the nuclei was stained with DAPI (blue).

7.3.2. piRNA-83679 and basal ovarian follicle development

To study the function of piRNA-83679, newly emerged *B. germanica* adult females were treated with an ASO targeting the piRNA, and effects were observed 7 days after the treatment.

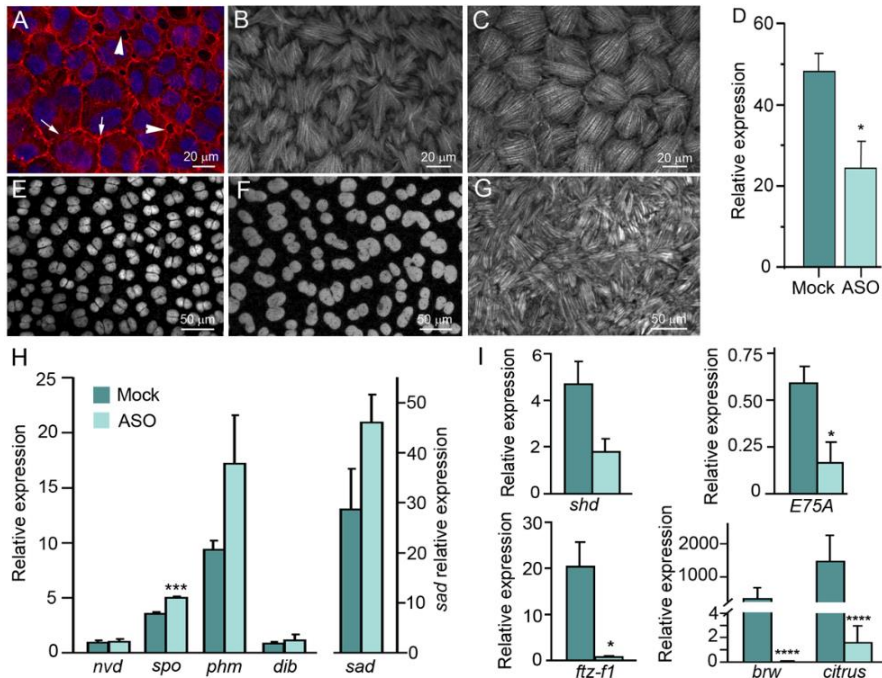


Figure 7.2. Effects of piRNA-83679 depletion in the ovaries of *Blattella germanica*. Newly emerged adult females were treated with ASO or Mock and dissected 7 days later. Images from A-C and E-G correspond to basal ovarian follicles. (A) Follicular epithelia, from a Mock-treated adult female, showing the follicular cells (FCs) distribution; cells are closing the intercellular spaces; arrows indicate closed intercellular spaces, and arrowheads indicate intercellular spaces that are still open. (B) F-actin distribution in the basal pole of FCs from a Mock-treated adult female in early chorion stage; the actin fibers in the basal pole of FCs are not completely packed. (C) F-actin distribution in the basal pole of FCs from a Mock-treated adult female in late chorion stage; the F-actin fibers are completely packed giving the FCs a round shape. (D) Expression levels of piRNA-83679 in 7-day-old *B. germanica* adult ovaries from freshly emerged females that were injected with Mock or ASO. Data represent copies of the piRNA per 1000 copies of *U6*, and are expressed as the mean \pm S.E.M. ($n = 3$). The asterisk indicates

In 7-day-old Mock-treated adult females, the binucleated FCs in the BOF, exhibit uniform distribution, with nuclei of same size and shape (Figure 7.2A, E) and begin to close intercellular spaces (Figure 7.2A, arrows). Upon completion of the chorion, the actin cytoskeleton surrounds the FCs, modifying their distribution and covering the surface of the basal pole of FCs in an orderly manner, packing the entire ovarian follicle (Figure 7.2B). Just before ovulation, the actin fibers wrap up the FCs, giving them a rounded shape (Figure 7.2C), which facilitates the contractions of the ovarian follicle needed for ovulation and oviposition.

piRNA-83679 levels in the ovaries were quantified in 7-day-old adult Mock- and ASO-treated females. In ASO-treated females, piRNA-83679 levels were significantly reduced ($p = 0.0107$) compared to Mock-treated females (Figure 7.2D). The FCs from the BOF from ASO-treated compared to Mock-treated females evidenced some morphological changes. These FCs of piRNA-83679-depleted females exhibited enlarged nuclei, heterogeneous in shape with bizarre morphologies (Figure 7.2F). Moreover, the distribution of the F-actin fibers in the basal pole of the FCs was disorganized (Figure 7.2G). The misaligned fibers did not follow the correct orientation on the ovarian follicle surface, and appeared overlapping different FCs.

Figure 7.2. (continued) statistically significant differences ($p = 0.01$). (E) Nuclei from FCs in Mock-treated females, showing the uniformity in size and distribution. (F) Nuclei from FCs in ASO-treated females, showing the different size and forms. (G) F-actin distribution in the basal pole of FCs of ASO-treated adult females, showing their disorganization; the F-actin microfilaments were stained with phalloidin-TRITC (red in A, white in B, C and G). DNA was stained with DAPI (blue in A, white in E and F). (H) Expression of the ecdysteroidogenic genes, *neverland* (*nvd*), *spook* (*spo*), *phantom* (*phm*), *disembodied* (*dib*), and *shadow* (*sad*). (I) Expression of *shade* (*shd*), *E75A*, *fushi tarazu-1* (*ftz-f1*), *brownie* (*brw*) and *citrus*. In H and I, data represent copies of mRNA per 1000 copies of *actin-5c* mRNA and are expressed as the mean \pm S.E.M. ($n = 3-5$). The asterisks indicate statistically significant differences respect to Mock-treated: * $p = 0.03$ (*E75A*); * $p = 0.02$ (*ftz-f1*); *** $p = 0.0003$ (*spo*); **** $p < 0.0001$ (*brw* and *citrus*).

Relevant changes in the mRNA levels of ecdysteroidogenic genes were detected (Figure 7.2H) in ovaries of ASO-treated females. While the expression of *nvd* remained unaffected, *spo* expression increased significantly by 41% ($p = 0.0003$). The expression of *phm*, *dib*, and *sad* showed a trend to increase, but the differences were not statistically significant compared to Mock-treated females (Figure 7.2H). Interestingly, the expression of *shd*, which encodes a 20-hydroxylase responsible for converting ecdysone into its active form, 20-hydroxyecdysone (20E), tended to decrease by an average of 61% (Figure 7.2I). This reduction in *shd* expression likely led to decreased availability of 20E, resulting in a significant reduction of *E75A* (71%; $p = 0.03$; Figure 7.2I) and a severe depletion of *ftz-fl* transcripts (94%, $p = 0.02$, Figure 7.2I). These disruptions in ecdysone signaling also caused a significant and extreme depletion of the chorion genes *citrus* and *brw* (99.89% and 99.95% respectively, $p < 0.0001$; Figure 7.2I).

7.3.3. piRNA-83679 function on reproduction and embryo development

To extend our study, we investigated whether depletion of piRNA-83679 in adult females could affect reproduction and embryo viability. Again, newly emerged adult females were treated with the same ASO targeting the piRNA, and then paired with males and observed until ootheca formation. The first effect observed was a significant delay in oviposition in ASO-treated females (8.11 ± 0.26 days; $n = 53$; $p = 0.013$), compared to Mock-treated insects (7.33 ± 0.08 days; $n = 38$).

Despite this delay, ASO-treated females carried the ootheca throughout the entire embryogenesis period (18.50 ± 0.26 ; $n = 32$) with no significant differences from Mock-treated females (18.81 ± 0.21 ; $n = 28$). However, although all the ASO-treated females successfully mated ($n = 32$), a significant number (25%, $n = 8$) of oothecae failed to produce nymphs. Furthermore, in the remaining ASO-treated females, the number of hatching nymphs was significantly reduced (36.29 ± 1.60 ; $n = 24$) compared to Mock-treated females (41.15 ± 0.74 ; $n = 27$; $p = 0.0062$). The lower number of hatching nymphs may be linked to the production of defective oothecae in several ASO-treated females (31.25%, $n = 10$), with shortened, curved or dried oothecae, or a combination of these defects, which often

resulted in misaligned eggs (Figure 7.3A and B), compromising hatching. The number of hatching nymphs from these malformed oothecae was drastically reduced (24.25 ± 3.64 nymphs; $n = 4$) and in some cases, no nymphs hatched at all ($n = 6$) (Figure 7.3B).

To further investigate how piRNA-83679 depletion affected embryo development, we examined 15-day-old oothecae from Mock- and ASO-treated females. At this stage, embryos from Mock-treated females (94 embryos from 4 oothecae) have completed the dorsal closure, and the tips of the antennae and the hind legs almost reached the seventh abdominal segment. Eye pigmentation is completed, and sclerotization of mandibles and legs is at the onset (Figure 7.3C) (Piulachs et al., 2010; Tanaka, 1976). In contrast, embryos from ASO-treated females (107 embryos from 3 oothecae) exhibited a wide range of phenotypic defects. Many embryos (62%) were morphologically similar to controls but showed less sclerotization (Figure 7.3D). The phenotypes of the remaining 38% of embryos displayed a variety of defects, ranging from eggs lacking the germinal band or with some tissue concentration in the ventral side, with the aspect of an amorphous mass (Figure 7.3E), to embryos with incomplete segmentation and with defective eyes (Figure 7.3F and G). Some embryos lacked eye pigmentation (Figure 7.3F), while others had eyes of incorrect shape (Figure 7.3H). The dorsal organ was still visible in this group of embryos (Figure 7.3H, arrow), and none of them showed signs of appendage sclerotization in the appendages, and in general, the legs were improperly sized and shaped (Figure 7.3F-I). In addition, in a few ASO-treated embryos, the fat body cells (urate cells and mycetocytes; see Tanaka, 1976) were more abundant than in Mock-treated ones (Figure 7.3I, white dots in the thorax and abdomen).

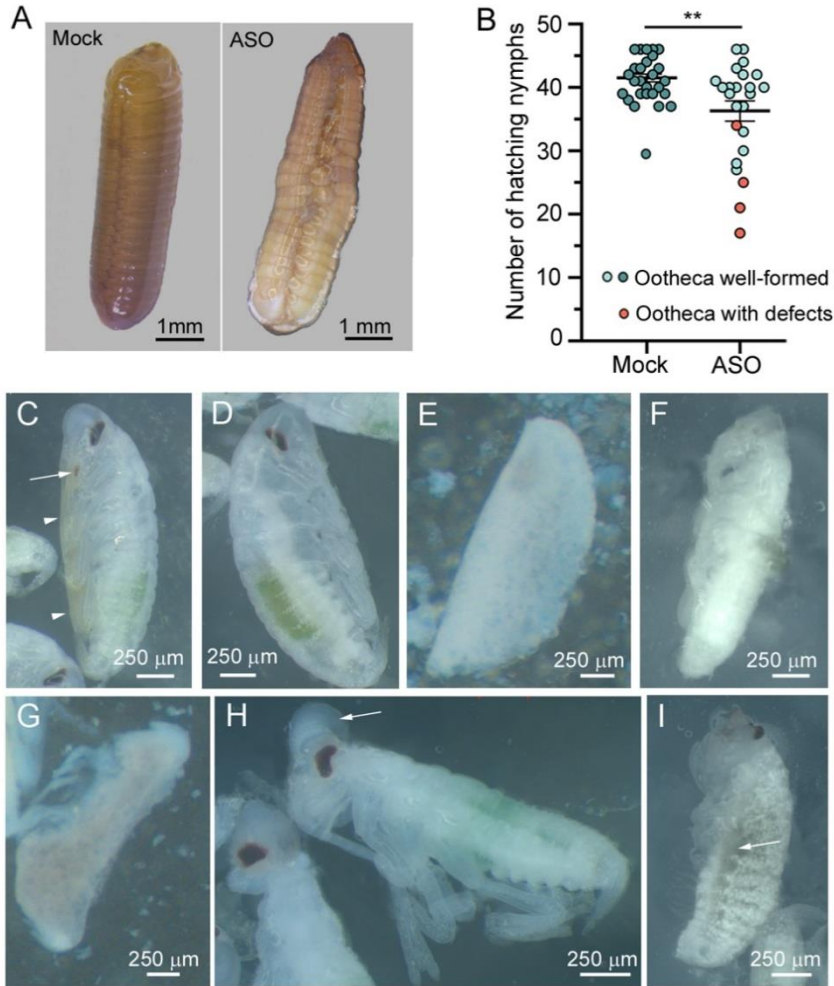


Figure 7.3. Effects of piRNA-83679 depletion on *Blattella germanica* embryogenesis. (A) Oothecae from Mock- and ASO-treated females; the later shows the eggs were not well-aligned. (B) Number of nymphs hatching from oothecae formed by Mock- and ASO-treated females. Each dot represents the total nymphs from one ootheca. Blue dots correspond to well-formed oothecae, and orange dots to defective oothecae. Data are represented as the mean \pm S.E.M. (Treated females, $n = 27$; Control females, $n = 24$). Asterisks indicate statistically significant differences (** $p < 0.01$). (C) Fifteen-day-old embryo from Mock-treated females. Segmentation is complete; the sclerotization of mandibles (arrow) and legs (arrowheads) already started. (D-I) Fifteen-day-old embryo from ASO-treated females. (D) Embryo similar to controls without sclerotized appendices. (E) Embryo with no signs of development. (F) Embryo with the different body parts differentiated; the appendages have some degree of development; the eyes are not

7.4. Discussion

The role of piRNAs as regulators of TEs and genome protectors is a well-established function. However, recent research has shown the importance of piRNAs as mRNA regulators. Thus, piRNA functions have been extended to processes as different as the maintenance of germinal stem cells, DNA repair mechanisms, sex determination, chromatin modifications, learning and memory, and cancer mechanisms (Gleason et al., 2018; Iki et al., 2023; Kiuchi et al., 2023, 2014).

Insect oogenesis is a highly regulated event involving multiple steps and processes, including germ cell proliferation, oocyte growth and maturation, vitellogenesis, and eggshell formation. These processes occur under the control of ecdysone and juvenile hormone (Alborzi and Piulachs, 2023; Bellés et al., 2024). Due to the efficiency and precision required, the regulation of this process entails different regulatory layers involving proteins, mRNAs, and non-coding RNAs, which have specific functions at different regulatory levels. Among the non-coding RNAs are the small non-coding RNAs that include the piRNAs studied here.

Our findings show that the piRNA-83679 is highly expressed in *B. germanica* ovaries, being present in somatic and germinal cells. Furthermore, piRNA-83679 levels in the ovary correlate with the key changes in the BOF, which are mainly related to the changes in the FCs program (Claycomb and Orr-Weaver, 2005; Irls et al., 2016, 2009b; Irls and Piulachs, 2014, 2011). The changes in piRNA-83679 expression during critical moments, such as the arrest of cytokinesis, the increase of

Figure 7.3. (continued) pigmented. (G) Similar to F but less advanced development; the legs are distinguishable, but the body segmentation was not apparent. (H) Embryo with a correct body development, however, the head has an abnormal morphology and the dorsal organ is still visible, these modifications determine a miss-localization of the head appendages; in addition, the legs appear to be larger than in controls. (I) Embryo with complete body segmentation; the head does not have the correct structure; the eyes are correctly pigmented, but the head appendages are not well defined; the legs are short reaching only the first abdominal segments; there is an increase of cells corresponding to the fat body that appeared like white dots.

polyploidy, or the endoreplication in the FCs, suggest a role in genome protection. However, piRNA-83679 likely has other functions since it is maternally provided to the embryo.

Using an ASO to deplete the piRNA-83679 allowed us to infer its functions in the adult ovary and the embryo of *B. germanica*. Reduction of piRNA-83679 levels in the ovary led to a delay in oviposition and malformations in the ootheca shape and size. These oothecae defects could explain the observed reduction in the number of emerging nymphs. Moreover, the expression profile of the piRNA-83679 in the ovary, and the observed oothecae malformations, suggest an effect of this piRNA on genes important at the end of the gonadotropic cycle, among them, ecdysteroidogenic genes expressed in the adult ovary (Ramos et al., 2020; Bellés et al., 2024). In most adult insects, when the prothoracic gland degenerates, the ovary becomes the main source of ecdysone, which acts then in an autocrine manner (Pascual et al., 1992; Romaña et al., 1995). In *B. germanica* adults, ecdysone is primarily needed at the end of the gonadotropic cycle to facilitate the endoreplication of some genome regions in the FCs, promoting chorion synthesis and facilitating the egg release into the oviduct (Alborzi and Piulachs, 2023; Bellés et al., 2024; Bellés et al., 1993). Depletion of piRNA-83679 led to reduce *shd* mRNA expression, which prevents the conversion of ecdysone to 20E, resulting in an overexpression of *phm*, *dib*, and *sad*. This suggests that piRNA-83679 may directly or indirectly repress the expression of these three genes, or that their mRNAs accumulate due to the *shd* reduction.

The inability to convert ecdysone to 20E disrupts 20E signaling, as shown by the lowered *E75A* expression. This weakened of 20E signaling affects the FCs program in the BOFs (Ramos et al., 2020), which in turn results in a decrease in the expression of chorion genes. Since the piRNAs have been described as repressors of mRNAs, the reduction of *shd* expression determined after the ASO treatment suggests that piRNA-83679 would inhibit a *shd* repressor.

The cytoskeleton in the BOF, which contributes to the egg release into the oviduct was also affected by the piRNA-83679 depletion. We had previously described that in *B. germanica* ovaries *ftz-f1* contributes to control the distribution of the cytoskeleton and its organization at the end of the gonadotropic cycle (Alborzi and Piulachs, 2023). Now, we have

observed that piRNA-83679-depleted females show a reduction of *ftz-fl* levels. This reduction resulted in the same phenotype obtained when *ftz-fl* was depleted by RNAi in adult females, which involved a decrease in ecdysone levels (Alborzi and Piulachs, 2023).

The diversity of phenotypes resulting from piRNA depletion could be attributed to its action on different mRNA targets. It is worth noting that the functions described here may represent only part of the roles of piRNA-83679 in *B. germanica* ovaries. The maternal provision of piRNA-83679 to the embryo suggests that it would play specific roles in early embryo development, a topic for future research. Nonetheless, our results show that ASOs-mediated piRNA depletion can be a useful approach to study the functions of these still mysterious sncRNAs.

Acknowledgments

We thank the financial support to the project PID2021-122316OB-I00 from the MCIN/AEI/ 10.13039/501100011033 and by ERDF, a way of making Europe, and to the Catalan Government (2021 SGR 00419). This work was supported by Pla de Doctorats Industrials de la Secretaria d'Universitats i Recerca del Departament d'Empresa i Coneixement de la Generalitat de Catalunya (grant number 2021 DI 059). The authors acknowledge the support of the publication fee by CSIC Open Access Publication Support Initiative through its Unit of Information Resources for Research (URICI).

7.5. Bibliography

- Alborzi, Z., & Piulachs, M. D. (2023). Dual function of the transcription factor Ftz-f1 on oviposition in the cockroach *Blattella germanica*. *Insect Molecular Biology*, 32(6), 689–702. <https://doi.org/10.1111/imb.12866>
- Aravin, A.A., Hannon, G.J., Brennecke, J. (2007). The Piwi-piRNA pathway provides an adaptive defense in the transposon arms race. *Science*, 318(5851), 761–764. <https://doi.org/10.1126/science.1146484>
- Bellés, X., Casas, J., Messeguer, A., & Piulachs, M. D. (1987). *In vitro* biosynthesis of JH III by the corpora allata of adult females of

- Blattella germanica* (L). *Insect Biochemistry*, 17(7), 1007–1010.
[https://doi.org/10.1016/0020-1790\(87\)90111-9](https://doi.org/10.1016/0020-1790(87)90111-9)
- Bellés, X., Cassier, P., Cerdá, X., Pascual, N., André, M., Rósso, Y., Piulachs, M.D. (1993). Induction of choriogenesis by 20-hydroxyecdysone in the german cockroach. *Tissue and Cell*, 25(2), 195–204. [https://doi.org/10.1016/0040-8166\(93\)90019-H](https://doi.org/10.1016/0040-8166(93)90019-H)
- Bellés, X., Maestro, J. L., & Piulachs, M. D. (2024). The German cockroach as a model in insect development and reproduction in an endocrine context. *Advances in Insect Physiology*, 66, 1–47. <https://doi.org/https://doi.org/10.1016/bs.aiip.2024.03.001>
- Bolger, A.M., Lohse, M., Usadel, B. (2014). Trimmomatic: a flexible trimmer for Illumina sequence data. *Bioinformatics*, 30(15), 2114–2120. <https://doi.org/10.1093/bioinformatics/btu170>
- Büning, J. (1994). *The Insect Ovary: Ultrastructure, previtellogenic growth and evolution*. Springer Dordrecht.
- Cerqueira de Araujo, A., Hugué, E., Herniou, E.A., Drezen, J.M., Josse, T. (2022). Transposable element repression using piRNAs, and its relevance to endogenous viral elements (EVEs) and immunity in insects. *Current Opinion in Insect Science*, 50, 100876. <https://doi.org/10.1016/j.cois.2022.100876>
- Claycomb, J., Orr-Weaver, T.L. (2005). Developmental gene amplification: insights into DNA replication and gene expression. *Trends in Genetics*, 21(3), 149–162. <https://doi.org/10.1016/j.tig.2005.01.009>
- Crooke, S.T., Baker, B.F., Crooke, R.M., Liang, X. (2021). Antisense technology: an overview and prospectus. *Nature Reviews Drug Discovery*, 20, 427–453. <https://doi.org/10.1038/s41573-021-00162-z>
- Davey, K. G. (1981). Hormonal control of vitellogenin uptake in *Rhodnius prolixus* Stål. *American Zoologist*, 21, 701–705. <https://doi.org/10.1093/icb/21.3.701>
- Davey, K. G., & Huebner, E. (1974). The response of the follicle cells of *Rhodnius prolixus* to juvenile hormone and antigonadotropin *in vitro*. *Canadian Journal of Zoology*, 52, 1407–1412. <https://doi.org/10.1139/z74-178>
- Gleason, R.J., Anand, A., Kai, T., Chen, X. (2018). Protecting and diversifying the germline. *Genetics*, 208(2), 435–471. <https://doi.org/10.1534/genetics.117.300208>
- Gou, L.-T., Dai, P., Yang, J.-H., Xue, Y., Hu, Y.-P., Zhou, Y., Kang, J.-Y., Wang, X., Li, H., Hua, M.-M., Gou, S.-T., Dai, P., Yang, J.-H., Xue, Y., Hu, Y.-P., Zhou, Y., Kang, J.-Y., Wang, X., Li, H., ... Liu, M.-F.

- (2014). Pachytene piRNAs instruct massive mRNA elimination during late spermiogenesis. *Cell Research*, 24, 680–700. <https://doi.org/10.1038/cr.2014.41>
- Harrison, M. C., Jongepier, E., Robertson, H. M., Arning, N., Bitard-feildel, T., Chao, H., Childers, C. P., Dinh, H., Dugan, S., Gowin, J., Greiner, C., Han, Y., Hughes, D. S. T., Huylmans, A., Kemena, C., Kremer, L. P. M., Lee, S. L., Lopez-ezquerria, A., Mallet, L., ... Bornberg-bauer, E. (2018). Hemimetabolous genomes reveal molecular basis of termite eusociality. *Nature Ecology & Evolution*, 2, 557–566. <https://doi.org/10.1038/s41559-017-0459-1>
- Hirakata, S., Siomi, M.C. (2016). piRNA biogenesis in the germline: From transcription of piRNA genomic sources to piRNA maturation. *Biochimica et Biophysica Acta (BBA) - Gene Regulatory Mechanisms*, 1859(1), 82–92. <https://doi.org/10.1016/J.BBAGRM.2015.09.002>
- Iki, T., Kawaguchi, S., Kai, T. (2023). miRNA/siRNA-directed pathway to produce noncoding piRNAs from endogenous protein-coding regions ensures *Drosophila* spermatogenesis. *Science Advances*, 9(29), eadh0397. <https://doi.org/10.1126/sciadv.adh0397>
- Irles, P., Bellés, X., Piulachs, M.D. (2009a). *Brownie*, a gene involved in building complex respiratory devices in insect eggshells. *PLOS ONE*, 4(12), e8353. <https://doi.org/10.1371/journal.pone.0008353>
- Irles, P., Bellés, X., Piulachs, M.D. (2009b). Identifying genes related to choriogenesis in insect panoistic ovaries by Suppression Subtractive Hybridization. *BMC Genomics*, 10, 206. <https://doi.org/10.1186/1471-2164-10-206>
- Irles, P., Elshaer, N., Piulachs, M.D. (2016). The Notch pathway regulates both the proliferation and differentiation of follicular cells in the panoistic ovary of *Blattella germanica*. *Open Biology*, 6(1). <https://doi.org/10.1098/rsob.150197>
- Irles, P., Piulachs, M.D. (2014). Unlike in *Drosophila* Meroistic Ovaries, hippo represses notch in *Blattella germanica* Panoistic ovaries, triggering the mitosis-endocycle switch in the follicular cells. *PLOS ONE*, 9(11), e113850. <https://doi.org/10.1371/journal.pone.0113850>
- Irles, P., Piulachs, M.D. (2011). Citrus, a key insect eggshell protein. *Insect Biochemistry and Molecular Biology*, 41(2), 101–108. <https://doi.org/10.1016/j.ibmb.2010.11.001>
- Jensen, S., Brasslet, E., Parey, E., Roest Crollius, H., Sharakhov, I. V., Vaury, C. (2020). Conserved Small Nucleotidic Elements at the Origin of Concerted piRNA Biogenesis from Genes and lncRNAs.

- Cells*, 9(6), 1491. <https://doi.org/10.3390/cells9061491>
- Kiuchi, T., Koga, H., Kawamoto, M., Shoji, K., Sakai, H., Arai, Y., Ishihara, G., Kawaoka, S., Sugano, S., Shimada, T., Suzuki, Y., Suzuki, M.G., Katsuma, S. (2014). A single female-specific piRNA is the primary determiner of sex in the silkworm. *Nature*, 509, 633–636. <https://doi.org/10.1038/nature13315>
- Kiuchi, T., Shoji, K., Izumi, N., Tomari, Y., Katsuma, S. (2023). Non-gonadal somatic piRNA pathways ensure sexual differentiation, larval growth, and wing development in silkworms. *PLOS Genetics*, 19(9), e1010912. <https://doi.org/10.1371/journal.pgen.1010912>
- Lambert, M., Benmoussa, A., Provost, P. (2019). Small Non-Coding RNAs Derived from Eukaryotic Ribosomal RNA. *Non-Coding RNA*, 5(1), 16. <https://doi.org/10.3390/NCRNA5010016>
- Langmead, B., Salzberg, S.L. (2012). Fast gapped-read alignment with Bowtie2. *Nature Methods*, 9, 357–359. <https://doi.org/10.1038/nmeth.1923>
- Le Thomas, A., Tóth, K.F., Aravin, A.A. (2014). To be or not to be a piRNA: Genomic origin and processing of piRNAs. *Genome Biology*, 15, 204. <https://doi.org/10.1186/gb4154>
- Livak, K. J., & Schmittgen, T. D. (2001). Analysis of relative gene expression data using real-time quantitative PCR and the $2^{-\Delta\Delta CT}$ method. *Methods*, 25(4), 402–408. <https://doi.org/10.1006/meth.2001.1262>
- Llonga, N., Ylla, G., Bau, J., Bellés, X., Piulachs, M.D. (2018). Diversity of piRNA expression patterns during the ontogeny of the German cockroach. *Journal of Experimental Zoology Part B: Molecular and Developmental Evolution*, 330(5), 288–295. <https://doi.org/10.1002/jez.b.22815>
- Love, M., Huber, W., Anders, S. (2014). Moderated estimation of fold change and dispersion for RNA-seq data with DESeq2. *Genome Biology*, 15, 550. <https://doi.org/doi:10.1186/s13059-014-0550-8>
- Martin, M. (2011). Cutadapt removes adapter sequences from high-throughput sequencing reads. *EMBnet.journal*, 17(1). <https://doi.org/10.14806/ej.17.1.200>
- O'Donnell, K.A., Boeke, J.D. (2007). Mighty Piwis defend the germline against genome intruders. *Cell*, 129(1), 37–44. <https://doi.org/10.1016/J.CELL.2007.03.028>
- Oberemok, V. V., Laikova, K. V., Repetskaya, A. I., Kenyo, I. M., Gorlov, M. V., Kasich, I. N., Krasnodubets, A. M., Gal'chinsky, N. V.,

- Fomochkina, I. I., Zaitsev, A. S., Bekirova, V. V., Seidosmanova, E. E., Dydik, K. I., Meshcheryakova, A. O., Nazarov, S. A., Smagliy, N. N., Chelengerova, E. L., Kulanova, A. A., Deri, K., ... Kubyshkin, A. V. (2018). A half-century history of applications of antisense oligonucleotides in medicine, agriculture and forestry: we should continue the journey. *Molecules*, 23(6), 1302. <https://doi.org/10.3390/molecules23061302>
- Pascual, N., Cerdá, X., Benito, B., Tomás, J., Piulachs, M.D., Bellés, X. (1992). Ovarian ecdysteroid levels and basal oöcyte development during maturation in the cockroach *Blattella germanica* (L.). *Journal of Insect Physiology*, 38(5), 339-343, 345-348. [https://doi.org/10.1016/0022-1910\(92\)90058-L](https://doi.org/10.1016/0022-1910(92)90058-L)
- Piulachs, M.D., Pagone, V., Bellés, X. (2010). Key roles of the *Broad-Complex* gene in insect embryogenesis. *Insect Biochemistry and Molecular Biology*, 40(6), 468–475. <https://doi.org/10.1016/j.ibmb.2010.04.006>
- Ramos, S., Chelemen, F., Pagone, V., Elshaer, N., Irlés, P., Piulachs, M.D. (2020). *Eyes absent* in the cockroach panoistic ovaries regulates proliferation and differentiation through ecdysone signalling. *Insect Biochemistry and Molecular Biology*, 123, 103407. <https://doi.org/10.1016/j.ibmb.2020.103407>
- Roberts, T., Langer, R., Wood, M.J.A. (2020). Advances in oligonucleotide drug delivery. *Nature Reviews Drug Discovery*, 19, 673–694. <https://doi.org/10.1038/s41573-020-0075-7>
- Rojas-Ríos, P., Simonelig, M., Rojas-Ríos, P., Simonelig, M. (2018). piRNAs and PIWI proteins: Regulators of gene expression in development and stem cells. *Development*, 145(17), dev161786. <https://doi.org/10.1242/dev.161786>
- Romaña, I., Pascual, N., & Bellés, X. (1995). The ovary is a source of circulating ecdysteroids in *Blattella germanica*. *European Journal of Entomology*, 92, 93–103.
- Rumbo, M., Pagone, V., & Piulachs, M. D. (2023). Diverse functions of the ecdysone receptor (EcR) in the panoistic ovary of the German cockroach. *Insect Biochemistry and Molecular Biology*, 156, 103935. <https://doi.org/https://doi.org/10.1016/j.ibmb.2023.103935>
- Senti, K.A., Jurczak, D., Sachidanandam, R., Brennecke, J. (2015). piRNA-guided slicing of transposon transcripts enforces their transcriptional silencing via specifying the nuclear piRNA repertoire. *Genes & Development*, 29, 1747–1762.

<https://doi.org/10.1101/GAD.267252.115>

- Tanaka, A. (1976). Stages in the embryonic development of the German Cockroach, *Blattella germanica* Linné (Blattaria, Blattellidae). *Kontyû*, 44(4), 512–525.
- Tanaka, E.D., Piulachs, M.D. (2012). Dicer-1 is a key enzyme in the regulation of oogenesis in panoistic ovaries. *Biology of the Cell*, 104(8), 452–461. <https://doi.org/10.1111/boc.201100044>
- Wang, J., Zhang, P., Lu, Y., Li, Y., Zheng, Y., Kan, Y., Chen, R., He, S. (2019). piRBase: a comprehensive database of piRNA sequences. *Nucleic Acids Research*, 47(D1), D175–D180. <https://doi.org/10.1093/NAR/GKY1043>
- Yamashita, T., Komenda, K., Miłodrowski, R., Robak, D., Szrajer, S., Gaczorek, T., Ylla, G. (2024). Non-gonadal expression of piRNAs is widespread across Arthropoda. *FEBS Letters*. <https://doi.org/10.1002/1873-3468.15023>
- Ylla, G., Piulachs, M.D., Bellés, X. (2017). Comparative analysis of miRNA expression during the development of insects of different metamorphosis modes and germ-band types. *BMC Genomics*, 18, 774. <https://doi.org/10.1186/s12864-017-4177-5>

7.6. Supplementary material

Table 7.S1. Primers used in the qRT-PCR reactions of small RNAs and mRNAs. F: primer forward, R: primer reverse.

Name		Primer sequence (5'-3')	Accession number
piRNA 83679	F	TTCGGTCTGTGCCGGTCTGGGGGACCTCC	-
Universal (Agilent)	R	GACGAGCTGCCTCAGTCGCATA	-
<i>U6</i>	F	CGATACAGAGAAGATTAGCATGG	FR823379
	R	GTGGAACGCTTCACGATTTT	
<i>actin-5c</i>	F	AGCTTCCTGATGGTCAGGTGA	AJ862721
	R	TGTCGGCAATTCCAGGGTACATGGT	
<i>dib</i>	F	GCAACAGACAATGGACCTCA	PSN36324
	R	AGATCCAATGCAACCTCCTC	
<i>E75A</i>	F	AATGAGTAGAGATGCGGTGCGGT	CAJ87513.1
	R	TCAGCGTCGGACAGTCTTAGTGA	
<i>ftz-fl</i>	F	TTGTACATCGACAAGACGCA	FM163377
	R	GTACATCGGGCCGAATTTGTTTTCT	
<i>nvd</i>	F	CTGGGGCCAGTCACAATACT	PSN31862
	R	GCAGGGGCTTGCAATGTAT	
<i>phm</i>	F	CTAGGCACCAGACACCTTC	PSN36025.1
	R	GCAAGCACTGTGTCTTCCAA	
<i>sad</i>	F	ATGAGGAGGTTTCAGGGTGTG	OE845190.1
	R	CTGGCCAGAAGTCATTTGGT	
<i>shd</i>	F	CACAGAGGCGCACAAGTTTA	PSN43891.1
	R	GTTCCCTTCAAAGTCCACA	
<i>spo</i>	F	GCCTTCATCATGTTGGCGTC	PSN30774.1
	R	CAGGTGTGGAGAGGTGTCTG	
<i>citrus</i>	F	TCGTGCTTTTCAATGTGCGTA	FN823078.1
	R	GGGAATCCAGGGTATTTGGAA	
<i>brownie</i>	F	CTCAGCACAAAGCCGTAGCA	FM253364.1
	R	CGTCGGCGTAAGCTTCGTAG	

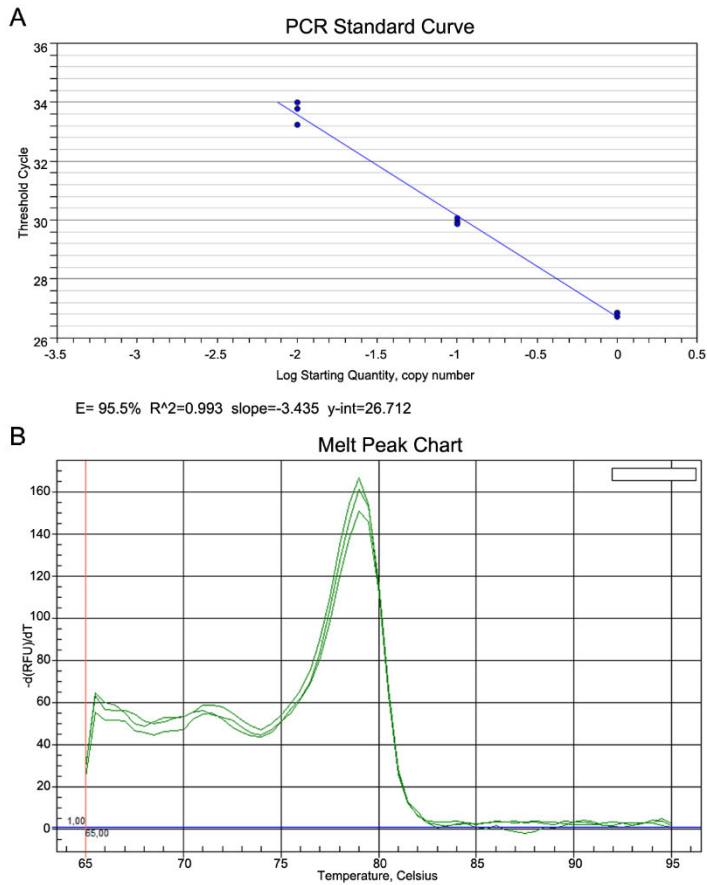


Figure 7.S1. (A) Standard Curve to calculate the efficiency of the primer pair used to quantify the piRNA-83679 expression. Efficiency was calculated with serial dilutions of ovarian cDNA. (B) Dissociation curve carried out after the amplification phase. The two panels are complementary and together validate the efficiency of the qPCR and the specificity of the primer pairs. qRT-PCR reactions were performed with iTaq Universal SYBR Green Supermix (Bio-Rad Laboratories). Amplification reactions were performed at 95°C for 5 min, 44 cycles of 95 °C for 10 s plus 62 °C for 40 s, followed by 95 °C for 1 min. Finally, to obtain the dissociation curve, the samples were heated from 60 to 95 °C with a measurement every 0.5 °C increase.

8. DISCUSSION

8.2. Bibliography

- Bachman, P., Fischer, J., Song, Z., Urbanczyk-Wochniak, E., & Watson, G. (2020). Environmental Fate and Dissipation of Applied dsRNA in Soil, Aquatic Systems, and Plants. *Frontiers in Plant Science*, *11*(21). <https://doi.org/10.3389/fpls.2020.00021>
- Bonina, V., & Arpaia, S. (2023). The use of RNA interference for the management of arthropod pests in livestock farms. *Medical and Veterinary Entomology*, *37*, 631–646. <https://doi.org/10.1111/mve.12677>
- Dubelman, S., Fischer, J., Zapata, F., Huizinga, K., Jiang, C., Uffman, J., Levine, S., & Carson, D. (2014). Environmental fate of double-stranded RNA in agricultural soils. *PLOS ONE*, *9*(3), e93155. <https://doi.org/10.1371/journal.pone.0093155>
- Farrus, N., Maestro, J. L., & Piulachs, M. D. (2024). CHMP4B contributes to maintaining the follicular cells integrity in the panoistic ovary of the cockroach *Blattella germanica*. *Biology of the Cell*, *116*(9), e2400010. <https://doi.org/10.1111/boc.202400010>
- Gonzalvo, J., Farrus, N., Escudero, J., Pujal, D., Bau, J., & Piulachs, M.D. (2024). A piRNA regulating oogenesis and embryo development in cockroaches. *bioRxiv*, 10.10.617606. <https://doi.org/10.1101/2024.10.10.617606>
- Oberemok, V. V., Laikova, K. V., & Gal'chinsky, N. V. (2024). Contact unmodified antisense DNA (CUAD) biotechnology: list of pest species successfully targeted by oligonucleotide insecticides. *Frontiers in Agronomy*, *6*, 1415314. <https://doi.org/10.3389/fagro.2024.1415314>
- Setten, R. L., Rossi, J. J., & Han, S. ping. (2019). The current state and future directions of RNAi-based therapeutics. *Nature Reviews Drug Discovery*, *18*, 421–446. <https://doi.org/10.1038/s41573-019-0017-4>
- Vélez, A. M., Narva, K., Darlington, M., Mishra, S., Hellmann, C., Rodrigues, T. B., Duman-Scheel, M., Palli, S. R., & Jurat-Fuentes, J. L. (2023). Insecticidal proteins and RNAi in the control of insects. In J. Jurat-Fuentes (Ed.), *Advances in Insect Physiology* (pp. 1-54). Elsevier. <https://doi.org/10.1016/bs.aiip.2023.09.007>
- Zhang, X., Zhang, J., & Zhu, K. Y. (2010). Chitosan/double-stranded RNA nanoparticle-mediated RNA interference to silence chitin synthase genes through larval feeding in the African malaria mosquito

(*Anopheles gambiae*). *Insect Molecular Biology*, 19(5), 683–693.
<https://doi.org/10.1111/j.1365-2583.2010.01029.x>

9. CONCLUSIONS

ANNEXES

ANNEXES

Table S1. Primers used for qRT-PCR measurements and biotechnologically dsRNA synthesis. dsRNA synthesis primers are underlined. The length of the amplicon, and the accession number of the sequence in the NCBI are indicated. F: Forward primer; R: Reverse primer.

Primer set		primer 5'-3'	Amplicon length (bp)	Accession number
<i>actin-5c</i>	F R	AGCTTCCTGATGGTCAGGTGA ACCATGTACCCTGGAATTGCCGACA	213	AJ862721
██████	█ █	████████████████████ ████████████████████	█	██████
<i>eIF4aIII</i>	F R	ATGGTGACATGCCACAAAAA GCAACACCTTTCCTTCCAAA	208	HF969254
██████	█ █	████████████████████ ████████████████████	█	██████
<i>Vg</i>	F R	CTGGGCATTTGACAACACAACAT TTGAAGAGCTGCTGGAGAGTTTG	116	AJ005115.2
██████	█ █	████████████████████ ████████████████████	█	██████
██████	█ █	████████████████████ ████████████████████	█	██████
<u>dsPolyH</u>	F R	ATCCTTTCCTGGGACCCGGCAA ATGAAGGCTCGACGATCCTAATCA	306	K01149
██████	█ █	████████████████████ ████████████████████	█	██████
██████ ██████	█ █	████████████████████ ████████████████████	█	██████

